VESSEL HEAVE DETERMINATION USING THE GLOBAL POSITIONING SYSTEM

P. J. V. RAPATZ

September 1991

PREFACE

In order to make our extensive series of technical reports more readily available, we have scanned the old master copies and produced electronic versions in Portable Document Format. The quality of the images varies depending on the quality of the originals. The images have not been converted to searchable text.

VESSEL HEAVE DETERMINATION USING THE GLOBAL POSITIONING SYSTEM

Phillip J.V. Rapatz

Department of Surveying Engineering
University of New Brunswick
P.O. Box 4400
Fredericton, N.B.
Canada
E3B 5A3

August 1991

PREFACE

This technical report is a reproduction of a thesis submitted in partial fulfillment of the requirements for the degree of Master of Science in Engineering in the Department of Surveying Engineering, August 1991. The research was supervised by Dr. David E. Wells, and funding was provided partially by the Natural Sciences and Engineering Research Council of Canada and by Nortech Surveys (Canada) Inc.

As with any copyrighted material, permission to reprint or quote extensively from this report must be received from the author. The citation to this work should appear as follows:

Rapatz, P.J.V. (1991). *Vessel Heave Determination Using the Global Positioning System.* M.Sc.E. thesis, Department of Surveying Engineering Technical Report No. 155, University of New Brunswick, Fredericton, New Brunswick, Canada, 129 pp.

ABSTRACT

This thesis investigation shows how the precise carrier-phase measurements available from the Global Positioning System in differential mode may be used to monitor the vertical motion of a ship — called heave. A model to utilize GPS observations in combination with ship attitude measurements has been devised and implemented. This model has been incorporated into a hydrographic navigation system being produced by Nortech Surveys (Canada) Inc. for the Canadian Hydrographic Service [Rapatz and Wells, 1990]. Testing of this model using a static data set indicates accuracy levels in the order of five centimetres or less. Comparisons of GPS measured heave with commercial heave sensor data during a ship cruise 100 kilometres offshore of Shelburne, N.S. reinforces this initial accuracy estimate.

The investigation illuminates some of the advantages, disadvantages and problems with using GPS for heave measurements and recommends areas of further research. The final conclusion is that used appropriately, GPS has the capability of accurately measuring vessel heave, even under circumstances in which commercial heave sensors may be incapable.

TABLE OF CONTENTS

LIST OF FIGURES

LIST OF TABLES

DEDICATION

This thesis is dedicated to Swee Leng, my wife and very best friend, and to my parents.

Their belief in me made me equal to the task.

ACKNOWLEDGEMENTS

I wish to acknowledge the special support, guidance and effort of Dr. D.E. Wells. There is no exaggeration when I say that without his encouragement, direction and example of tireless work, this thesis would never have been started let alone completed.

As well I would like to acknowledge the time and effort of Swee Leng Rapatz in the proofreading and critique of this thesis. Her contribution improved the work immeasurably.

The financial support for this research has been provided by several sources: National Sciences and Engineering Research Council (NSERC) of Canada Strategic Grant entitled "Applications of Differential GPS", principle investigator Dr. J. Tranquilla; NSERC Operating Grant entitled "Global Positioning System Design / Online Tides", principle investigator Dr. D.E. Wells; NSERC Operating Grant entitled "Integration of Hydrographic Systems", principle investigator Dr. D.E. Wells; Nortech Survey Canada Inc. contract entitled "Development of a Heave Compensation Algorithm", principle investigator Dr. D.E. Wells.

I wish to thank the Geophysics Division of the Geological Survey of Canada (GSC) and the Atlantic Geoscience Centre, GSC for providing equipment and resources for the collection of the data and for illustrating both scientific professionalism and enthusiasm.

Finally, a warm thanks to all my colleagues and friends in the Department of Surveying Engineering. In particular, Nick Christou, Jan Garmulewicz and Derrick Peyton provided me with daily examples of how friendship, the exciting exchange of ideas and personal commitment can combine to make a difficult task that much easier.

CHAPTER ONE
SCOPE OF THESIS

This thesis investigates the use of the NAVSTAR Global Positioning System (GPS) in a differential mode to precisely measure vessel heave — the vertical displacement of a ship from an equilibrium position. The issues affecting the use of differential GPS for heave determination addressed by this thesis are divided into two areas; the first dealing with the GPS signal itself and the second how to best use the motion information obtained from the signal. Of principle interest in the first case is the role which ambiguity resolution, satellite geometry and signal integrity play in the determination of the short term antenna motion. An appropriate model has been designed which utilizes the GPS derived antenna motion and pitch and roll information to resolve the vessel heave.

This thesis will show that heave determination using GPS is possible, accurate and even advantageous. The practical approach that has been taken, while perhaps not definitive, at the very least gives proof of concept and provides accurate vessel heave measurements from GPS signals.

1.1   Motivation

The forces that act on a ship and the motions generated by those forces are factors which limit ship based activities. Early in the history of sailing, measurements of vessel speed, pitch and roll were possible using crude instrumentation [Blagoveshchensky, 1962]. In contrast, heave resisted measurement other than qualitative observation for a much longer time. Early measurement techniques, including hull mounted pressure sensors and electrical conducting strips, suffered from the variability of the elevation of the water

surface used as the reference datum [Lattwood and Pengelly, 1967] and have largely been replaced by accelerometer based heave sensors.

Even though such heave sensors can potentially achieve accuracies in the order of three percent of the range of motion experienced [Hopkins and Adamo, 1981], they suffer from a number of problems which limit their range of operations [Rapatz, 1989]. GPS signals, by being independent of the vessel, offer the possibility of eliminating some of these problems thereby increasing accuracy and expanding the conditions under which accurate measurements can be made. However, the use of GPS introduces its own difficulties and these need to be identified and addressed.

1.2   Historical Background

In 1985, GPS measurements were observed aboard an airplane during flight in order to monitor height changes in a dynamic mode [Mader, 1986]. Rigid control observations were taken before, during and after the flight to control the experiment. The technique involved using strictly carrier phase observations and solving for the change in position between the starting point and the observation epoch. The accuracy of the experiment was determined by the mis-closure between height measurements from GPS measurements and control measurements. Results from this investigation indicated rms accuracies for GPS height measurements of 30 cms or better with the potential for much higher accuracies.

Attitude determination studies using GPS have been conducted showing the possibility of measuring short period motions with a high precision [Evans, 1985, 1986]. These studies are designed to evaluate GPS capabilities in precise vessel attitude monitoring and possible enhancement or replacement of inertial navigation systems. Difficulties include signal noise levels, cycle slips and satellite geometry; all of which are factors in the accuracy of the measurements.

A GPS kinematic test was undertaken by Nortech Surveys of Canada Inc. [Nortech, 1987]. During this test, carrier phase observations were obtained that, when processed, showed a height signal with a sinusoidal character. It was theorized that this signal was the heave of the ship on which the GPS antenna was located. Unfortunately, there were no additional sensors aboard the ship that might have confirmed this observation. Even so, the evidence of the capacity of GPS for heave measurement was quite clear.

The goal of continuing investigations into kinematic GPS , using various platforms such as boats, cars and airplanes, is to provide real-time, centimetre level positioning. These investigations are related to this thesis in that the nature of the problem is similar, however the requirements that are associated with the general kinematic problem are much more stringent than is necessary for heave determination. More details on these requirements are given in Chapters Two and Three. Some problems that are currently being addressed by these studies are again geometry considerations, cycle slip recovery and ambiguity resolution [Landau, 1989 and Hatch, 1989].

1.3   Investigation Procedure

The investigation procedure followed for this thesis was developed to provide proof for the initial postulation that differential GPS is capable of measuring vessel heave and then to develop a practical utilization of this theory. This consisted of developing techniques to appropriately utilize GPS measurements, testing using static data, collecting field data and finally, evaluating the results of processing the field data.

The technique used for determining heave from GPS measurements utilizes the high precision with which the carrier phase signal can be measured to determine the relative movements of the GPS antenna from epoch to epoch. Refining the motion determination

into height changes from epoch to epoch and integrating gives height motion over time. Appropriate datum selection and low frequency filtering, combined with pitch and roll measurements allow the determination of vertical motion of any point on a vessel.

This technique was tested using a data set from a static baseline collected during a 1986 observing campaign on Vancouver Island and north western Washington State [Kleusberg and Wanninger, 1987]. The result of processing this data set should of course indicate zero vertical motion over time and this assumption was used to confirm the algorithm. The accuracy of this test is influenced by the static nature of the data set and the more precise signal measurements possible under low dynamics. These test results indicate a precision level in the order of a few centimetres or less.

In determining potential accuracy, many aspects have been considered. The GPS system accuracy is central to this issue. In order to assess this accuracy as it relates to heave determination, rough estimates of error contributions have been relied on, supplemented by continuing research in the area of kinematic GPS. Considering all practical sources of error and the conditions under which the system would be expected to operate, it was felt that centimetre level accuracy was certainly attainable. In fact, field data obtained for this thesis indicates that accuracies in the order of five centimetres are already achievable.

In order to fully confirm the initial expectations of this study, it was necessary to collect data under field conditions using controlled observations from different sensors. In June of 1988, the CSS HUDSON was used to collect multi-sensor data. The cruise lasted for ten days and took place approximately 100 miles off-shore of Nova Scotia, Canada. The sensors included mechanical heave sensors, pitch/roll sensors, three axis accelerometers and two Texas Instruments series 4100 GPS receivers, one of which was located ashore at Shelburne, N.S.

The data collected at sea and on shore occupied 80 megabytes of floppy disk space and much pre-processing was required to reduce the observations to a usable format. GPS data was processed on a day-by-day basis and then compared against data from other sensors. The discussion of the results of these comparisons form the core of Chapter 5.

1.4   Contributions of This Thesis

Section 1.2 indicated that research into the use of differential GPS to measure vessel attitude was begun only recently and that the issue of heave measurement is relatively untouched. The unanswered questions from the 1987 Nortech research project formed the basis for the goals of this investigation: namely show that GPS can measure vessel heave and assess the accuracy and reliability of GPS derived heave. In carrying out the mandate of the investigation, the following contributions have been made:

- The ability of GPS to measure vessel heave has been clearly confirmed and is a significant development. Although it had been previously suspected that GPS was capable of this capacity, deterministic studies had yet to be performed [Nortech, 1987]. This thesis clearly demonstrates a further use for GPS hitherto not realized and opens the door for further development of this technique in the future.

- A practical heave determination algorithm was constructed during the course of this investigation in response to a request by Nortech Surveys of Canada Inc. This heave algorithm takes into consideration some of the difficulties encountered during the research and represents a simple yet effective approach to heave determination. This algorithm is currently being used in a micro-computer based GPS positioning system developed by Nortech under contract to the Canadian Hydrographic Service [Rapatz and Wells, 1990].

• The accuracy of differential GPS heave determination has been clearly demonstrated in the case of the initial algorithm. This accuracy is currently plus or minus five centimetres and is limited by such factors as signal noise, satellite geometry, cycle-slips and long baselines. The sensitivity of GPS heave determination to some situations has been illustrated and this information can be used to define conditions under which the technique is appropriate. The results from comparing the control measurements with the GPS heave estimates hint at the potential improvement of GPS heave measurement accuracy by as much as an order of magnitude.

1.5   Thesis Outline

Chapter One — *Scope of Thesis* is an introductory section outlining the framework of the study. It introduces the motivation behind the investigation within the context of the historical background and sketches the investigation procedure followed. The contributions of this thesis are elucidated and the structure of the written work is described.

Chapter Two — *A Ship in Motion* describes the physical dynamics of a ship that the new technique is attempting to monitor. The chapter begins with the driving forces behind ship motions, continues with the physical ship/sea interaction and the resulting motions experienced. The remaining sections deal with the establishment of a basis for measurement, the different techniques available and the importance of a measurement datum.

Chapter Three — *GPS Derived Heave* deals with the issues involved in using GPS for heave determination. The chapter begins with sections describing the Global Positioning System and the types of measurements possible. The techniques used for determining positions with GPS measurements are outlined with emphasis on moving receivers. The

chapter concludes by illustrating the particular technique used for resolving the heave motion of the antenna and the ship itself.

Chapter Four — *Field Data* outlines the collection of data in the field. Sections deal with both GPS data collection and data from the mechanical motion sensors. Details of the data decoding, cleaning, pre-processing are given for both data types.

Chapter Five — *Processing And Comparisons* gives the results for processing and comparison of the two sets of data. The criteria used for the comparison and evaluation of the data are explained, followed by interpretation of the differences between GPS data and the control data. The chapter ends with a summary of the comparison statistics.

Chapter Six — *Discussion and Conclusion* summarizes the preceding chapters in this thesis and draws conclusions from the results of the investigation. A review of the goals of the thesis are contrasted with a discussion of the effectiveness of the study. The future of GPS as a heave sensor is elaborated upon in conjunction with the previous sections and finally recommendations are given regarding future research and application of this technique.

1.6 Chapter Summary

Chapter One has introduced the scope of this thesis investigation by introducing the concept of differential GPS heave determination, describing the motivation behind the work, and relating some of the historical background regarding research in differential GPS and heave measurement. Completing the overview of the thesis, the procedure followed in the investigation and the structure of the subsequent report on this work has been described, followed by a concluding section which clearly states the goals of the research and details the scientific contributions made.

CHAPTER TWO
A SHIP IN MOTION

The modelling of ship motions on the ocean has intrigued sailors and ship owners wishing

to assess and extend the sea worthiness of their vessels. The problem however is that ship

motion is a complicated interaction between the air, sea and ship's hull. Researchers use

models, statistics, simplistic assumptions and the experience of mariners with varying

degrees of success. This chapter introduces some of the basic concepts and definitions

used in studying ship motion with the emphasis on the vertical motion – known as heave.

The following sections introduce ocean waves as the dominant driving force of ship

motion, basic theory of ship statics and motions, and the deterministic mathematical model.

Some heave measurement techniques are described and the importance of vertical datums in

vertical motion studies is discussed.

2.1　Waves

Undulations of the surface of a body of water, called waves, will provoke the motion of

any object resting on the surface of the water. Waves are formed as a result of disturbances

from three main sources:

- air/sea interaction at the surface;
- seismic disturbances;
- tidal forces [Price and Bishop, 1974].

Waves created by the first source are of direct interest when studying vessel motions as

they are more persistent, energetic and frequent than the other two.

Wind driven waves are typically classified according to their height, wavelength, period

and fetch. Waves which have a wavelength greater than twice the depth of the water, called

translational waves, are affected by the presence of the water bottom and have a speed c_s which is independent of the wave frequency. Oscillatory or free waves on the other hand are not affected by the presence of the bottom but their speed c_d is frequency or wavelength dependent [Bowditch, 1984]. These relationships can be seen in the following equations:

$$c_d = \sqrt{g\frac{L}{2}\pi} \tag{2.1}$$

$$c_s = \sqrt{gD} \tag{2.2}$$

where:

g   -   acceleration due to gravity;

L   -   wavelength;

D   -   water depth [Forrester, 1984].

There are two major theories regarding the development of wind driven waves, both assuming an energy transfer at the boundary between the air and water but differing in the mechanism. The first claims that shear stresses on the water surface set up by the wind is the source of the energy transfer, whereas a later theory states that the mechanism is the turbulently changing pressure right at the air-sea interface [Price and Bishop, 1974]. In either case this energy transference occurs immediately when the wind begins to blow. Winds with a speed of less than two knots will instantly cause ripples on the water, whereas flows greater than two knots will begin to develop more stable gravity waves [Bowditch, 1984]. These two theories do not fully account for the observed rates of wave generation and are still in question. Much more complicated, non-linear formulations and more study of the actual mechanisms are required to adequately model this complex process [Price and Bishop, 1974].

Ocean waves, when under the influence of the wind, have a shape closely related to trochoidal waves. This wave shape is mathematically defined as the continuous line

formed by the path of a fixed point within a circle as that circle is rolled along a straight line [Rawson and Tupper, 1968]. As the wave moves out from under the wind's influence, the wave height diminishes and the wave shape decays to a sinusoidal shape. The difference between the two wave shapes can be seen in Figure 2.1. The trochoidal wave shape is used for some fundamental predictions but, for deterministic studies, is usually replaced by the mathematically simpler sinusoidal wave shape [Blagoveshchensky, 1962].
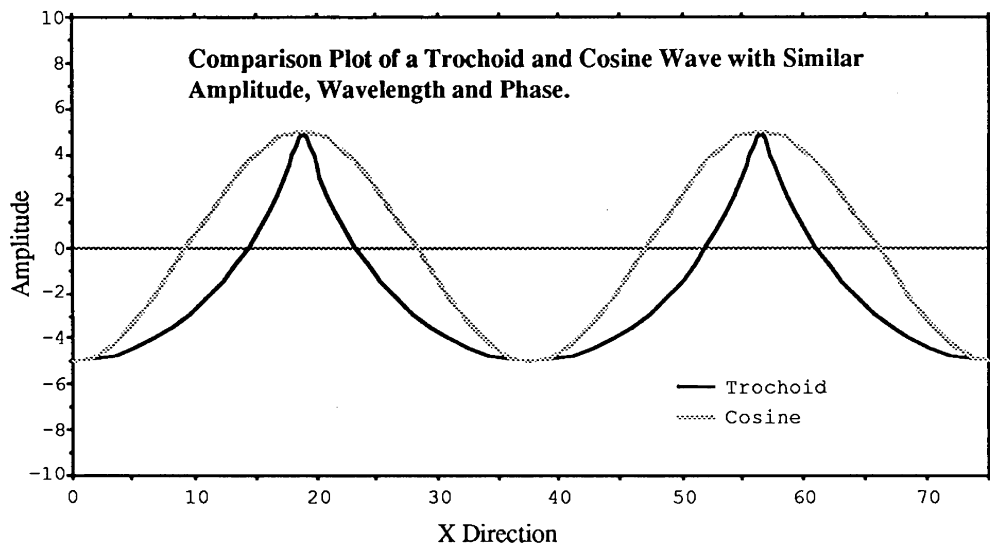
Figure 2.1 – Trochoidal vs. Sine Wave

Ocean waves can also be treated as a random process that is best characterized by statistical properties. Some effort has been given to finding a representative wave energy spectrum for an area based on observations of wave height, direction and frequency. As the wind continues to blow at a constant velocity for some time, the energy of the wave spectrum approaches a peak at a particular frequency ω_0. This characteristic frequency is inversely proportional to the velocity of the wind. The cutoff equilibrium spectrum is the simplest model of the wind spectrum.

$$\Phi_{\xi\xi}(\omega) = Ag^2\omega^{-5} \qquad \omega > \omega_c \qquad (2.3)$$

$$= 0 \qquad \text{otherwise}$$

A   —   Amplitude of wave;

g   —   gravitational acceleration;

ω —   frequency;

ω_c —   cutoff frequency.

This model is not frequently used as it relies on the relationship between frequency and wave energy whereas modern models have attempted to relate the wave energy spectrum to the wind velocity.

2.2 Ship Statics

The study of the forces which act on a floating object at rest on a still surface is called statics. Static forces are the result of the gravitational force acting downwards and the buoyancy restoring force acting upwards. The buoyancy restoring force and the gravitational force do not in general, act through the same point. The gravitational force acts through the centre of gravity of the ship whereas the buoyancy restoring force, following Archimedes principle, acts through the centroid of the space submerged in the water [Rawson and Tupper, 1968]. When these two forces do not act in the same line, such as when the vessel is somehow moved from its rest position, then the ship can exist in three states: stable equilibrium where the restoring force is such that the ship will return to its original rest position, unstable equilibrium where the restoring force is such that the ship will move away from its original rest position, and neutral equilibrium where the ship neither moves towards or away from the rest position [Lattwood and Pengelly, 1967]. Obviously, ships are designed to be in stable equilibrium under most circumstances.

2.3 Ship Motions

A ship can be considered a rigid body floating upon still or disturbed water. The motions of a ship are described using a three dimensional reference frame where six quantities can be measured: rotations about each of the axes and translations in the direction of each of the axes. These motions are coupled and therefore not easily interpreted when looking for insight into the behavior of the ship. The common terminology and definitions are presented below and are with respect to the equilibrium position [Blagoveshchensky, 1962].

Roll   –   Rotation about the longitudinal axis. Positive if the starboard (right) side is low. Negative if the port (left) side is low.

Pitch   –   Rotation about the transverse axis. Positive if the bow is raised.

Yaw   –   Rotation about the vertical centre axis. Positive if the bow is to starboard.

Heave   –   Translation in the vertical direction. Positive when the ship moves downward.

Surge   –   Translation in the longitudinal direction. Positive in the forward direction.

Sway   –   Translation in the transverse direction. Positive in the starboard direction.
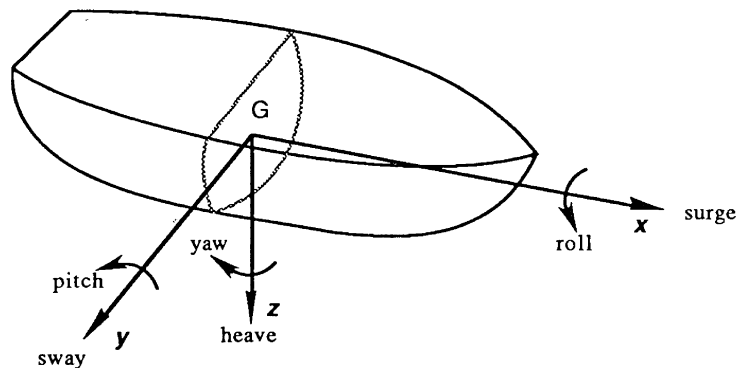
[Rawson and Tupper, 1967]

Figure 2.2 – Ship Motions

The oscillatory motions described above are individually characterized according to the parameters A-amplitude, T-period and ϕ-phase, which are familiar from basic wave theory. In the study of ship motions the maximum velocity and acceleration of the motion is measured along with the roll intensity which is the amplitude doubled [Blagoveshchensky, 1962].

2.4   Reference Frames

For the purposes of studying ship motions in response to a driving force, a set of appropriate reference frames must be considered. The most useful set of reference frames will allow transformation of observations in the local ship reference frame to an external reference frame. The parameters which relate the different reference frames are the six orientation and displacement measures from section 2.3, the ship's heading, the ship's speed and the ship's initial geographic position.

The four intermediate reference frames that are typically utilized in ship motion studies are:

1) OXYZ— A left hand system, origin fixed to the initial position of the ship, X axis oriented North (local topocentric).

2) O'X'Y'Z'— A left hand system, origin as above, X axis oriented along the heading of the ship.

3) $O^*X^*Y^*Z^*$— A right hand system, origin fixed to the ship, axes follow axes of the vessel when it is motionless and in equilibrium;

4) $O^\dagger X^\dagger Y^\dagger Z^\dagger$— A right hand system, origin fixed to the ship, axes fixed to the axes of the vessel itself.

The first reference frame OXYZ has a fixed origin and orientation. The OXY plane lies on and is tangent to the average ocean surface and the Z axis points vertically up. The initial orientation and origin can be arbitrary but it is customary to choose North as the X axis and the position of the vessel at time $t = t_0$ respectively. The second reference frame O'X'Y'Z' is in all ways the same as the first with the exception that the X' axis is oriented along the ship heading. This reference frame naturally makes the assumption that the ship heading is constant between time $t = t_0$ and $t = t_i$. These two reference frames are necessary for relating the position and orientation of the ship with respect to geographical coordinate systems.

Relationship Between Local Topocentric Coordinate System
Origin at t(o) and Ship Based System at t(n)
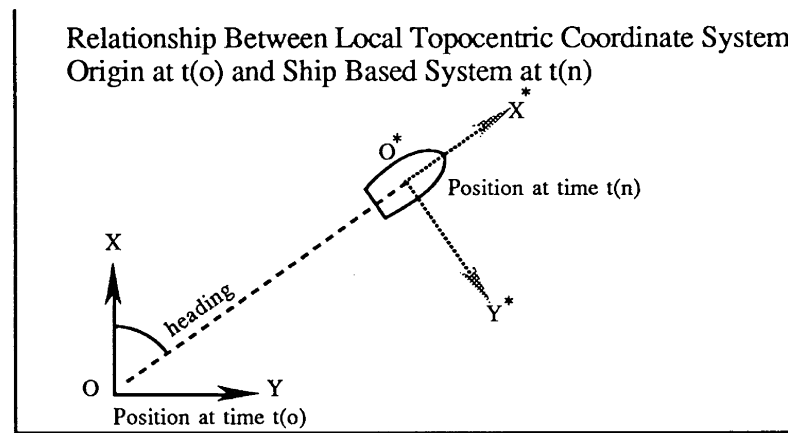
Figure 2.3 – Local Coordinate System to Ship Based System

Reference frames that allow measurement of the ship's orientation with respect to its static position have the origin fixed at the centre of gravity of the vessel. The equilibrium reference frame $O^*X^*Y^*Z^*$ allows the reference axes to be aligned with the ship axes such that X^* is pointing along the longitudinal axis, Y^* is aligned with the beam axis and Z^* vertically downward given that the ship is not influenced by the motion of the waves, i.e. that it is at rest in equilibrium. The final reference frame $O^{\dagger}X^{\dagger}Y^{\dagger}Z^{\dagger}$ is a ship fixed frame where the axes are fixed with the axes of the vessel and follow the motion of the vessel. It

is in this reference system that the relative coordinates of the motion sensors are determined.

2.4.1 Transformations

Given the assumption that the rotation angles are small, the coordinate transformations may be performed using rotation and reflection matrices where the general form is:

$$\bar{r}' = T(\omega_1, \omega_2, \omega_3) \cdot \bar{r} + \bar{r}'_0 \tag{2.2}$$

where:

$\bar{r}'$ — vector in the second system;

$\bar{r}$ — vector in the first system;

$\bar{r}'_0$ — position of the origin of the first system in the second system;

T — general transformation matrix consisting of a series of rotations R and reflection P;

$\omega_1, \omega_2, \omega_3$ — rotation angles about the axes of the first system.

[Vaníček and Krakiwsky, 1988]

Using this general form then:

$$T(\omega_1, \omega_2, \omega_3) = R_1(\omega_1) \cdot R_2(\omega_2) \cdot R_3(\omega_3) \cdot P_1 \cdot P_2 \cdot P_3 \tag{2.3}$$

where:

$$R_1(\omega_1) = \begin{bmatrix} 1 & 0 & 0 \\ 0 & \cos(\omega_1) & \sin(\omega_1) \\ 0 & -\sin(\omega_1) & \cos(\omega_1) \end{bmatrix} \qquad R_2(\omega_2) = \begin{bmatrix} \cos(\omega_2) & 0 & -\sin(\omega_2) \\ 0 & 1 & 0 \\ \sin(\omega_2) & 0 & \cos(\omega_2) \end{bmatrix}$$

$$R_3(\omega_3) = \begin{bmatrix} \cos(\omega_3) & \sin(\omega_3) & 0 \\ -\sin(\omega_3) & \cos(\omega_3) & 0 \\ 0 & 0 & 1 \end{bmatrix} \text{ and}$$

$$P_1 = \begin{bmatrix} -1 & 0 & 0 \\ 0 & 1 & 0 \\ 0 & 0 & 1 \end{bmatrix} \qquad P_2 = \begin{bmatrix} 1 & 0 & 0 \\ 0 & -1 & 0 \\ 0 & 0 & 1 \end{bmatrix} \qquad P_3 = \begin{bmatrix} 1 & 0 & 0 \\ 0 & 1 & 0 \\ 0 & 0 & -1 \end{bmatrix}$$

To describe the relationships between the four reference systems the following transformations can be used:

From system 4 ($O^\dagger X^\dagger Y^\dagger Z^\dagger$) to system 3 ($O^* X^* Y^* Z^*$):

$$\bar{r}_3 = R_1(\text{-Roll}) \cdot R_2(\text{-Pitch}) \cdot R_3(\text{-Yaw}) \cdot \bar{r}_4 + t_4 \tag{2.4}$$

where:

$t_4 \qquad - \quad \text{translation vector} = \begin{bmatrix} \text{-surge} \\ \text{-sway} \\ \text{-heave} \end{bmatrix}$

from system 3 ($O^* X^* Y^* Z^*$) to system 2 ($O'X'Y'Z'$):

$$\bar{r}_2 = P_3 \cdot \bar{r}_3 + \bar{r}_{o2} \tag{2.5}$$

where:

$\bar{r}_{o2} \qquad - \quad$ coordinates of the ship fixed origin with respect to origin of system 2.

from system 2 ($O'X'Y'Z'$) to system 1 (OXYZ):

$$\bar{r}_1 = R_3(\text{-heading}) \cdot \bar{r}_2 \tag{2.6}$$

The reverse transformation is easily accomplished by reversing the process and following the appropriate rules for handling matrix operations.

2.5 Mathematical Model

In deterministic studies of ship motion simplifying assumptions are made to alleviate mathematical complications. These assumptions are generally taken to be that the ship is rigid, it is operating at a constant speed and that the ship's heading is at some arbitrary angle to the direction of sinusoidal waves [Price and Bishop, 1974]. The equation used is the well known 2nd order differential equation describing damped, forced motion.

$$(M+A)\,\ddot{q}(t) + B\,\dot{q}(t) + C\,q(t) = q_o e^{i\omega_e} \tag{2.7}$$

where:

(M+A)   –   the virtual mass matrix and is made up of the contributions of the mass and inertial tensor of the ship as well as that of the water entrained by the ship movements;

B   –   the damping matrix;

C   –   the restoring force matrix;

q(t)   –   the output vector consisting of amplitudes of the surge, sway, heave forces and the amplitudes of the roll, pitch, yaw forces;

q₀   –   considered the input vector which is a combination of translation and rotation movements in the directions of the equilibrium axes;

ω_e –   encounter frequency.

The matrices **(M + A)**, **B**, **C** can be considered constant over time [Price and Bishop, 1974]. The reference frame is the ship based equilibrium frame and:

$$q_o = \begin{bmatrix} X \\ Y \\ Z \\ k \\ m \\ n \end{bmatrix} ; \quad q(t) = \begin{bmatrix} x(t) \\ y(t) \\ z(t) \\ \omega_1(t) \\ \omega_1(t) \\ \omega_1(t) \end{bmatrix} \tag{2.8}$$

where:

X, Y, Z   –   amplitudes of surge, sway, and heave;

k, m, n   –   amplitudes of pitch, roll, and yaw;

x(t), y(t), z(t)   –   surge, sway, and heave motions in the $O^*X^*Y^*Z^*$ reference frame;

$\omega_1(t), \omega_2(t), \omega_3(t)$ –   pitch, roll, and yaw orientations with respect to equilibrium axes [Price and Bishop, 1974].

2.6 Measurement Techniques

Early motion sensors used very simple principles in their design in order to measure ship attitude and motion. Pitch and roll measurements were made using mechanical or hydro-mechanical inclinometers. Yaw measurements consisted of course deviations from course made good. These types of measurements follow similar principles today but are more refined in terms of accuracy and reliability. Heave measurements on the other hand, are a more difficult proposition. Measurement techniques have changed substantially and reflect a great improvement in accuracy and suitability to the ocean environment.

2.6.1 Hydrodynamic

Typical early heave sensor designs were electrostatic strips and pressure sensors. The electrostatic strip utilized the conductivity of sea water to assist in measuring the height of the water along a metal strip attached to the side of the ship [Caldwell, 1955]. The pressure sensor was fixed to the side of the ship and provided a continuous measurement of the pressure of the water column above the sensor [Grover, 1954]. As the ship moved up and down the water pressure at the sensor head decreased or increased. A simple formula $P = \rho gh$ is used to extract the height h, where P is pressure, ρ is water density and g is acceleration due to gravity.

These techniques, while offering direct measurement of the water height with respect to the ship's hull, have no way of distinguishing whether the water level change is due to the motion of the ship such as rolling or due to changes in the sea surface such as is caused by waves etc [Tucker, 1955]. These extraneous changes of the water level in direct contact with the hull cause significant measurement errors and limit the usefulness of hydrodynamic techniques to times when the sea surface is very calm.

2.6.2 Survey Measurement

One technique that can be very accurate is optical measurement using conventional surveying instrumentation. Observing various points on the vessel as it undergoes motion enables one to track the roll, pitch and heave. The main limitations are the rapidity with which the measurements must be made, the range limitation of the optical instruments (usually less than five kilometres) and the coordination required for observations from different vantage points. These restrictions limit the application of this technique to near shore research projects [Renouf, 1987].

2.6.3 Photographs

Photographs or motion pictures, taken from either on board the vessel or from another vantage point, can provide a unique visual record of a ship's motions [Blagoveshchensky, 1962]. However, unless some kind of positional control can be added to the picture, it is difficult to perform quantitative measurements. Photographs have been successful however, in quantitatively assessing the driving function of the sea surface itself.

2.6.4 Accelerometer Based Heave Sensors

The particular type of heave sensor used to provide control measurements for this investigation have a single accelerometer installed on a self-stabilizing platform. These devices are usually but not always located near or at the centre of gravity of the vessel where the sensor will not experience tangential accelerations other than those due to heave. Should the device experience motions outside its dynamic range, the resulting output will be unreliable. When the sensor is placed away from the point of interest, other orientation sensors monitoring the pitch and roll of the vessel must be used. The roll and pitch may

then be used in the transformation of the motion from the sensor location to the point of interest.

2.6.4.1   The Reference Platform

The self-stabilized platform on which the heave sensing accelerometer is installed, is used as the horizontal reference plane and attempts to compensate for the rotational motions so as to remain perpendicular with respect to the gravity normal at all times. As well, the platform is designed to be insensitive to short period horizontal translational motions. The platform has some resonant oscillation period which is a function of the characteristics of the platform as well as the medium in which the working parts are immersed. However these motions, which can be the result of wave action, ship maneuvering and pitch and roll, become significant as the frequency of the motion approaches the natural oscillation frequency of the platform [Staples et al., 1985]. The resulting horizontal accelerations will cause the orientation of the reference platform to change with respect to the gravitational normal and the accelerometer will no longer register the vertical acceleration alone but a component of both the vertical and horizontal accelerations experienced.

2.6.4.2   The Acceleration Signal

To calculate the vertical position of the sensor with respect to its equilibrium position, the vertical acceleration is doubly integrated and sampled [Renouf, 1987]. However, because the signal from an accelerometer oriented vertically will always contain a constant component as well as spurious low frequency components, the integrator will eventually become overwhelmed. For this reason, low frequency signals must be heavily filtered from the output signal with a consequent loss of information [Zielinski, 1986].

There are two ways of handling output from the accelerometer. The signal, which is analogue by nature, can be processed using an analogue filter and integrator or it can be discretely sampled, and then digitally filtered and integrated. Analogue filtering and integration technique can only use past data providing near real time output. Digital techniques, by storing the information, can provide either near real time results or, smoothed results that are lagged in time [Hopkins and Adamo, 1981].

Filtering techniques are limited in that they are designed to be insensitive to periodic motions within a specific frequency pass band. The appropriate band width chosen in the filter and integrator design is determined by the conditions the sensor is expected to operate in. For vessel operations on the ocean, a low frequency cutoff point of close to 0.05 Hz and a high frequency cutoff point of 1 Hz are commonly used [Renouf, 1987].

2.6.4.3   Centripetal Acceleration

One difficulty with accelerometer based heave sensors is their sensitivity to all accelerations, not just those in the vertical direction. Even though the sensor platform attempts to remain perpendicular to the normal gravity vector, small deviations will occur due to the pitch and in particular the roll of the vessel. If the sensor package is located some distance from the rotational axis then centripetal accelerations will occur during rolling motion. The sensor is incapable of distinguishing this acceleration from linear acceleration and is one reason that the manufacturers recommend locating the sensor at the centre of gravity of the vessel.

A simple calculation can indicate the range of error this centripetal acceleration can introduce and that must be filtered out. Given a point 10 metres above the roll axis of the vessel and experiencing a roll of ± 2° then, assuming simple harmonic motion as an

approximation and looking at one half the cycle i.e. roll from one side to the other, the heave sensor will show a change of height of:

$$h = \frac{4\pi^2 A^2}{16\, r} = 0.11 \text{ metres} \tag{2.9}$$

where:

A   — amplitude of the horizontal range of motion;

r   — height above the roll axis.

2.6.4.4   Limitations

The accuracy of the accelerometer based heave sensors is dependent upon how well the overall system reacts to the particular conditions. Each heave sensor is designed to accommodate only a certain range of motion and a certain range of motion frequency. As the range and frequency of the motion begin to approach the design cutoffs of the instrument, the data becomes unreliable. The requirement for heavy low frequency filtering constitutes a significant limitation because the heave data is distorted by the filtering process. Forward and backward smoothing which reduces this distortion, is only possible by including the "future" data [Gelb, 1974]. This means that the output is delayed in time.

A limitation that is peculiar to heave sensors with a self stabilizing platform or suspension is the natural resonance frequency of the platform oscillation. As the frequency of the driving force approaches the resonance frequency of the platform, the platform becomes sensitive to this motion and becomes misoriented with respect to the gravity normal. This situation can invalidate the resulting heave signal. The resonance frequency of the platform is generally designed to be much lower than the expected frequency of the wave induced motion of the vessel. Unfortunately, some ship motions such as course alterations approach this resonance frequency thereby causing spurious heave signals.

Most manufacturers recommend that the heave sensor data during a period of course alteration and for some minutes afterward, not be used until after the platform has reached equilibrium again [DataWell, n.d. and TSS, n.d.].

2.7 Vertical Datums

The heaving motion of a ship is generally considered to be periodic and to oscillate about a fixed plane [Price and Bishop, 1974]. The process of measuring the heaving motion of the ship requires that the fixed plane or vertical datum be appropriately established depending upon the nature of the heave and how the measurements will be used. Absolute heave can be considered the vertical departure of the ship from a general, time invariant surface such as the geoid or the ellipsoid. This would be the case when attempting to monitor slowly changing displacements such as tidal motion in addition to the wave induced motion of the ship. Relative heave on the other hand can be considered the vertical displacement with respect to a locally established datum which is assumed to be fixed over a finite period of time.

In the case of measuring relative heave, the vertical datum is chosen such that the datum represents a surface of constant elevation throughout the period of measurement. Physical meaning is given to this datum by requiring that the reference surface be parallel to the geoid whose normal is, by definition, aligned with the normal of the gravity vector [Vaníček and Krakiwsky, 1988]. The geoid represents a surface of constant potential, i.e. the surface to which an homogeneous fluid would conform to under the influence of gravity and no other forces. The ocean can for some purposes be considered such a homogeneous fluid and therefore provides a useful physical reference surface [Vaníček and Krakiwsky, 1988].

GPS measurements however, are made with respect to the ellipsoid, a completely mathematical construct positioned to best conform to the actual shape of the equi-potential surface in the area of interest. The use of the ellipsoid as a reference surface overcomes the awkwardness of establishing the geoid's position and its variability due to the inhomogeneous density distribution of the Earth. The advantage of such a mathematical construct is that observations made with respect to this reference surface can be mathematically related to observations in another reference system. Unfortunately, generally the geoid and the ellipsoid are not coincident and therefore the physical interpretation of measurements made with respect to the ellipsoid can be obscure.

The challenge is to establish a relationship between the two datums so that measurements in one system may be used and compared in another. In this instance, the heave signal being sought is relative in nature and can be measured with respect to the local mean ocean level. The ocean surface however, is rarely at rest and is being constantly affected by phenomena such as tides, winds, currents, pressure disturbances and regions of differing sea water density. Averaging the local sea surface over a period of time significantly longer than the expected period of the heave motion produces an adequate datum for relative heave measurements and is the technique used by accelerometer based heave sensors.

The GPS height signal obtained from the antenna point is with respect to the ellipsoid and therefore not related to the geoid. However, by realizing that the antenna is constrained to oscillate about the mean ocean level, the GPS height signal can be time averaged to estimate the position of the mean sea surface with respect to the ellipsoid. Subtracting this estimated surface from the original signal transforms the GPS heights into heave measurements. The time period chosen for averaging the GPS height signal should be

significantly longer than the expected heave period of between one and twenty seconds but will also depend on biases in the GPS signal which are discussed in Chapter Three.

2.8 Chapter Summary

Chapter Two has introduced the study of ship motions by describing the basic concepts involved. The motions and their measurement with particular emphasis on heave has been given to help introduce the problem. Particular emphasis has been given to accelerometer based heave sensors as this was the system used for control measurements in the investigation. A discussion of the importance and relationship between various vertical datums concludes this chapter.

CHAPTER THREE
GPS DERIVED HEAVE

This chapter describes the technique adopted in this thesis for using the Global Positioning System to estimate vessel heave. A brief review of GPS together with the possible observables is given to provide the necessary background prior to introducing GPS heave determination. The mathematical techniques involved in GPS heave determination are described and the chapter is concluded by presenting test results using static data that indicate the potential of this new heave measurement tool.

3.1   Background of GPS

The Global Positioning System is a satellite based radio navigation system designed to provide 24 hour, three dimensional positions throughout the world. The mandate for construction, testing and operations has been assumed by the United States Department of Defense and the availability of the system to civilian users is to be consistent with U.S. security interests.

The control segment of the GPS is composed of tracking stations, ground control and information dissemination services. Tracking stations are located in Hawaii, Colorado Springs, Ascension Islands, Diego Garcia and Kwajalein [Jones, 1989]. The tracking stations monitor satellite signals and transmit the relevant information to the master ground control in Colorado Springs. Ground control determines orbital and clock parameters and returns this information to the tracking stations which "up-load" it to the satellites.

The space segment of the GPS is to be made up of 24 satellites orbiting in six different orbital planes with a nominal inclination of 55 degrees and period of 12 sidereal hours

[Green et al., 1988]. The satellites currently in orbit are made up of a dwindling number of Block I or experimental satellites and an increasing number of Block II or operational satellites. The constellation is designed such that at least four satellites will be above the horizon when viewed from any point on earth at virtually any time [Wells and Kleusberg, 1989].

3.2 Observables

The observables from the GPS satellites are obtained from monitoring two L-band radio frequencies; L_1 (1575.42 MHz) and L_2 (1227.60 MHz) [Remondi, 1985]. The satellites send imbedded information on the two carrier frequencies using coded modulations of phase. Decoding these alterations of phase permits the receiver to observe and record timing pulses being sent from the satellites as well as other data such as broadcast ephemeris and satellite health status indicators. Stripping this modulation from the signal leaves a smooth carrier signal the phase of which can be monitored and measured by most types of GPS receivers. These carrier-phase measurements have both advantages and disadvantages over code measurements.

3.2.1 Pseudo-ranges

A pseudo-range is the difference between the time of transmission of a coded pulse measured by the satellite's clock and the time of reception as determined by the receiver clock [Wells et al., 1986]. This value is not an estimate of the true time difference because in general, the time frames of both the satellite and the receiver are misaligned. This misalignment of the time frames along with other biases affecting the pseudo-range, can be estimated using various techniques described in Wells et al. [1986]. The corrected time

difference is multiplied by the nominal speed of light to convert to the units of range. The following equation describes the pseudo-range observable.

$$P_i^k(t) = \rho_i^k(t) + c[dt^k(t) - dT_i(t)] + d_{ion}(t) + d_{trop}(t) + \epsilon(t); \qquad (3.1)$$

where:

$P_i^k(t)$ — the observed pseudo-range between satellite k and receiver i at time t;

$\rho_i^k(t)$ — the actual range between satellite k and receiver i at time t;

c — nominal speed of light in a vacuum;

$dt^k(t)$ — satellite clock offset from GPS time at time t;

$dT_i(t)$ — receiver clock offset from GPS time at time t;

$d_{ion}(t)$ — correction due to ionospheric refraction of the signal at time t;

$d_{trop}(t)$ — correction due to tropospheric refraction of the signal at time t;

$\epsilon(t)$ — residual errors due to effects not being modelled;

and:

$$\rho_i^k(t) = \sqrt{(x^k-X_i)^2 + (y^k-Y_i)^2 + (z^k-Z_i)^2} \ , \qquad (3.2)$$

where:

x^k, y^k, z^k — cartesian coordinates of satellite k;

X_i, Y_i, Z_i — cartesian coordinates of receiver i.

3.2.2 Carrier-phase

The most common method of carrier-phase measurement $\phi_i(t)$ is to beat the incoming carrier signal being received with the carrier signal being internally created by the receiver. The phase of the resulting signal is monitored and when integrated over a period of time, is a measure of the doppler shift of the satellite signal [Wells et al., 1986]. The typical carrier-phase measurement is the accumulated count of cycles, integer and fractional, that

have passed the antenna point between the time of startup and time t. There are other methods available including the SERIES approach and interferometry, but these techniques are not commonly used [Remondi, 1985]. Much like the pseudo-range observable, a misalignment of the two respective timing clocks will exist as well as atmospheric effects that must be accounted for when formulating the following carrier-phase observation equation.

$$-\lambda\phi_i^k(t) = \rho_i^k(t) + c[dt^k(t) - dT_i(t)] - d_{ion}(t) + d_{trop}(t) + \lambda N_i^k + \varepsilon(t) \qquad (3.3)$$

where:

λ	–	wave length of the signal at the L_1 or L_2 frequency
$\phi_i^k(t)$	–	the observed accumulated phase measurement in cycles between satellite k and receiver i
$\rho_i^k(t)$	–	actual range between satellite k and receiver i (see equation 3.2)
c	–	nominal speed of light in a vacuum
$dt^k(t)$	–	satellite clock offset from GPS time at time t
$dT_i(t)$	–	receiver clock offset from GPS time at time t
$d_{ion}(t)$	–	correction due to ionospheric refraction of the signal at time t
$d_{trop}(t)$	–	correction due to tropospheric refraction of the signal at time t
N_i^k	–	integer cycle ambiguity in the carrier-phase signal
$\varepsilon(t)$	–	residual errors due to effects not being modelled.

3.2.3 Satellite Coordinates and Clocks

The two observation equations 3.1 and 3.3 make explicit use of the satellite coordinates plus the characteristics of the satellite clock behaviour. Two methods of determining orbit information are the use of satellite orbit ephemerides and short or long arc orbit solutions. Orbit solutions essentially solve for the orbital parameters along with the network

parameters and are generally only applicable to networks spanning large areas. Orbit ephemerides, either predicted or post computed, are commonly used for most GPS applications [Wells et al., 1986].

An ephemeris is a collection of parameters which describes the motion of a satellite and are generally valid for a short period of time— in the order of hours. The selection of these parameters is not unique, however a particular set of parameters called Keplerian elements is commonly chosen [Vaníček, 1973]. The main Keplerian elements are:

- right ascension of the ascending node,
- inclination of the orbital plane,
- argument of perigee,
- semi-major axis of the elliptical orbit,
- eccentricity of the orbit,
- mean anomaly [Wells et al., 1986].

The predicted GPS ephemeris is disseminated via the GPS broadcast message, a series of coded phase modulations impressed upon the carrier wave. The ephemeris consists of Keplerian elements, their velocities, trigonometric corrections to the elements and appropriate corrections to the satellite clock. This signal is decoded and recorded by most receivers. The precise GPS ephemerides are post-computed and made available by US-National Geodetic Service [Remondi, 1986]. This ephemeris normally consists of satellite positions at equal increments of time along with velocities which aid in the interpolation process [Casey, 1986].

The primary clocks on board the satellites are cesium atomic clocks with a frequency stability of better than 10^{-11}s and a frequency drift of better than 10^{-14} s/s [McCaskill and Buisson, 1985]. GPS clocks are monitored closely by ground control and a representative second order polynomial is used to predict the clock behaviour. The coefficients from this

polynomial approximation are then up-loaded to the satellites and broadcast by the satellites as part of their ephemeris message [Wells et al., 1986].

3.3 Errors and Biases

The elements of the observation equations 3.1 and 3.3 are all affected by random noise, biases and errors. The noise, biases and errors are effects that can be attributed to both GPS satellites and receivers. The term biases when used in conjunction with GPS generally means those factors which force the signal measurements away from the expected theoretical mean. It is implied that these factors can be modelled and eliminated or at least reduced through different techniques. Biases which affect GPS measurements are attributable to three sources; satellite biases, receiver biases and observation dependent biases.

Errors on the other hand, are those residual factors which cannot be accounted for, either through neglect or the limitation of the model. The contribution made to GPS measurement errors may be categorized similarly to biases. A description of some of the dominant effects and how they can be reduced using different techniques will be discussed in the ensuing sections.

3.3.1 Signal Noise

The signal noise is most often thought of as the statistically random fluctuations of the signal as it departs from an errorless model. This noise is due to the internal electronic limitations of the receiver. The magnitude of the GPS signal noise has been characterized by the rule of thumb that the noise is 1% of the signal wavelength [Wells et al., 1986]. In the case of the carrier signal the wavelength is approximately 20 centimetres which translates to ±2 mm of expected noise. Noise in the order of ±3 metres is expected for the

pseudo-range measurement following this guide. Newer receivers which are incorporating better technology have been reported to have obtained noise levels better than 0.5 % of the signal wavelength [Ashtech, 1989].

These estimates of signal noise levels are dependent upon the tracking of the satellites signal from a stationary position. This allows the receiver to severely restrict the band-width of the monitoring loop and thereby reduce the amount of noise. In a situation where the receiver is experiencing accelerations, it is often necessary to relax the band-width restriction. In such a situation where the band-width of the monitoring loop has been widened to accommodate expected accelerations, the signal noise will be increased significantly [Evans et al., 1985].

3.3.2 Satellite Biases

Satellite dependent biases are the result of uncertainties in both the satellite position and the satellite clock. The satellite position uncertainties stem from errors in the ephemeris information used in the position calculations which in turn depend on the factors involved in monitoring and predicting the motion of the satellites by the ground control segment of the system. The clock biases are deviations of the satellite time frame from the nominal GPS time frame and will affect both code and pseudo-range observations equally. In general, satellite biases are considered uncorrelated between satellites [Wells et al., 1986].

3.3.3 Receiver Biases

Receiver biases are dependent upon factors present at the receiver station site. The receiver clock will in general not be coordinated with the satellite clocks, again affecting both pseudo-range and carrier-phase observations equally. Uncertainty in initial station

coordinates will have a limited effect on the final results when using differential GPS techniques [Santerre, 1989].

3.3.4 Observation Dependent Biases

Observation dependent biases are a function of either signal propagation or related directly to the nature of the observation types. The propagation of the signal through the atmosphere is affected by the atmospheric constituents. The earth's atmosphere can be separated into two representative regions; the troposphere — ranging from the surface to approximately 50 kms and the ionosphere — from 50 kms to over 1000 kms [Wells et al., 1986]. Each region will affect the signal propagation differently, acting as a refractive medium. The ionosphere is typically a dispersive medium where the refraction is frequency dependent whereas the tropospheric effect is frequency insensitive [Wassef and Kelly, 1988].

The ambiguity of the carrier-phase is an example of an observational bias related to an observation type. The measurement of the phase of a carrier cycle inherently leaves the integer number of cycles between transmitter and receiver unknown. The correct solution of this bias potentially results in the most accurate application of GPS measurements.

3.3.5 Errors

Measurement errors are those biases that have not been accounted for, either through neglect or ignorance. The effects of these errors will eventually propagate through to the final results in some way determined by the use of the measurements in the observational model. Some of the factors which can be considered errors are; multipath, antenna imaging, uncorrectable cycle-slips, residual bias errors and antenna phase centre movement [Wells et al., 1986].

Multipath and imaging are site dependent errors caused by signal reflections or antenna imaging effects due to the makeup of the surrounding station site. This effect is correlated between days at the same site but not between station sites. It is generally difficult to account for and reduction is accomplished through careful site selection.

Phase centre movement on the other hand, is the result of anisotropic shape of the phase envelope of the antenna. The effective position of the antenna changes with the direction of the signal wave front being monitored by the antenna. This change in position can be as large as centimetres depending on the construction of the antenna and the direction of the signal wave front but is in general two to three centimetres for the normal range of motion expected on a ship [Tranquilla, 1991].

Cycle-slips occur when the carrier wave signal being monitored by the receiver is blocked or the signal strength severely reduced. When this happens the receiver loses track of the integer number of cycles that have passed. After tracking is re-established the new integer cycle count can be any arbitrary value depending on how the receiver is designed. Cycle slips can be corrected using a variety of techniques, including using double differences, different combinations of the L1 and L2 frequency [Wells and Kleusberg, 1989] and variations of "on the fly" ambiguity resolution [Seeber and Wübbena, 1989]. Cycle-slip correction techniques improve with the increasing number of satellites being simultaneously tracked, but are generally less effective when the receiver is moving.

Residual bias effects not accounted for by modelling include high frequency atmospheric effects, residual clock terms, and residual orbital errors. The magnitude of these errors will depend on factors such as the atmospheric variability, precision of models used and the techniques used to reduce the bulk of the effect.

3.3.6 Satellite Geometry

The measure of the contribution of the satellite positions to the accuracy of the solution is known as the geometrical dilution of precision (GDOP) and is made up of the square root of the trace of the covariance matrix of the position parameters being solved for [Wells et al., 1986]. The covariance matrix $C_{\hat{x}}$ of the unknowns $\hat{x}$ is a statistical measure of the accuracy of the estimates of the unknowns [Vaníček and Krakiwsky, 1988] and is a result of the least squares solution technique that will be described in the next section. The covariance matrix is in part a function of the first derivative of the observation equations which is made up of the direction cosines of the satellites with respect to the receiver as well as other elements. Research into the reliability of $C_{\hat{x}}$ as statistical indicator of GPS position accuracy has shown it to be overly optimistic due to the presence of unmodelled errors (see section 3.3.3) and correlations in the observations [Wells and Kleusberg, 1989].

Investigation of the formulation of the GDOP shows that it is inversely proportional to the volume of the special tetrahedron formed by the tips of the unit vectors reaching from the receiver to the four satellites in the unique solution scenario [Mertikas, 1983]. From the preceding discussion it may be concluded that the overall effect of the errors in the GPS measurements is governed by the "geometry" of the satellites involved.

3.3.7 Selective Availability

Selective availability (S/A) is the US Department of Defense policy of intentionally degrading the GPS satellite signals and orbital information such that the accuracy of an absolute position is limited to 100 metres [Jones, 1989]. The intentional degradation is in the form of satellite clock dithering and alterations of the broadcast ephemeris [Wells and

Kleusberg, 1989]. Signal differencing will reduce the effect of both S/A strategies but more research is needed to understand the full implications of the S/A policy [Wells and Kleusberg, 1989].

3.4   Differencing

Operation of GPS in differential mode allows the linear combination of GPS observations which can be an effective technique for eliminating or at least reducing common biases. Biases which are affected by the different levels of differencing are the satellite clock bias, the receiver clock bias, the orbit bias and to some extent the atmospheric propagation bias. The basic linear combinations of observations which are useful are differences between satellites, between receivers and between epochs. Each of these combinations reduces a particular bias. This technique can be carried even further where it is possible to produce linear combinations of the basic linear combinations such that double differences come from differencing single differences and triple differences come from differencing double differences. There are three possible combinations of double differences depending on the requirements: between satellites and between receivers; between satellites and between epochs; and between receivers and between epochs.

In this thesis, double and triple differences are used in the processing of the GPS data and they are described below along with the biases they reduce. The convention adopted from Wells et al. [1986] is to use the uppercase delta (Δ) and nabla (∇) symbols to refer to between receiver and between satellite differences respectively. The lower case delta δ is used to represent differences between epochs.

3.4.1 Receiver–Satellite Double Differences ($\nabla\Delta$)

Double differences are formed by differencing observations taken at the same epoch first between satellites and a common receiver and then between resulting differences having the same satellite pair and different receivers. This results in the following equation for double difference pseudo-range observations derived from equation 3.1:

$$\nabla\Delta P(t) = \nabla\Delta\rho(t) + \nabla\Delta d_{ion}(t) + \nabla\Delta d_{trop}(t) + \nabla\Delta\varepsilon(t), \tag{3.4}$$

and for double difference carrier-phase observations derived from equation 3.3:

$$\nabla\Delta\Phi(t) = \nabla\Delta\rho(t) + \lambda\cdot\nabla\Delta N - \nabla\Delta d_{ion}(t) + \nabla\Delta d_{trop}(t) + \nabla\Delta\varepsilon(t). \tag{3.5}$$

where:

$\Phi(t)$ —   carrier-phase observation in distance units ($= \lambda\cdot\phi(t)$)

Comparing equations 3.1 and 3.3 with equations 3.4 and 3.5, it can be seen that both the satellite and receiver clock biases have been eliminated. As well, under the assumption that the two receivers are close enough together for the atmospheric effects to be highly correlated, it can be assumed that the double difference equations greatly reduce the effect of the atmospheric biases. This is true more so for the ionospheric effect than it is for the tropospheric effect which is a more local phenomenon and not well correlated with surface conditions [Wells et al., 1986].

3.4.2 Triple Differences ($\delta\nabla\Delta$)

Triple differences are now formed by differencing the double difference observations having the same satellite and receiver pairs and occurring in adjacent epochs. In this

instance the formulation is really only effective for carrier-phase observations and therefore only that form is given below:

$$\delta\nabla\Delta\Phi = \delta\nabla\Delta\rho - \delta\nabla\Delta d_{ion} + \delta\nabla\Delta d_{trop}. \qquad (3.6)$$

The integer ambiguity N which is still a part of the previous relevant equations is no longer represented in equation 3.6. It should be clear that by performing triple differencing, it is possible to either eliminate or greatly reduce the effect of the satellite and receiver clock biases, the orbital biases, the atmospheric biases and the integer ambiguity unknown.

3.5   Precise Vertical Motion with GPS

The technique for solving for the vertical motion of the GPS antenna combines both the pseudo-range observable and the carrier-phase observable. The pseudo-range supplies initial estimates of position whereas the carrier-phase supplies the precision of the estimate of change in position. The change of position estimate is transformed to a change of height estimate with respect to the ellipsoid. Transformation of the changes in height with respect to ellipsoid to heave estimates with respect to the geoid is performed via high pass filtering.

3.5.1 Characterization of the Problem

Much research has been done recently to achieve kinematic GPS positions accurate at the centimetre level, examples of which can be found in Remondi [1988], Wells and Kleusberg [1989], and Seeber and Wübbena [1989]. However, all the work is predicated upon the knowledge of the integer ambiguities in the carrier-phase observations. For this reason, much research has been directed towards solving for the integer ambiguities using various techniques such as in Hatch [1989] and Seeber and Wübbena [1989]. This field of

research and application promises to reveal startling results and indeed has already done so. However, there are some limitations, especially when viewed with respect to the problems being solved in this thesis.

In particular, the problem of ambiguity resolution is greatly affected by such factors as distance between receivers, signal noise, geometry and the number of visible satellites. In some cases, these factors can affect the results enough to make ambiguity resolution impossible [Abidin, 1989,1990]. Using an estimate of the integer ambiguities has the inherent risk of distorting the results by such a degree as to make them unusable. In the case of heave determination, the solution must be to develop a technique that does not rely on these estimates but is still accurate enough to produce usable results.

This can be done through solving for the change in position of the antenna from epoch to epoch. The technique for solving for and using this information requires developing a model for the change in position and dealing with the lack of vertical datum information. This model and the assumptions used are given in the following sections.

3.5.2 Observation Equation

The mathematical model for the change in position based on the change in phase between epochs is based on the observation equation 3.2. However, the change in position or δX is not explicit in equation 3.2 and must be derived. One technique is to alter the observation equation to include the parameter δX. This can be done by differentiating the observation equation with respect to time and then re-integrating over the time difference between two adjacent epochs. The result is an observation equation giving the change in phase as a function of the change in position.

The phase velocity can be derived from equation 3.4 by taking the time derivative:

$$\frac{\partial \nabla \Delta \Phi}{\partial t} = \frac{\partial}{\partial t} \left[\nabla \Delta \rho(t) + \lambda \cdot \nabla \Delta N - \nabla \Delta d_{ion}(t) + \nabla \Delta d_{trop}(t) \right]$$

$$= \frac{\partial}{\partial t} \left(\nabla \Delta \rho(t) \right) + \frac{\partial}{\partial t} \left(\lambda \cdot \nabla \Delta N \right) - \frac{\partial}{\partial t} \left(\nabla \Delta d_{ion}(t) \right) + \frac{\partial}{\partial t} \left(\nabla \Delta d_{trop}(t) \right), \qquad (3.7)$$

assuming that the double difference ambiguity is a constant and that the atmospheric corrections are negligible one is left with:

$$\frac{\partial \nabla \Delta \Phi}{\partial t} = \frac{\partial}{\partial t} \left(\nabla \Delta \rho(t) \right). \qquad (3.8)$$

Using the Chain Rule for differentiation, equation for $\rho(t)$ given in equation 3.1 and assuming that the double difference observation is between receivers i, j and satellites k, l results in:

$$\frac{\partial \nabla \Delta \Phi}{\partial t} = \frac{\partial}{\partial X_i} \left(\nabla \Delta \rho(t) \right) \cdot \frac{\partial X_i}{\partial t} + \frac{\partial}{\partial X_j} \left(\nabla \Delta \rho(t) \right) \cdot \frac{\partial X_j}{\partial t}$$

$$+ \frac{\partial}{\partial x^k} \left(\nabla \Delta \rho(t) \right) \cdot \frac{\partial x^k}{\partial t} + \frac{\partial}{\partial x^l} \left(\nabla \Delta \rho(t) \right) \cdot \frac{\partial x^l}{\partial t} \qquad (3.9)$$

where:

X_i, X_j —   Receiver coordinate vectors

x^k, x^l —   Satellite coordinate vectors

Given that receiver **i** is the stationary receiver, then the differentiation of X_i with respect to time equals zero. This new observation equation on its own is of limited usefulness since instantaneous phase velocity is not an observable. However, if we linearize the problem by assuming that the contributions of phase acceleration over a short time period is quite small [Peyton, 1990], then it is possible to re-integrate equation 3.9 over the period spanning two adjacent epochs. The result is an observation equation that is a linear function of δX_j.

$$\int_{t_1}^{t_2} \frac{\partial \nabla \Delta \Phi}{\partial t} \, dt \approx \delta \nabla \Delta \Phi$$

$$\approx \frac{\partial}{\partial X_j}\left(\nabla\Delta\rho(t_{12})\right)\cdot\delta X_j + \frac{\partial}{\partial x^k}\left(\nabla\Delta\rho(t_{12})\right)\cdot\delta x^k + \frac{\partial}{\partial x^l}\left(\nabla\Delta\rho(t_{12})\right)\cdot\delta x^l \quad (3.10)$$

where:

$$t_{12} \quad - \quad \frac{(t_1 + t_2)}{2}$$

At this point there are a number of possibilities when it comes to solving for δX_j. For example, using measurements from four satellites results in three double difference observation equations similar to equation 3.10. A unique solution can be obtained from these three equations and three unknowns; i.e. δX_j, by solving for them as a set of simultaneous equations. This technique is efficient but does not allow for the over determined case nor does it give useful statistical information about the solution. In this thesis, the least squares technique is used to solve for the changes in position from epoch to epoch, based on the observation equation 3.10.

3.5.3 Mathematical Model

The least squares technique described by Wells and Krakiwsky [1971] and Mikhail [1976] is based on a generalized mathematical model for the combined method:

$$F(x,l) = 0 \quad\quad (3.11)$$

where:

x   –   Vector of unknown parameters

l   –   Vector of observations

For the purposes of the least squares technique, equation 3.11 is linearized using Taylor's series expansion, about an initial point x^o, and limited to the first two terms in the series. Linearization gives:

$$F(x,l) = F(x^o,l) + \frac{\partial F}{\partial x}\bigg|_{x^o,\,l}(x\text{-}x^o) + \frac{\partial F}{\partial l}\bigg|_{x^o,\,l}(v) = 0$$

or

$$w + A\delta + Bv = 0 \qquad (3.12)$$

where:

w   –   Misclosure vector

A   –   First design matrix

B   –   Second design matrix

v   –   Vector of residuals

δ –   Vector of corrections to the initial estimates of the unknowns $(x-x^o)$

In the situation of solving for changes in position using the observation equation 3.10 above, it is clear that the unknown parameters are the changes in the coordinates of receiver j and the known parameters the satellite coordinates and the coordinates of receiver i with the associated covariance information.

3.5.4 Normal Equations

Given the mathematical model in equation 3.12, the least squares technique applies the additional criterion that the sum of the squares of the weighted residuals be a minimum i.e.:

$$\hat{v}^T P \hat{v} = \text{minimum.} \qquad (3.13)$$

where:

$\hat{v}^T$ –   The transpose of the least squares estimate of the observation residual vector

P   –   The inverse of the covariance matrix C_l of the observables (also known as the observation weight matrix)

The Lagrange technique can be used to solve this extremum problem, the details of which can be found in Wells and Krakiwsky [1971]. The solution of this problem, called the normal equations, can be expressed in a hypermatrix form:

$$\begin{bmatrix} \mathbf{P} & \mathbf{B}^T & \mathbf{0} \\ \mathbf{B} & \mathbf{0} & \mathbf{A} \\ \mathbf{0} & \mathbf{A}^T & \mathbf{0} \end{bmatrix} \cdot \begin{bmatrix} \hat{\mathbf{v}} \\ \hat{\mathbf{k}} \\ \hat{\boldsymbol{\delta}} \end{bmatrix} + \begin{bmatrix} \mathbf{0} \\ \mathbf{w} \\ \mathbf{0} \end{bmatrix} = \mathbf{0} \tag{3.14}$$

where:

$\hat{\mathbf{k}}$ –   the least squares estimate of the vector of Lagrange multipliers.

The normal equations can be reduced to solve explicitly for the unknowns by partitioning the hypermatrix and eliminating $\hat{\mathbf{k}}$ so that:

$$\hat{\boldsymbol{\delta}} = -\left(\mathbf{A}^T(\mathbf{B}\mathbf{P}^{-1}\mathbf{B}^T)^{-1}\mathbf{A}\right)^{-1} \cdot \mathbf{A}^T(\mathbf{B}\mathbf{P}^{-1}\mathbf{B}^T)^{-1}\mathbf{w} \tag{3.15}$$

The covariance information can be derived by using the propagation of covariance, equation 3.15 and information from equation 3.13. To begin:

$$\mathbf{w} = F(\mathbf{x}^o, \mathbf{l})$$

from equation 3.11. Using the covariance law:

$$\mathbf{C}_w = \mathbf{J}_w \mathbf{C}_l \mathbf{J}_w^T$$

where:

$\mathbf{C}_w$ –   Covariance matrix of the misclosure vector $\mathbf{w}$.

$\mathbf{J}_w$ –   The Jacobian matrix of the misclosure vector $\mathbf{w}$.

$$\mathbf{J}_w = \left.\frac{\partial F}{\partial \mathbf{l}}\right|_{\mathbf{x}^o, \mathbf{l}} = \mathbf{B} \implies \mathbf{C}_w = \mathbf{B}\mathbf{C}_l\mathbf{B}^T$$

Following the same procedure for equation 3.15 we find:

$$C_{\hat{\delta}} = J_{\hat{\delta}} C_w J_{\hat{\delta}}^T,$$

where:

$J_{\hat{\delta}}$ -   The Jacobian matrix of the correction vector $\hat{\delta}$ with respect to w

Substituting and cancelling appropriately results in:

$$C_{\hat{\delta}} = \left(A^T (B C_l B^T)^{-1} A \right)^{-1}. \tag{3.16}$$

Equations 3.15 and 3.16 are the result of linearization of a non-linear observation equation. For this reason, it is necessary to iterate both equations by setting:

$$x_i^o = x_{i-1}^o + \hat{\delta}_{i-1} \tag{3.17}$$

and reintroducing equation 3.17 into equation 3.12 until the magnitude of the elements of $\hat{\delta}$ fall below some realistic threshold level.

3.5.5 Coordinate Transformations

The coordinate transformations are based on transforming cartesian coordinates to curvilinear coordinates (ellipsoidal geographic) and back again. The transformations follow set mapping theory such that: $T : R^3 \rightarrow R^3$, $S : R^3 \rightarrow R^3$ and $T^{-1} = S$ where T and S are mapping functions and adhere to the Inverse Transformation Theorem [Hurley, 1980].

3.5.5.1   PLH to XYZ

The transformation from ellipsoidal coordinates to cartesian coordinates is straight forward and direct. The following equations and symbol definitions can be found in Vaníček and Krakiwsky [1988].

$$r = T(u)$$

$$= \begin{bmatrix} x \\ y \\ z \end{bmatrix} = \begin{bmatrix} (N+h)\ \cos\phi\ \cos\lambda \\ (N+h)\ \cos\phi\ \sin\lambda \\ (Nb^2/a^2+h)\ \sin\phi \end{bmatrix} \qquad (3.18)$$

given:

$$N = \frac{a^2}{(a^2\cos^2\phi + b^2\sin^2\phi)^{1/2}} \qquad (3.19)$$

where:

T	—	transformation function;
r	—	position vector (x,y,z);
u	—	vector of ellipsoidal coordinates (ϕ,λ,h);
N	—	prime vertical radius of curvature;
a,b	—	semi-major, semi-minor axis of the reference ellipsoid.

3.5.5.2   XYZ to PLH

The inverse transformation from cartesian to ellipsoidal coordinates is not straight forward but there are two possible approaches: the first is an iterative solution; the second is a direct solution. The iterative solution is given here whereas the direct solution may be found in Vaníček and Krakiwsky [1988]. Beginning with the two initial approximations:

$$N_o = a,$$

$$h_o = \sqrt{x^2 + y^2 + z^2} - a$$

then iterate:

$$\phi_{i+1} = \tan^{-1}\left\{ \frac{z}{p} \cdot \frac{1}{\left(1 - \frac{e^2 N_i}{N_i + h_i}\right)} \right\} \qquad (3.20)$$

where:

$$p = (N+h)\cos\phi = (x^2 + y^2)^{1/2} \tag{3.21}$$

$$h_i = \frac{p}{\cos\phi_i} - N_i \tag{3.22}$$

and N is as in equation 3.19.

ϕ_i is solved for using equation 3.20, then N and h are updated using equations 3.19 and 3.22 and the cycle repeated. Once $(\phi_{i+1} - \phi_i)$ is less than some practical threshold limit, λ can be solved for directly using:

$$\lambda = \tan^{-1}\left(\frac{y}{x}\right) \tag{3.23}$$

from equation 3.18.

3.5.5.3 Error Propagation

The transformation of the covariance matrix follows the propagation of variances as described in section 3.5.4 and the theory of transformations [Hurley, 1980]. The Jacobian matrix of transformation is developed from equation 3.18.

$$\mathbf{J_T(u)} = \begin{bmatrix} -(M+h)\sin\phi\cos\lambda & -(N+h)\cos\phi\sin\lambda & \cos\phi\cos\lambda \\ -(M+h)\sin\phi\sin\lambda & (N+h)\cos\phi\cos\lambda & \cos\phi\sin\lambda \\ (M+h)\cos\phi & 0 & \sin\phi \end{bmatrix} \tag{3.24}$$

$$M = \frac{a(1-e^2)}{(1-e^2\sin^2\phi)^{3/2}} \tag{3.25}$$

where:

M   — meridional radius of curvature;

e   — eccentricity of the ellipsoid.

With the exception of the singularity at the poles, the determinant of $\mathbf{J_T}$ is unequal to zero and therefore $\mathbf{J_T}$ has an inverse. Using the theorem of inverse transformations then [Hurley, 1980]:

$$J_S(r) = J_T(u)^{-1}$$

$$= \begin{bmatrix} -\sin\phi\cos\lambda/(M+h) & -\sin\phi\sin\lambda/(M+h) & \cos\phi/(M+h) \\ -\sin\lambda/[(N+h)\cos\phi] & \cos\lambda/[(N+h)\cos\phi] & 0 \\ \cos\phi\cos\lambda & \cos\phi\sin\lambda & \sin\phi \end{bmatrix} \qquad (3.26)$$

therefore by the covariance law;

$$C_u = J_S(r) \cdot C_x \cdot J_S(r)^T \qquad (3.27)$$

3.5.6 Heave from GPS Measurements

After the changes in position from epoch to epoch have been transformed from a cartesian coordinate system to an ellipsoidal coordinate system, the changes in height can be extracted. The essential requirement then is to estimate the vertical position of the point of interest at each epoch and to establish an appropriate datum. It should be clear that these changes in height must be integrated to represent the actual vertical movement of the antenna. The data is in the form of discrete data and so must be treated as a summation:

$$H(t_n) = \sum_{i=1}^{n} \Delta H_{ti} + C_H \qquad (3.28)$$

where:

$H(t_n)$ —   The height of the antenna at time t which is the nth epoch

ΔH_{ti} —   The individual changes in height that have been determined

C_H —   A constant offset that is, by definition of the problem and solution, unknown and is a function of the position of the point at the time of the first epoch of measurement.

    Essentially this process can be considered a running summation of the changes in height to produce a running estimation of the vertical position of the point.

3.5.6.1   Datum Establishment

Movement of the GPS antenna can be characterized by horizontal movement in the X and Y direction and vertical movement in the Z direction with respect to the local equilibrium coordinate system. In order to measure the departure of the ships antenna from the equilibrium position using GPS, not only must the epoch by epoch position of the antenna be monitored, but the epoch by epoch position of the equilibrium position of the antenna as well. It is this last requirement that poses the most difficulties in estimating GPS heave.

For the purpose of estimating vessel pitch and roll, a single GPS antenna is of little value when seeking the horizontal equilibrium position of the antenna. The epoch by epoch equilibrium position of the antenna is constantly changing and is a function of the overall ship direction and speed. Various filtering or averaging techniques are possible, but would depend heavily on the equilibrium position changing smoothly and regularly. Instead, pitch and roll may be quite adequately modelled using various and relatively inexpensive inclinometer devices.

The vertical equilibrium point of the antenna on the other hand is much more restricted in the nature of its motion. The vertical equilibrium point is forced to follow the mean water level in so far as the buoyancy specifications of the vessel and the sea conditions do not alter. This is a much more stringent restriction than that of the horizontal equilibrium point and may be put to advantage in forcing the definition for the vertical datum.

The above discussion leads to one of the major underlying assumptions of this thesis: the short term average of the GPS heave signal (over a few minutes) should closely follow the mean water level and have a nearly zero slope — any departure from this assumption can be construed as a bias and be removed.

3.5.6.2   Residual Heave Signal

Once the vertical motion signal has been extracted and the datum established and applied, the true vertical heave can be determined by noting the departure of the vertical signal from the estimated datum. This residual signal is the vertical motion of the antenna. It should be noted that the heave experienced at the antenna is the composite of all rotational motions of the ship as well as the translational heave motion. Translating the residual heave signal from the antenna to the point of interest is accomplished using the transformations outlined in section 2.4.1.

3.5.7 Test Results (Static Data)

A necessary precursor to using the above technique is to test the algorithm on a data set where a predictable result can be anticipated. This can be accomplished either through using control measurements with another independent system or by restricting the conditions under which the measurements take place. A most effective method for initial testing of kinematic algorithms such as that being used in this thesis is to use static baseline data.

Static baseline data has the benefit of giving predictable results using real measurements and allowing some realistic assessment of achievable accuracy and potential errors. A static baseline should, by definition, yield results that show zero heave movement. Any departures from this zero hypothesis will be induced by measurement noise, measurement errors such as those described in section 3.3.3 and model errors.

The baseline data chosen for this initial testing is from a 1986 observation campaign undertaken jointly by Canada and the US and covering an area of south-west Vancouver

Island and north-west Washington State [Kleusberg and Wanninger, 1987]. The two

stations were Race Rocks (RR) in Canada and Tucker (TU) in the U.S. The measurements

were performed using Texas Instruments 4100 GPS receivers at a 15 second data rate,

spanning just under one hour. The final results give a baseline of 20103.08 metres.

This data was processed using the GPS height determination technique described in

sections 3.5.1 – 3.5.5. As can be seen from the results in Figure 3.1, the departures of the

height signal from a zero mean reach ± 5 centimetres at individual times during the one

hour recording session but the overall trend is flat as is to be expected from static data.
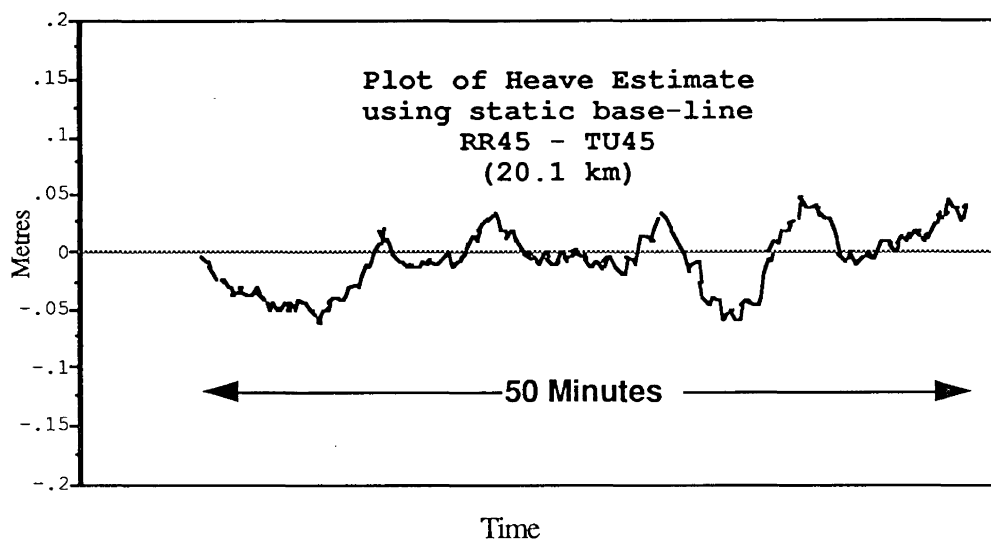
Time

Figure 3.1 – Static Base-line Test

The conclusion to be reached from the results of this initial test is that with TI 4100

data, the technique is capable of producing results with an accuracy of better than 5

centimetres over a baseline of some 20 kilometres. Based on this conclusion, an

assessment of the potential accuracy of the technique under conditions of longer baselines

and different dynamics can be extrapolated.

3.6 Chapter Summary

This chapter discussed the role GPS plays in determining changes in height from epoch to epoch. The discussion was prefaced by a description of GPS and an overview of the observations possible using the system. The relative contributions of the systematic and random biases and errors along with some techniques to reduce or eliminate these problems was presented. The mathematical formulation of the problem, the solution and error propagation was described complete with relevant coordinate transformations. The chapter was concluded with the results of a static baseline test of the algorithm that indicated the technique is capable of accuracies equal to or better than five centimetres.

CHAPTER FOUR
FIELD DATA

This chapter deals with the collection and processing of field data during the 1988 cruise aboard the CSS Hudson [Hudson, 1988]. This data was used to confirm the experimental theory and to gain experience with some of the conditions and problems encountered at sea. The chapter begins with a brief description of the data collection process and the equipment used. The subsequent sections deal with measurements obtained from GPS, the accelerometer based heave sensors and the pitch and roll sensor.

4.1 Equipment Used

Two dual frequency P-code TI4100 GPS receivers were provided by the Geophysics Division of the Geological Survey of Canada (GSC), each having a maximum data update rate of 1.2 seconds. Three heave sensor systems were used; two TSS Model 320 Heave Compensators were supplied by Technical Survey Services Ltd. of England, one of which was loaned free of charge, and one Datawell HIPPY 120b Heave Sensor was provided by the Canadian Hydrographic Service Québec regional office. Each of these heave sensor packages has accuracy specifications and data rates of five centimetres or better and five hertz or better respectively.

4.2 GPS Antenna Installation

TI4100 GPS receivers are composed of a signal processor, a data archiving device and an antenna connected to the processor unit via a 100 foot coaxial cable. The siting of the antenna is critical in reducing measurement biases and errors described in Chapter Three whereas the location of the signal processor unit and the data archiving box can be decided

by convenience alone. The location of the satellite receiver antenna, both on board the CSS Hudson and at the Shelburne, N.S. shore station, was dictated by the requirement of full visibility and the reduction of multipath and imaging. The latter was accomplished by siting the antenna as much as was possible, away from electrically reflective surfaces and conductive objects.

Aboard the CSS Hudson, the highest point on the ship, the mast head, was chosen for the antenna site. The disadvantage of this site is that the mast head undergoes accelerations due to roll and pitch that are in general much more exaggerated than those experienced at other points on the vessel. The top of the navigation mast aboard the CSS Hudson is approximately twenty metres above and ten metres aft of the forward laboratory.

At the Shelburne, N.S. shore site, roughly 100 kilometres from the expected location of the ship, the receiver was located on the premises of a Department of the Environment (DOE) weather station. A suitable site was found for the antenna and the receiver was located in the shelter of the DOE offices and was manned by personnel from the GSC.
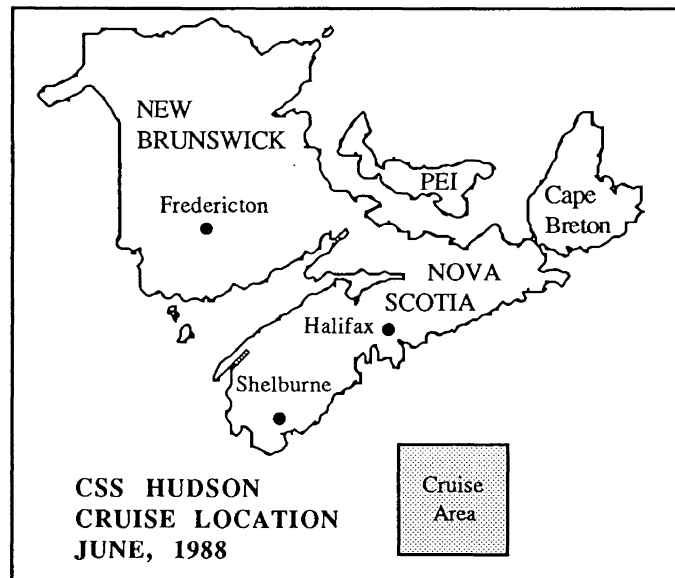

NEW BRUNSWICK

Fredericton

PEI

Cape Breton

NOVA SCOTIA

Halifax

Shelburne

CSS HUDSON
CRUISE LOCATION
JUNE, 1988

Cruise Area

Figure 4.1 – Cruise Location

4.3 Heave Sensor Installation

The location of a heave sensor will affect the character of the heave signal as well as the accuracy of that signal. Important considerations when siting the heave sensors are the vertical accelerations experienced—which they are designed to respond to, and the rotational accelerations. Very large vertical accelerations can exceed the sensor specifications and contaminate the resulting heave signal. The effects of rotational accelerations are filtered to some degree, but the larger the magnitude, the larger the residual error. The effect of excessive vertical accelerations and rotational accelerations can be minimized by locating the sensor along the roll axis of the vessel and preferably on the pitch axis as well.

The three heave sensors were positioned in two locations on board CSS Hudson; the Datawell Hippy 120b and one TSS Model 320 sensors in the forward weather deck laboratory, and the second TSS Model 320 sensor in the central gravity laboratory (see Figure A.1). The two sensors in the forward lab were separated by approximately three metres in the x direction and 1 metre in the z direction. The forward lab is approximately 25 metres forward of and five metres above the gravity laboratory which is the nominal centre of gravity for the vessel. Vertical motions measured by the two forward sensors are greater in magnitude than those measured in the gravity laboratory and include a component due to rotation of the vessel about the pitch and roll axis. This location was chosen due to the physical constraints imposed by the size and weight of the HIPPY 120b and had the advantage of being physically closer to the GPS antenna.

4.4 Data Logging

Data from both heave sensors were logged on a single IBM compatible micro-computer connected using standard cabling and connectors. Data collection from the HIPPY 120b required an analog-to-digital (AtoD) conversion board in the computer, whereas the TSS Model 320 sensors required a standard RS 232 serial communications port.

The logging program, written in BASIC programming language, used a one pulse per second signal taken from the TI4100 GPS receiver to trigger a data collection loop from both the TSS Model 320 heave sensors and the AtoD board. The data was time tagged using the computer clock and stored in American Standard Code for Information Interchange (ASCII) format on a 20+20 megabyte floppy disk drive.

Data from the GPS receiver was recorded using a data collection program written by personnel of the Geophysics Division of the GSC [Beach, 1988]. The program was written in PASCAL for an IBM compatible 386 computer with a Bernoulli 20+20 Megabyte floppy disk drive system. Communications interrupts were used to signal the presence of data at the communication port which was decoded and stored on the Bernoulli floppy disk drive system. Each data record was time tagged using GPS time as tracked by the receiver.

The two logging system clocks were synchronized using the one PPS signal from the GPS receiver and the current GPS time from the receiver display unit. The current time from the receiver, advanced by roughly 30 seconds, was keyed into the computer and an interrogation loop started. When the time displayed on the GPS control display unit was just short of the keyed in time, the computer was manually instructed to reset the clock and start timing at the very next PPS signal from the receiver. This method worked adequately

in the majority of cases resulting in signals from the external sensors and the GPS receiver begin synchronized within one integer second of each other. Any mis-synchronization of an integer second was subsequently easy to recognize and correct during post processing.

4.5   Data Archiving

Recording rates of once every 1.2 seconds for the GPS observations and once every 1 second for the heave and accelerometer observations meant a data collection rate of 2.1 megabytes per hour. This data was initially stored on 20 megabyte Bernoulli disks. All GPS observations were recorded in binary file structure and all heave observations were recorded in ASCII file structure.
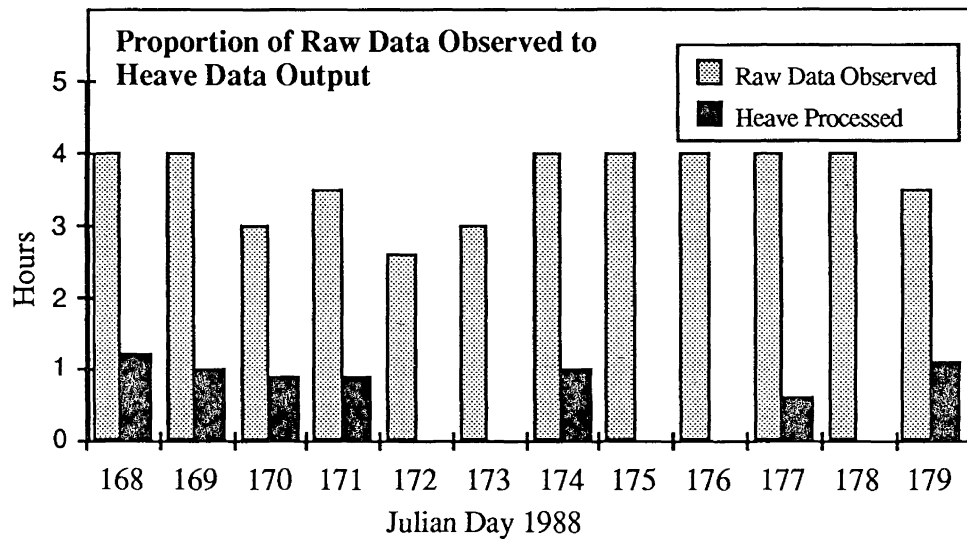
Figure 4.2 – Raw vs. Processed Data

Over 100 Macintosh formatted disks were required to complete the transfer of the data from the Bernoulli disk using standard data communications software. A summary of the proportion of raw data collected during the cruise vs. the amount of data finally processed for heave is presented in Figure 4.2. This figure illustrates the amount of data lost to all the various problems as described in this chapter.

4.6   Problems and Solutions

The quality of the data set collected was compromised by a number of factors and events that occurred during the 1988 CSS Hudson cruise. The problems encountered resulted from a combination of inadequate preparation and unpredictable events. To help the reader understand the character of the data and the final processing results, the following subsections briefly describe some of the problems as well as the efforts to correct them.

4.6.1 Bad Ephemeris Data

Collection of ephemeris data during the observation periods was intermittent and unreliable. This was postulated to be caused by both the receiver and independent logging software. The ephemeris data recorded during the observation session was generally corrupted and unusable. The cause of the corrupted data is unknown and the logging software is the main suspect. The fault could not be corrected during the cruise and it was necessary to obtain replacement ephemerides from the Geodetic Survey of Canada and precise ephemeris information for the same period of time from the U.S. National Geodetic Survey (USNGS). This set of broadcast ephemeris also contained corrupted data and was finally replaced with precise ephemerides supplied by the USNGS. Final processing was performed using the precise ephemeris as described by Remondi [1986].

4.6.2 Mismatching Time Tags

Texas Instruments Navigator software was used to operate the TI4100 GPS receiver at the maximum 1.2 second data rate. The version of the software used did not establish a common reference timing sequence with which to initiate the data collection loop and the result was that the observations did not occur simultaneously at the two receiver stations,

being shifted with respect to each other by some random fraction of 1.2 seconds. This problem did not arise with the other data rates and is likely an oversight in that version of the software.

Interpolation of the carrier phase observations using a polynomial fitting technique was necessary to achieve simultaneous observations required for the differencing technique. The process was implemented by fitting a low degree polynomial to the carrier-phase data from the shore based station. This function was then used to interpolate a value for the relevant epoch observed on board the ship. This same technique applied to pseudo-range observations was less successful due to high signal noise.

4.6.3 Equipment Failure

Various events and malfunctions occurred affecting the collection and quality of the data.

- On board the CSS Hudson, a power supply used to operate the TI4100 did not function properly, thereby draining the internal battery and causing data loss. This problem was not correctly diagnosed until day 173 and was finally redressed by replacing the faulty piece of equipment.

- The independent pitch and roll sensor designated as the primary attitude sensor was accidentally dropped and rendered inoperable during installation; back up information came from the Hippy heave compensator package which has its own built-in attitude sensor.

- On shore, the GPS antenna suffered a direct hit by lightning. The current generated along the antenna cable was sufficient to destroy the receiver and observations were suspended during days 175 and 176 until a replacement was delivered from Ottawa.

4.6.4 Inconsistent Data Logging

The problems with data logging constituted one of the more frustrating aspects of the data set. Again, it is not clear if it was the receiver software or the logging program which could not keep up with the high data rate but the result was frequent data gaps. The data gaps are inconsistent in nature and cannot be attributed to a particular channel or satellite. Although the nominal data rate was 1.2 seconds, the effective data rate when averaging over a long term was approximately 2 seconds. This data rate is close to the limiting sampling rate as dictated by the period of the actual heave signal. However, the random nature of the data gaps alleviates somewhat the danger of aliasing the signal.

4.6.5 Master Station Position

An accurate position of the master station in Shelburne, Nova Scotia was never obtained. Estimates were made using single station pseudo-range observations, however due to signal biases and errors these estimates are not better than ± 25 metres. This poor position estimate for the Shelburne station will introduce a slowly changing bias (in the order of a metre) into the heave estimates as a function of the satellite constellation geometry and the baseline length [Santerre, 1989]. The heave algorithm developed for this thesis is not affected by this type of bias because of the bias removal inherent in the datum determinations. However, if required, it may be analyzed using covariance propagation as developed in Section 3.5.5.3.

4.7   Data Quality Indicators

Typically when discussing the quality of GPS data from a static baseline or a tightly controlled kinematic survey, one looks at the residuals of the signals when compared

against a nominal signal constructed using the calculated position solution. This type of analysis is inappropriate in the context of a loosely controlled dynamic data set as in this thesis, because of the lack of redundant data. There are other less refined criteria by which the quality of GPS observations may be judged, independent of a position solution. These include looking at:

- range differences [Vaníček, 1985];

- ionospheric delay measurements [Vaníček, 1985];

- signal to noise ratios;

- velocity measurements [Garmulewicz, 1989];

It should be stressed that these are qualitative rather than quantitative indicators. Range differences are the separation between the satellite to receiver distance as measured by the pseudo-range signal and the carrier-phase signal. A smooth and continuous divergence of the two ranges is caused by ionospheric delays but a sharply discontinuous difference indicates the presence of a cycle-slip or other error.

Range differences:

$$RD_{L1}(t_i) = [P_{L1}(t_i) - P_{L1}(t_o)] - [\phi_{L1}(t_i) - \phi_{L1}(t_o)] \lambda_{L1} \qquad (4.1)$$

where:

RD   —   Range Difference

P   —   Pseudo-range measurement in distance units

$\phi_{L1}, f_1, f_2, \lambda_1$ —   as described in Chapter Three.

The ionospheric delay is a measure of the dispersive effect of the ionosphere on the GPS signal at the two different carrier frequencies. The absolute value of the ionospheric delay can be replaced with a relative value in this particular case and therefore the integer ambiguities need not be known. As with the range differences the magnitude of the relative

ionospheric delay should change slowly and smoothly, any sudden divergence or discontinuity indicates a cycle-slip or error.

Ionospheric delay:

$$\text{IonDel}_{L1}(t_i) = \frac{(f_2^2 - f_1^2)}{f_2^2} [\phi_{L1}(t_i) - \phi_{L2}(t_i) \frac{f_1}{f_2}] \qquad (4.2)$$

where:

IonDel_{L1} —   Ionospheric Delay;

ϕ_{L1} —   as described in Chapter Three;

f_1, f_2, λ_1 —   as described in Chapter Three.

The signal-to-noise ratio (S/N) is an internal receiver parameter which is a measure of the ratio of the intensity of the signal being received with the intensity of the noise at that signal frequency. A low S/N indicates that the reliability of the data may be in question. The S/N is not available on all receiver models but is a component of the TI 4100 measurement record. Phase velocity measurements are available on a TI 4100 receiver in the form of the phase difference measured over a 160 ms time period. This measurement is quite noisy and useful only as a crude quality indicator [Garmulewicz, 1989].

In the case of data obtained for this thesis, the constantly changing position and attitude of the ship imposed constraints on the assessment of data quality. The GPS data was initially filtered to exclude data with very low signal-to-noise ratios and those measurements with obvious time tagging errors. Secondary processing analyzed the change in range differences between the pseudo-range and carrier phase signals, as well as the ionospheric delay using the L1 and L2 carrier phase signal.

4.8 Quality Assessment

The data cleaning procedure was aimed at eliminating corrupted data, recognizing and correcting spikes in the data, and recognizing and correcting cycle-slips in the carrier-phase signal. The range difference and ionospheric delay in equations 4.1 and 4.2 were used for quality assessment in this stage of the processing. These two signals are expected to change slowly and smoothly and where the signals exhibit a sudden change in character or become discontinuous, then it may be postulated that a data spike or a cycle-slip has occurred or the data is in some way corrupted. The data set collected for this thesis contained a significant number of data spikes and cycle-slips as well as periods of corrupted data.

A data spike occurs when the data exhibits two significant departures from the smoothly changing signal; one in either the positive or negative direction, and a second of equal magnitude in the opposite direction. The signal that contains a data spike exhibits this departure only for the epoch affected and thereafter behaves normally. Once a data spike is recognized, it must be eliminated. A cycle-slip on the other hand is a discontinuity in the measurement signal which is characterized by a jump or multiple jumps in either direction. Once a cycle-slip is detected, it can be corrected given the appropriate circumstances.

The dual frequency data available from the TI4100 presents the opportunity to examine the signal on both frequencies. When the signal is corrupted on one frequency or measurement type, the error can be corrected using the other frequency or data type. This type of data cleaning is generally a preliminary technique and suffers from the inability to effectively correct departures that occur simultaneously in both frequencies.

The procedure followed during this process located either the spike or cycle-slip by detecting a discontinuity in both the range difference and ionospheric delay signal. At that point a choice was presented according to the particular combination of discontinuities in either of the two signals and either the L1 or L2 frequency. When the spike or cycle-slip was uncorrectable, the data was eliminated or in the case of a cycle-slip, a new file was opened and the subsequent data was assumed to be part of an independent observing session.

The results from this cleaning and the subsequent output files were plotted. Sessions where enough cycle-slips occurred so as to make observation sequences less than ten minutes in duration were ignored. Visual appraisal of the graphical output from this cleaning process indicates noise levels for pseudo-range measurements to be in the order of two to ten metres and for the carrier-phase from 1 to 5 cm.

Subsequent analysis of the results of further processing of the GPS data indicated that a few cycle-slips escaped proper detection and correction. These errant cycle-slips and data spikes were below the detection threshold of the techniques employed, typically two or three cycles, and their effects become apparent in the later stages of processing.

4.9   Heave Sensor Data

Data from the mechanical or accelerometer based heave sensors were collected to be used as control measurements with which to compare the GPS results. The factors which affect the nature and quality of the data are the sensor locations and the data collection technique. This section identifies biases in the data and evaluates the noise of the heave sensor signals.

4.9.1 Data Quality Flag

Data quality control can be carried out either while collecting the data or during post processing. In the case of heave sensors, pre-processing quality control is a function of monitoring parameters describing the sensor environment. While processing the data, it is possible to monitor the characteristics of the signal and use their behaviour to indicate the reliability of the data. In particular, the TSS Model 320 heave processor sets a quality flag indicating the suspect nature of the data when these descriptive parameters exceed the pre-defined constants. The HIPPY 120b heave sensor on the other hand does not have these capabilities and there are no indications if and when the heave signal becomes biased.

4.9.2 Biases and Errors

Heave compensators are designed to reduce the effects of horizontal or rotational accelerations through filtering and self-stabilizing sensor platforms. Where the motions experienced exceed the specifications of the sensor platform, biases and errors will be introduced into the resulting heave signal. Accelerations with a component acting in the horizontal direction will result in a misorientation of the sensor platform. The self-stabilizing system will act against this horizontal component unless the acceleration has a characteristic period close to the resonant frequency of the sensor platform. This is the case during vessel maneuvers, causing the heave signal to be invalid for a period of time and requiring a significant settling down time after the vessel makes a turn. This effect was apparent during vessel maneuvers and was most clearly evident in the roll signal from the Hippy 120b heave sensor.

4.9.3 Direct Comparisons

Direct comparisons between the two different models of heave sensors have been carried out in order to estimate the noise contribution of each sensor. Whereas these two sensors were not occupying exactly the same place, the locations were close enough to infer the composite noise in the two signals. A study of the relationship between the two heave sensors was performed in 1989 and the report is included in Appendix A of this thesis. The study indicated that the noise level or level of disagreement between the two sensors is a function of the magnitude of the heave signal itself. As well, any system dependent biases show up in the residual signal either in the form of increased residuals, phase dependencies or deviations from the zero mean.

4.9.4 Noise Levels

The noise in the heave signals from both GPS and independent sensors contribute to the magnitude of the residual signal. Using the residual signal alone, it is not possible to determine what percentage of the signal each sensor is responsible for. At best, based on the expected error specifications of the two instruments, a preliminary estimate of the percentage can be obtained. An error analysis performed on the data indicated that the TSS Model 320 exhibited a noise level some fifty percent greater than the HIPPY 120b (see Appendix A). A summary of the analysis of the residual signal between the two sensor is presented in Table 4.2 (also see Appendix A).

Table 4.1 – Error Summary

STATISTIC	DAY 174	DAY 175
Average Heave (approx)	± 0.5 m	± 1.5 m
Dominant Period (approx)	7 sec	9 sec
Residual Mean	2.7 cm	2.9 cm
Residual Std Dev.	4.8 cm	15.5 cm
Largest Differences	0.3 m	-0.7 m
Predicted RMS Error	2.1 cm	3.5 cm

4.9.5 Spectral Analysis

Spectral analysis of the heave signal from the two forward heave sensors has been performed to gain insight into the constituent frequency content of the signal. Two different days of data representing periods of both low and high dynamics were analyzed (see Appendix A). Of special interest was any low frequency contribution that could be present due to system bias.

This study concluded that, as expected, the majority of the spectral density was concentrated in frequency bands close to the mean heave period. Power spectrum density plots of the data series from the two heave sensors and the residual series indicated however, that some significant power existed in the lower frequencies. As both heave sensors should filter any low frequency signals, the results suggest that the internal processing and filtering were contaminating the measurements to some degree.

It appeared that, during periods of large motion, the TSS Model 320 introduced the majority of low frequency power whereas during periods of lesser motion, the HIPPY 120b introduced a dominant offset into the measurements. This offset appears to be a constant associated with the HIPPY 120b and falls within the specifications given for the

sensor. Further, the study indicated that a scale factor difference existed between the two sensors where the TSS Model 320 was producing a larger magnitude heave signal than the HIPPY 120b even though the two sensors were located nearly side by side. It was unclear which of the two sensors was responsible for this difference.

In summary, both sensors introduced a small low frequency bias into the heave signal. The HIPPY 120b introduced an offset during periods of low dynamics and the TSS Model 320 was responsible for biases during periods of high dynamics. As well, there existed a small scale factor difference between the two instruments [Rapatz, 1989].

4.10 Chapter Summary

This chapter described the procedure and circumstances under which the field data was collected and processed. The problems with the data set and the collection process was described along with their relationship to the overall data quality . Finally an assessment of the data quality was performed and a data collection summary presented.

CHAPTER FIVE
GPS HEAVE RESULTS & COMPARISONS

The final stage of this thesis investigation was the processing of the data collected at sea. The bulk of the processing effort went into transforming the GPS measurements into heave estimates. Once GPS derived heave estimates had been obtained for the antenna point, the remainder of the processing was necessary to provide direct comparisons between the GPS heave signal and the signals obtained from the accelerometer based heave sensors. Finally, an assessment of the residuals between the two systems was made to determine the success of the GPS heave determination technique.

5.1   Processing Organization

The processing was organized into modular operations to better manage the large quantity of data as well as allow greater flexibility when testing the algorithms. The order and details of the procedures used are given in the following subsections.

5.1.1 Interpolation and Differencing of GPS Measurements

The problem of non-concurrent GPS observations from both the shore station and the ship has already been mentioned in Section 4.6.2. Computing double difference data as described in Section 3.4.1 requires simultaneous measurements and therefore made it necessary to interpolate the signals. The signal from the shore station was chosen as the reference for the interpolation as it was expected to change smoothly without large variations.

A moving, ten epoch polynomial fit of degree two was chosen as the representative function to model the carrier-phase signal. The choice of the data window size and the degree of the polynomial was based on such factors as efficiency, speed and accuracy. Testing of the interpolation technique using shore station data showed that the interpolation accuracy was typically in the order of one centimetre and always less than three centimetres. Increasing the polynomial order and the data window size did not significantly increase the accuracy but did significantly affect the speed of calculation.

Upon completion of the interpolation, single differences between the shore station and the ship were calculated. These single differences were subsequently corrected for satellite clock errors and used to create double difference files. The satellite ephemeris was used to calculate satellite coordinates based on the corrected transmission time of the signals taken from the shore station and the ship. These coordinates were included in the double difference files.

5.1.2 Delta H

The double difference observations were used in the adjustment procedure described in Chapter Three. Upon input to the adjustment package each successive pair of observations were differenced once again. The pseudo-range observations were used to determine an initial position for the ship's antenna. The accuracy of this position, because of the noise in the pseudo-range signal, was generally ± 25 metres. This initial position, along with its representative covariance matrix, was combined with the carrier-phase observations to determine the change in coordinates between two epochs. The change in coordinates was transformed into ellipsoidal geographic coordinates according to Section 3.5.5 and the changes in height extracted. These results were then stored in a file for later use.

5.1.3 Datum Determination

Analysis of the data obtained during the adjustment process indicated that significant slowly changing biases of a few metres remained in the resulting height information. These biases were made up of: an indeterminate offset due to the first epoch being positioned at an arbitrary point of the motion cycle, a constant bias due to residual biases in the satellite signals, inaccurate Shelburne station coordinates and random biases due to remaining cycle-slips and multipath. It was necessary to remove these biases through filtering in order to equate the resulting GPS determined motion with the ship's heave.

The filtering was accomplished by using two variation of polynomial fitting to the GPS height signal. Given a set of observations that behave smoothly and continuously:

$$(y_i, x_i), i = 1, k$$

$$y = f(x) \approx a_0 + a_1x + a_2x^2 + ... + a_nx^n$$

$$= \sum_{j=0}^{n} a_jx^j \qquad (5.1)$$

where:

x	–	independent observations;
y	–	dependent observations;
a_j	–	polynomial coefficients;
k	–	number of points in data set;
n	–	degree of the polynomial.

The coefficients are estimated using the least squares technique with k points.

The first method used was an n degree polynomial fit to the entire signal of k data points. The typical data set contained 1500 points and spanned 45 minutes. This had the effect of producing a much smoother estimate of the vertical datum. The disadvantage was

that if the variation in the existing signal biases had a high frequency in comparison to the data set time span, then the fixed window technique would not be effective in reducing the biases.

The second method used a moving m-point window, n degree polynomial function, such that m << k, to extract the low frequency bias from the GPS height signal. This technique is better able to follow higher frequency changes in the biases and can operate in real time but pays a penalty by increasing the datum estimation noise.

In either case the high pass filtering assumes that the low frequencies apparent in the signal are of little consequence over the time period of interest, in this case in the order of minutes. The resulting residual signal from the polynomial fit can be considered to have been adjusted to the local datum as established by the mean height of the antenna. This mean height over the period of the fit is an approximation of the height of the antenna when the ship is resting in stable equilibrium.

5.1.4 Phase Alignment

Comparison of the GPS derived heave with the accelerometer based heave sensors required that there be no phase offset between these signals. The phase alignment between the GPS heave signal and the other heave sensor signals is dependent upon the timing functions used in time-tagging the different records as well as the system dependent data polling delays. The data collection and time-tagging procedures have been described previously in Chapter Four. The possible reasons for misalignment in time between the GPS and the accelerometer based heave sensors are:

- incorrect initialization of the timing clock (wrong by integer seconds);
- data polling delay (wrong by fractions of a second).

The data polling delay is equipment related and depends on the time necessary to access and sample the two serial ports and seven registers of the AtoD conversion board. Using the specifications quoted for all the equipment, this time delay was expected to be less than 0.1 of a second and therefore insignificant [Rapatz, 1988]. The wrong initialization of the timing routine on the other hand introduces timing errors of integer seconds which result in a significant misalignment of the signals. While all data sets experienced a consistent misalignment of one second, indicating that there was an oversight in the initializing procedure, random slips in the timing occurred infrequently. This misalignment in time was immediately apparent when viewing a plot of both signals together or a plot of the residuals from the signal differencing and was corrected by adjusting the time-tags of the heave sensor data by the amount of the estimated offset in integer seconds.

Figure 5.1 shows an overplot of the two heave signals without any corrections. The character of the two signals is very similar. However, it is quite apparent that a misalignment or phase error exists between the two signals. Based on the previous discussion of the time tagging procedure, it can be assumed that the magnitude of the phase error is integer seconds. The reference clock used is the GPS clock and therefore adjustments were made to the time tagging of the heave sensor signals. Figure 5.2 demonstrates that after a one second correction, the two signals are now coincident in phase. Figure 5.2 shows more clearly the similarity of the character of the two signals but a small difference still exists caused by the signals being generated at two different places aboard the ship. Also note that the plotting package, by drawing straight lines between the points causes the two signals to appear dissimilar even though this is just an artifact.
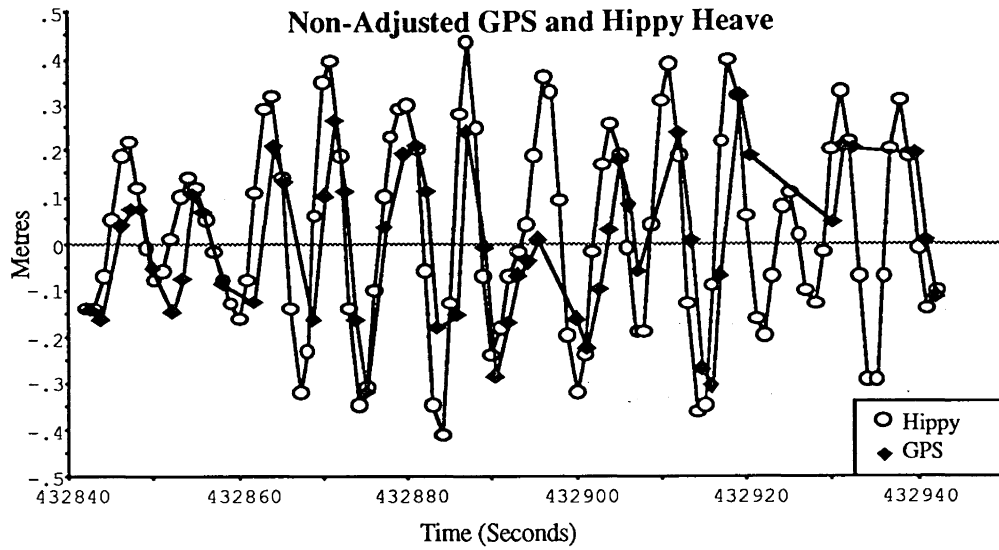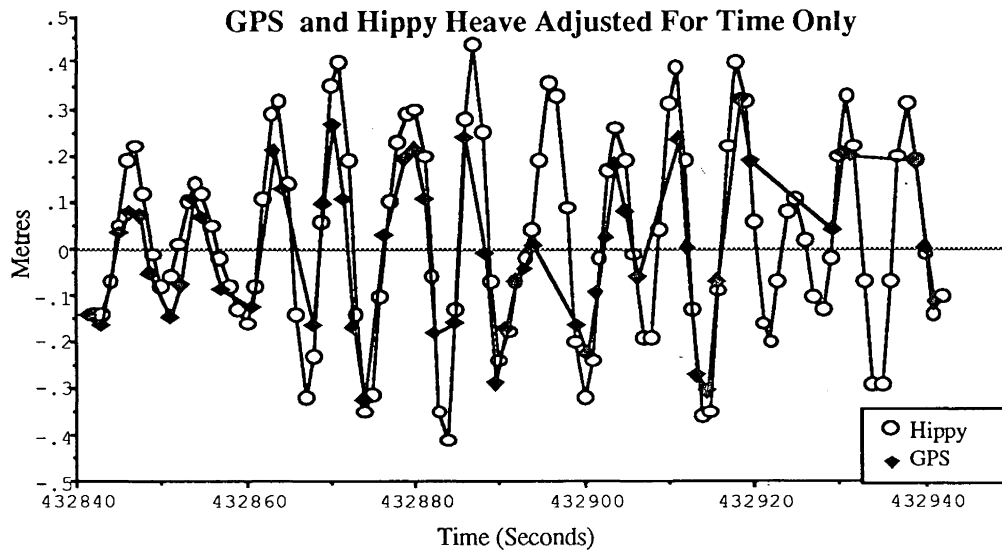
Figure 5.1 – Unadjusted Hippy & GPS Heave

Figure 5.2 – Hippy & GPS Heave Adjusted for Time Offset

5.1.5 Coincidence of the Signals

During the data collection process the different sensors were neither coincident in space nor

were they all sampled at the same time. For example, the GPS antenna was sited some 25

metres away from the other sensors and was sampled at a different rate. Figure 5.2

illustrates the significant difference in sampling rates for the GPS and heave sensor signals. Resampling of the signals was necessary to provide coincident observations for differencing. The constant, high data rate of the heave sensor signal provided a good reference signal and cubic spline interpolation was used to sample it at coincident times with the GPS estimates of heave [Atkinson and Harley, 1983]. All signals from the accelerometer based heave sensors were resampled, including the pitch and roll signals.

The GPS antenna and other sensors, occupying different locations, each monitored a different heave signal. To adjust for the difference in positions, the GPS heave estimate was translated to the positions occupied by the various heave sensors using the algorithm described in Chapter Two. The coordinates of all the relevant points of interest aboard the ship were taken from both physical measurements on the vessel and from scaled construction plans. The accuracy for these coordinates has been estimated to be ± 0.5 metres for all points except for the GPS antenna which, because of its location, was estimated to be ± 1 metre. Figure 5.3 shows the result of translating the GPS signal shown in Figure 5.2 and plotting it over the original heave sensor signal. Clearly the GPS signal now follows the heave sensor signal much more faithfully.
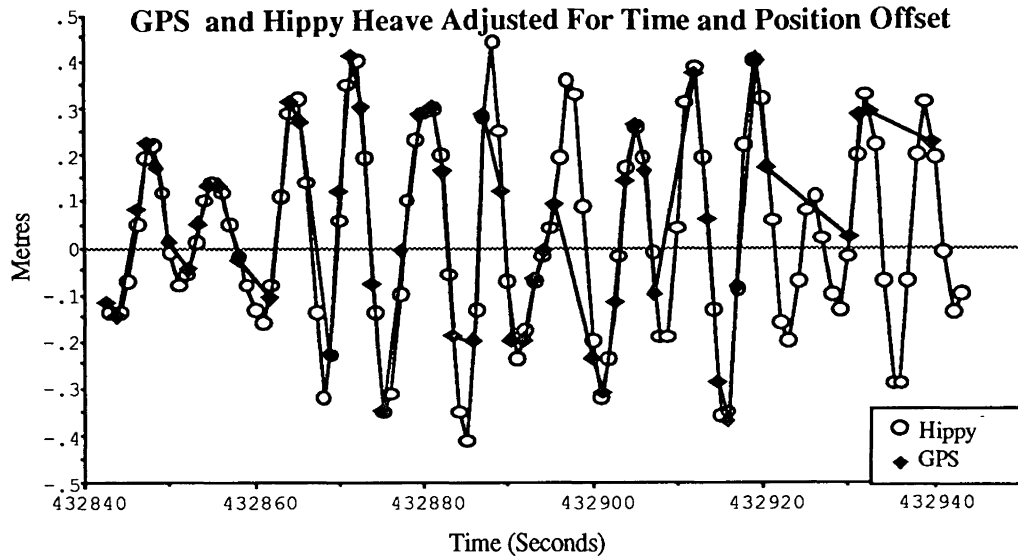
GPS and Hippy Heave Adjusted For Time and Position Offset

Figure 5.3 – Hippy & GPS Heave Adjusted for Time & Position Offset

5.2 Criteria For Comparisons

Researchers have had much difficulty in attempting to quantify the quality of the results produced using GPS. Typically, GPS has been able to meet or exceed the accuracy of most conventional techniques when used in various applications and the problem has been to establish a standard to which the GPS technique can be compared. The difficulty of providing such a standard presents itself when trying to quantify and assess the accuracy of GPS heave determination in this investigation.

Accelerometer based heave sensors were used to provide control measurements, the installation of which were discussed in the previous chapter. It is the comparison between these heave sensor measurements and the GPS derived heave that provides the basis for an assessment of the success of the GPS technique. Unfortunately the heave sensors themselves suffer from various degrees of noise and bias thus complicating the comparisons.

To proceed with the comparison, several characteristics of the signals were identified as influencing the results. These characteristics were; the phase alignment between the GPS and heave sensor signals, the magnitude of the residuals when the GPS heave is differenced with the heave sensor signals, the measurement noise in the signals, datum drifts between the signals and the frequency dependence of the residual signal with respect to the input signals. Each of these characteristics were analyzed to establish their overall contribution to the errors in the technique.

5.3 Residuals Between GPS And The Other Sensors

The residual signal that results when differencing the GPS heave estimate with the other heave sensors will contain the effects of the signal characteristics described above. The residual signal therefore can be assessed with these criteria in mind. The general assessment of the residual signals from the field data is discussed in the following subsections.

5.3.1 Magnitude of Residuals

The magnitude of the residuals after differencing the two processed signals represents a significant indication of the success of the GPS heave determination technique. These residuals and their size are governed by a number of factors affecting both signals. The residuals from differencing the two different signals have been obtained for all three heave sensor locations.

Using the assumption that the residual signal is random in nature, then the simplest way of describing the signal is to determine the first two moments of that signal — the population mean and variance. The two moments are defined such that:

$$E[X(t)] = \mu_x = \int_{-\infty}^{\infty} x f(x) dx \qquad (5.1)$$

$$E[X^2(t)] = \sigma^2_x = \int_{-\infty}^{\infty} x^2 f(x) dx \qquad (5.2)$$

where:

E[...]   — expectation operator;

$f(x)$ — probability density function;

μ_x — population mean;

σ^2_x — population variance.

Equations 5.1 and 5.2 may be reformulated for discrete data resulting in the familiar equations for sample mean and standard deviation.

$$\bar{x} = \frac{1}{n} \sum_{i=1}^{n} x_i \qquad (5.3)$$

$$s^2 = \frac{1}{n-1} \sum_{i=1}^{n} (x_i - \bar{x})^2 \qquad (5.4)$$

where:

n   — number of samples

x_i — i^{th} sample

$\bar{x}$ — sample mean

s   — sample standard deviation

The mean and standard deviation of the residual signal were calculated for all the relevant observation files and a summary of this data will be presented in Section 5.6.

As a counterpoint to the residual signal between GPS and the heave sensors, the difference between the two adjacent heave sensors was also determined and assessed. The

separation between the two sensors was small enough to allow direct comparison. Applying pitch and roll corrections to this signal only increased the noise level. This difference signal was used as an indication of the noise level in the heave sensor signals themselves. A study in 1989, based on analyzing this difference signal, concluded that the contribution made to the residual signal by each sensor was roughly proportional to the stated specifications which indicated that the TSS model 320 heave sensor can have less than half the accuracy of the Hippy 120b heave sensor [Rapatz, 1989]. This conclusion may be borne out by the consistently higher standard deviation of the GPS - TSS1 residual signal when compared to the GPS - Hippy residual signal (see Section 5.6).

5.3.2 Datum Differences

Datum determination is an important factor in the accuracy of the GPS heave technique. The datum is established using the hypothesis that the heave signal has a zero mean over a short time period. This hypothesis is not exactly true due to sea level variations like tides or alterations in the stability characteristics of the vessel, but for the time period of interest, the assumption is close enough to reality. By fitting a smooth low degree polynomial to the GPS data it is possible to remove the majority of the slowly changing biases. The remaining signal is expected to represent the departure of the antenna from the antenna equilibrium position.

To a large degree, the type of fit and the order of the polynomial depends upon the nature of the bias remaining in the GPS heave. In this investigation, two variations of polynomial fitting were attempted. The first was a low order polynomial fit to the entire data set, i.e. for as much as one hour of observations. The extent to which this was successful was determined by the length of the data span and the variability in the GPS bias effect. The shorter the data span, the fewer number of files joined together and the

smoother the GPS bias, the better the datum estimate. As the data departed from these ideal conditions, greater success was achieved using a moving low order polynomial with a data window of a small number of points, typically 100 spanning 200 seconds. The effect of changing the number of points and the degree of the polynomial fit has been investigated in Rapatz and Wells [1990] and is summarized in Figure 5.4. This figure shows the rms of the datum estimation error when altering the parameters of the polynomial fitting technique.

Bar Chart of RMS for Solutions using Various Numbers of Points and Degrees of Polynomials (Data Set From HIPPY 120b Compensator)
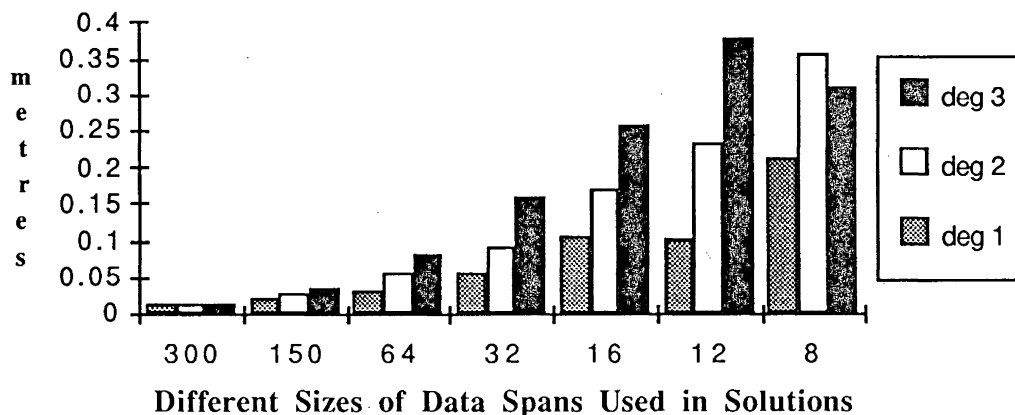

Figure 5.4 – Response to Differing Degrees & Window Sizes

The report concluded that a smaller data window followed changing biases in the GPS signal more closely, whereas a larger data window reduced the overall noise in the determined datum.

The moving polynomial fit was more successful in reducing the GPS bias effect encountered during the field exercise. In particular, the moving window technique was successful in constraining the effect of cycle-slips and other one-time-biases to within half the time span of the fitting window. An example of the effect of using a single fixed window of 1200 points (40 minutes) versus a moving window of 100 points (3.3 minutes)

as described above may be seen in Figure 5.5 which shows the resulting residual signal
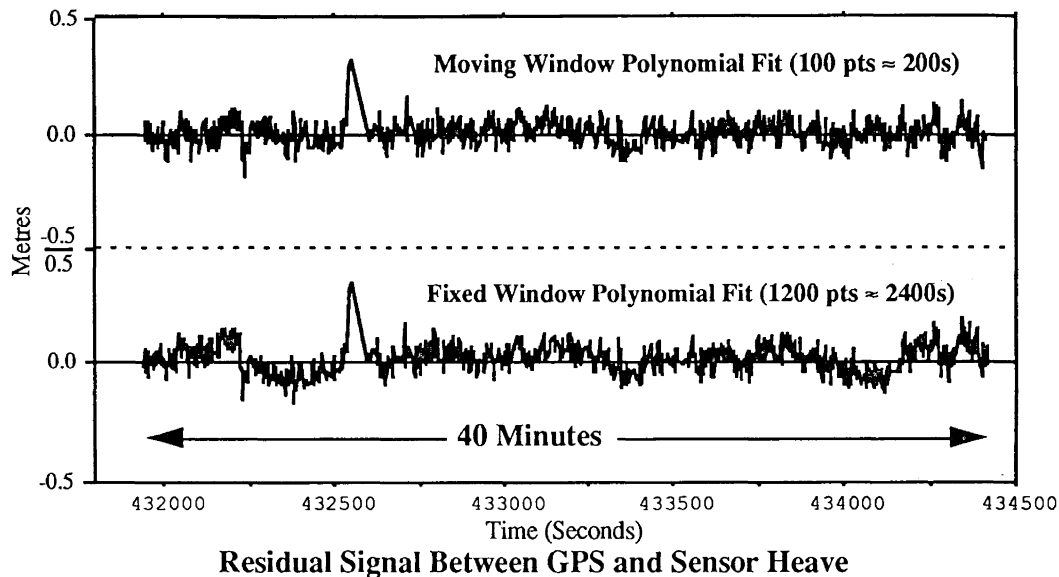
between the GPS heave and the Hippy heave sensors.

Residual Signal Between GPS and Sensor Heave

Figure 5.5 – Result of Different Polynomial Fit Variations

5.3.3 Spectral Analysis

Spectral analysis of both the heave data and the residual signal was used to gain insight into

the contributing constituent frequencies. The bandwidth chosen for investigation ranged

between 0.5 and .005 hertz which corresponds to periods of 2 and 200 seconds

respectively. Figure 5.6 shows the spectral density plot for the GPS heave estimate after it

has been sampled and translated to the heave sensor location. The predominance of of the

signal power is concentrated around a frequency of 0.13 hertz which corresponds to a 7.7

second period. The peak at this frequency represents the actual heave motion due to the

ship responding to the driving force of the waves. There exists a low frequency

component and a constant contribution in the higher frequencies which represents the
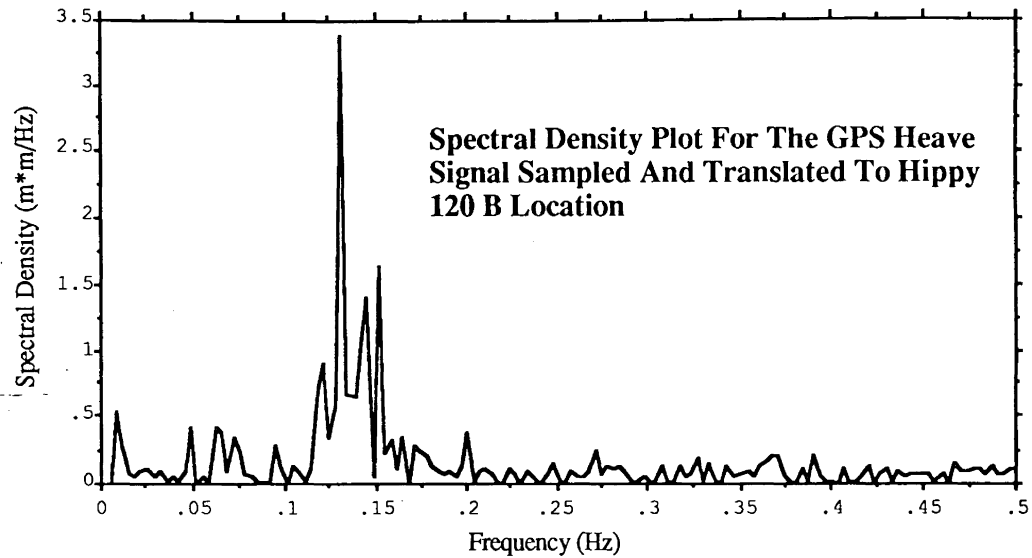
higher frequency noise.

Figure 5.6 – Spectral Density Plot of GPS Heave

In contrast, Figure 5.7 shows the majority of the power in the residual signal has

moved to lower frequencies with a residual peak remaining at 7.7 seconds. The implication

is that the resulting residual signal may be dependent upon the wave induced motion i.e. the

magnitude of the residual signal may be related to the magnitude of the heave experienced.

The high frequency noise contribution is constant but has increased due to the extraction of

some of the wave frequency contribution and the addition of the noise in the Hippy heave

sensor signal. The majority of the remaining power in the lower frequencies can be

attributed to residual bias in the GPS signal that has not been removed in the datum
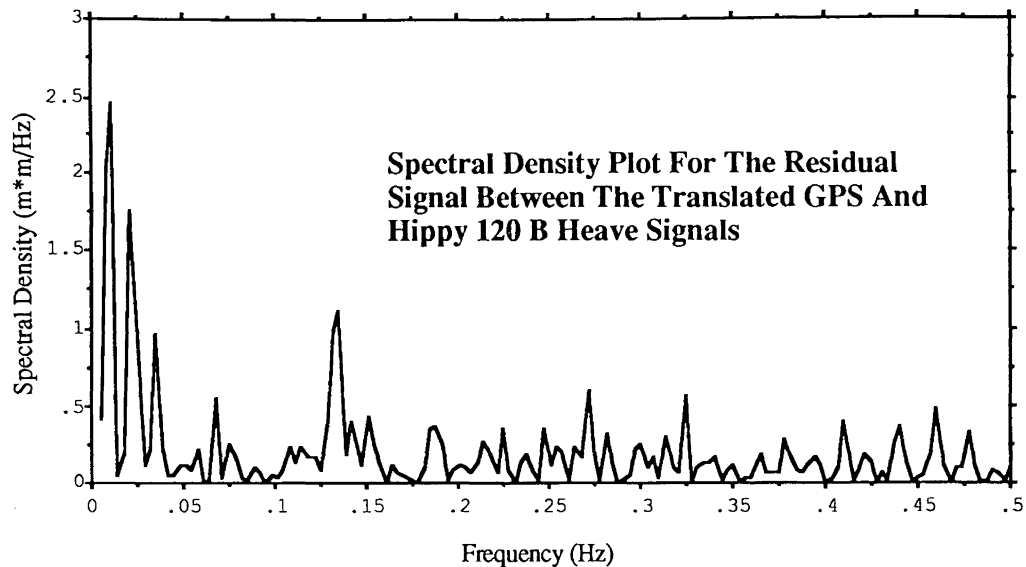
determination process.

Figure 5.7 – Spectral Density Plot of Residuals Between GPS & Hippy

5.4   Typical Results

The purpose of this section is to show some typical results obtained from this data set. The plots in the next subsections are results from Day 170 and Day 179, 1988 respectively. Day 170 represents a typical day with somewhat restrained vertical motion. Day 179 on the other hand represents the largest range of motion for which data was obtained during the three week cruise. Recall that the GPS antenna and the two forward heave sensors were located a good distance forward of the nominal pitch rotation centre of the ship and therefore the heave signal registered will be somewhat exaggerated in comparison to the motion experienced aft of these sensors.

5.4.1 High Dynamics

Day 179 exhibits heave measurements from the forward laboratory with a maximum of roughly ± 2 metres with an overall standard deviation of 0.6 metres. This day experienced

the largest magnitude of heave during which GPS measurements were successfully observed. Figure 5.8 shows a plot of the estimated heave from GPS and Figure 5.9 shows the residual plot after differencing the GPS heave estimate with the heave from the Hippy 120b heave sensor.
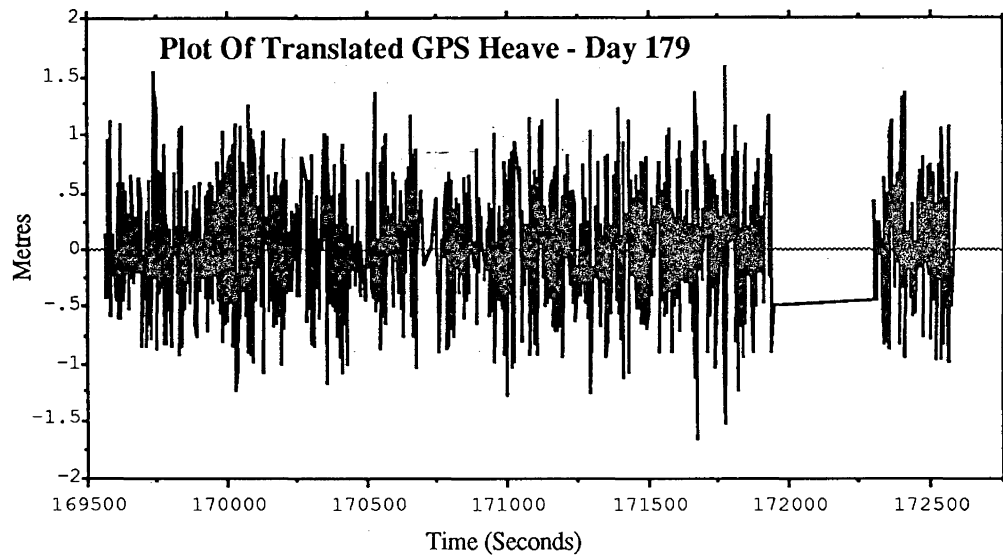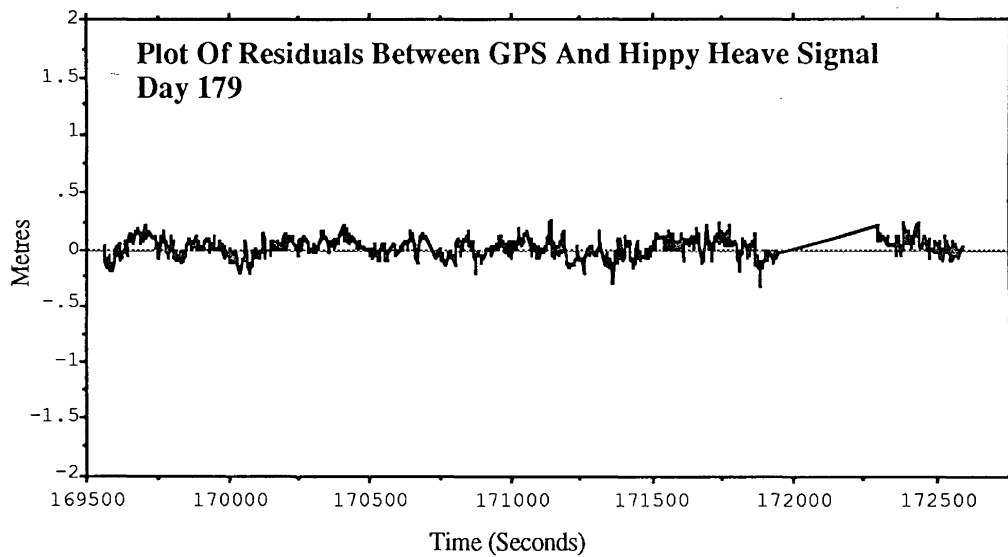

Figure 5.8 – GPS Heave Day 179

Figure 5.9a – Hippy Residual Signal Day 179
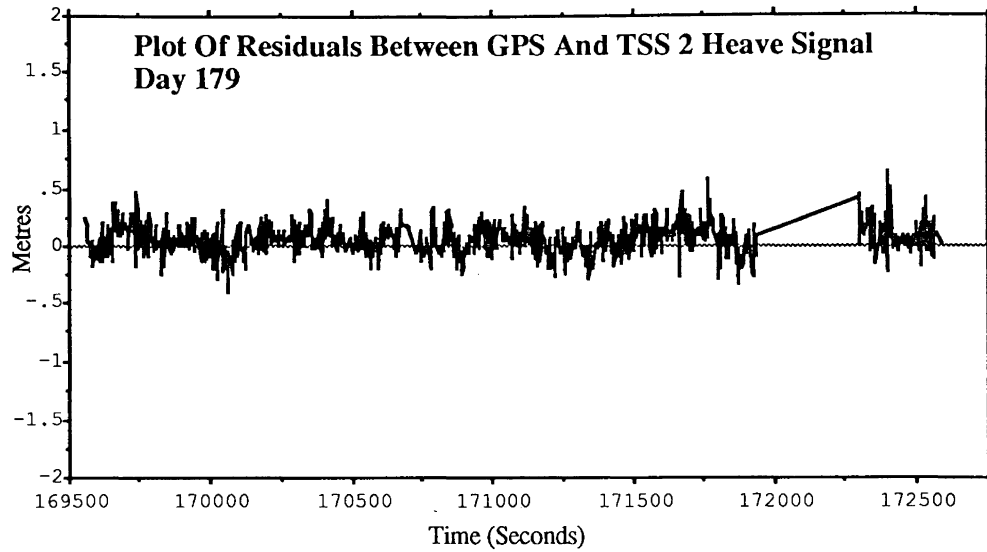
Figure 5.9b – TSS 2 Residual Signal Day 179

5.4.2 Low Dynamics

Day 170 exhibits a generally smaller range of motion with maximum amplitudes of ± 1.0

metres with an overall standard deviation of 0.35 metres. The results from this day differ

from the previous example in that the residual signal is generally smaller and there is clearly

less noise in the datum determination. The spike seen at the beginning of residual plot is

most likely due to a small cycle-slip in the GPS data.
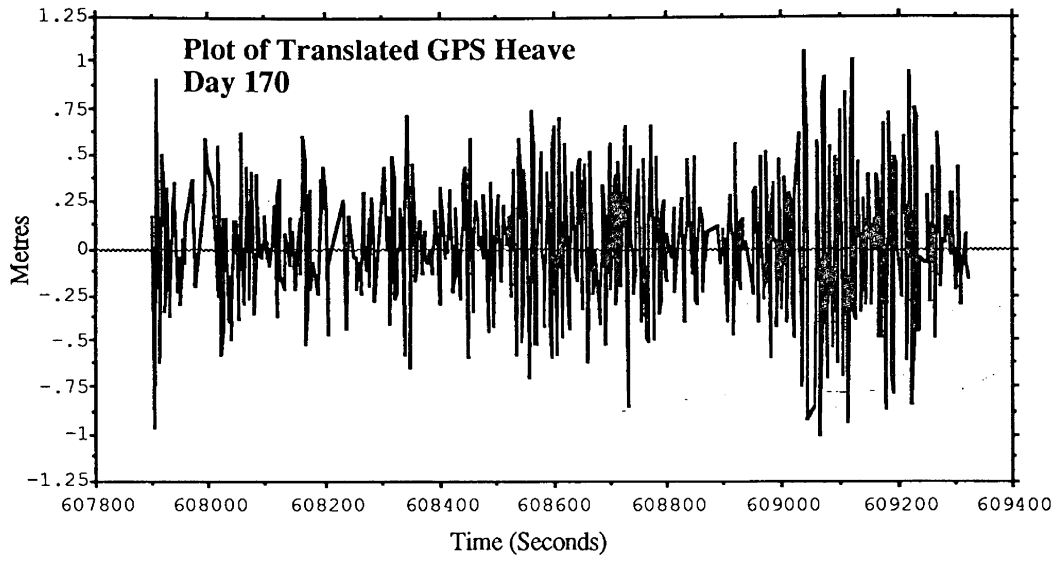
Figure 5.10 – GPS Heave Day 170
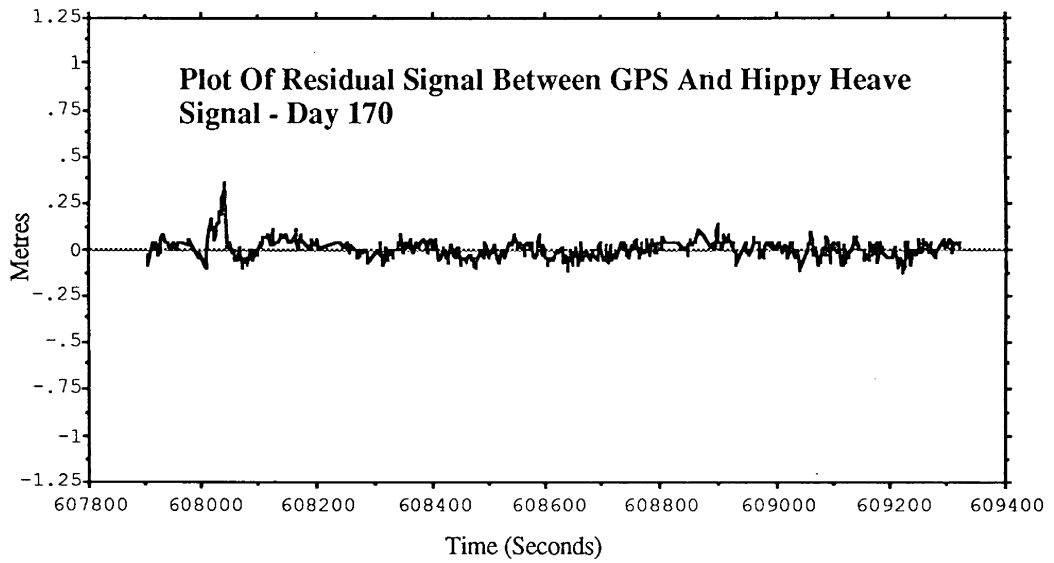
Figure 5.11a – Hippy Residual Signal Day 170
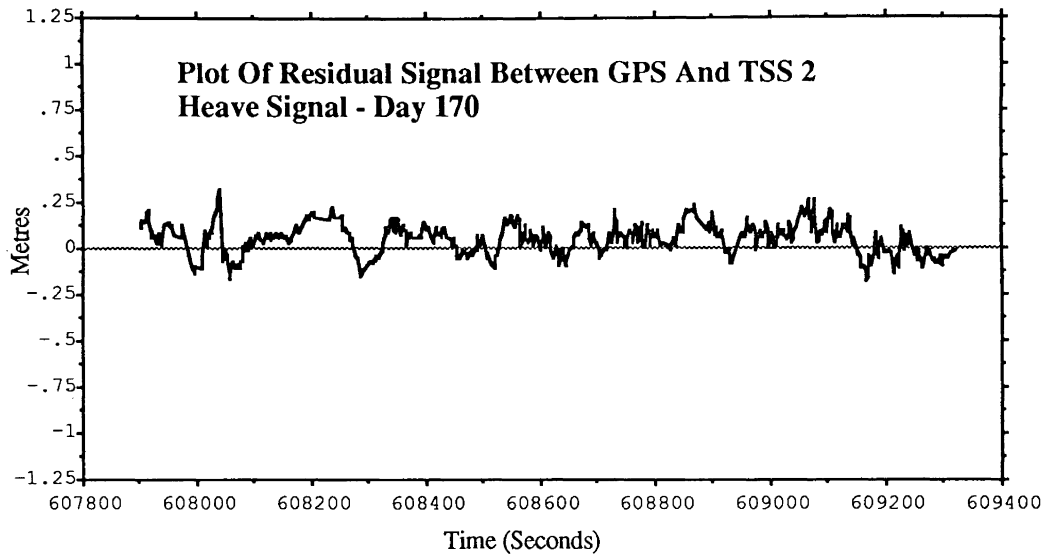
Figure 5.11b – TSS 2 Residual Signal Day 170

5.5 Error Contributions

All the factors affecting the character of the residual signal come from either the GPS signal or the heave sensor signal. Their effects will be present in one or all of the characteristics described in Section 5.3. These factors are summarized in Table 5.1 where the Magnitude column refers to the error seen in the input signal and Impact on GPS Heave column refers to the upper limit expected as the error is mapped into the vertical. In general Table 5.1 is a worst case estimate and typical GPS heave measurements should have a higher accuracy.

Table 5.1 – Error Impact

Errors	Magnitude	Impact on GPS Heave
carrier-phase noise	≤ 1 cm	≤ 5 cm
cycle-slips	≤ 5 cycles	≤ 1 m
data interpolation error	≤ 3 cm	≤ 10 cm
datum determination error	≤ 10 cm	≤ 10 cm
pitch / roll errors	$\leq 1°$ of arc	≤ 5 cm
heave sensor noise	≤ 3 cm + 3 %	
heave sensor bias	≤ 5 cm	

The above factors all constitute limitations on the effectiveness of the GPS heave determination technique investigated for this work.

5.5.1 Effect of Noise

The noise in the GPS signal is a combination of factors discussed in Chapter Three. The overall effect of this noise on the heave signal will be a function of the geometry of the satellite constellation which directly affects the transformation of the errors in the signal into errors in change in height estimates. This mapping is directed according to Section 3.5.5.3. The dilution of precision which is a measure of the geometry of the satellite constellation, represents a geometrical magnification factor of the signal errors and has been discussed in Section 3.3.4.

The noise in the heave sensor data on the other hand will map directly into the residual signal. As discussed in Section 5.3.1 the average magnitude of the error in the heave signal can be deduced from the difference signal between the two adjacent heave sensors.

5.5.2 Effect of Cycle-Slips

The effect of cycle-slips in heave determination is related to the success in the determination and correction of the cycle-slips. The data cleaning process removed the majority of the cycle-slips in the data but due to the low resolution of the techniques available, some cycle-slips in the order of a few cycles clearly went undetected. Cycle-slips of this size introduce a one time bias into the heave signal whose magnitude will depend on the satellite position and how the effect of the cycle-slip maps to the vertical. Once a slip occurs, the high pass filtering will tend to smooth out the effect but will also tend to spread it into the heave estimate within the range of the data window used by the filter. An example of this effect can be seen in Figure 5.12 from Day 171. The peak in the signal represents where a cycle-slip was not removed from the data and the slope of the heave signal on either side of that peak indicates how the effect is spread to the surrounding data via the filtering process. It should be noted that when a moving window is used in the filter, the majority of the effect is located close to the original peak and is limited to the width of the data window itself. Figure 5.12 illustrates the importance of discovering and correcting all cycle-slips in the GPS data before applying the heave estimation technique.
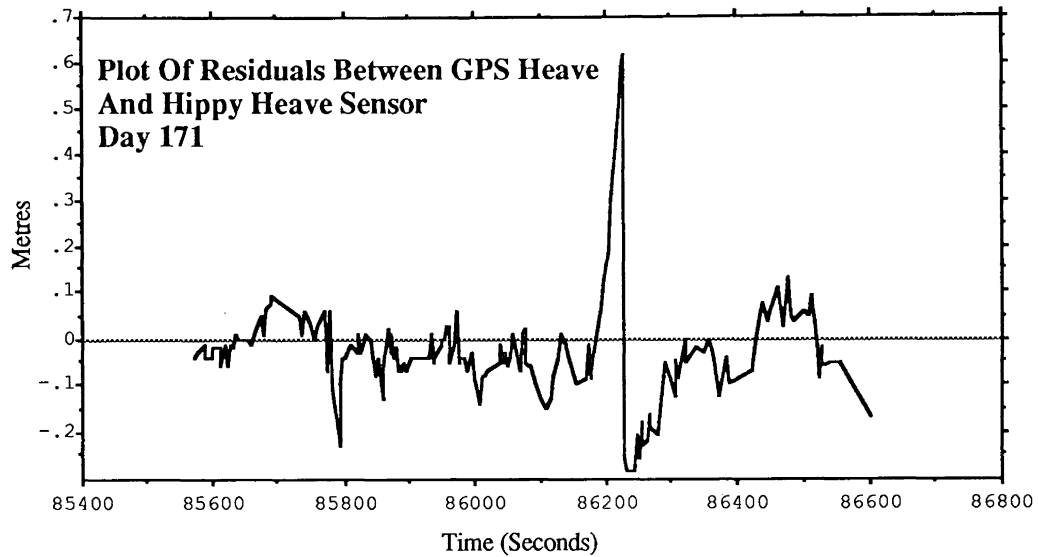
Figure 5.12 – Effect of Cycle-Slip in GPS Heave

5.5.3 Effect of Errors in Datum Determination

The datum determination technique used in this investigation attempts to model and remove the low frequency bias in the GPS heave signal. The success of this technique will be evident in the residual signal where the remaining bias will be contained. Depending on the frequency of this bias, the effect will appear to be constant in nature or slowly periodic. Such a periodicity in the residual signal is evident from Figure 5.5 and Figure 5.7. Any errors in determining the datum will map directly into the heave estimate. The assumptions made regarding the use of time averaging to estimate the equilibrium position of the ship are clearly appropriate to within a few centimetres during medium dynamics.

5.5.4 Effect of Heave Sensor Bias

Heave sensor biases are made up of an offset in the heave signal, a scale error and possible offsets and scale errors in the pitch and roll information. In the case of the heave estimate,

datum offsets and scale factor errors are functions of the internal design of the sensor and in fact the Hippy heave signal appeared to have a constant two centimetre positive offset [Rapatz, 1989]. The offset in the heave estimate will map directly into the residual signal and cause a nonzero mean, but not affect the standard deviation. The scale factor error on the other hand will not affect the mean of the residual signal but will cause an increase in the standard deviation. These errors can be compensated for after testing the sensor and determining their magnitude.

Pitch and roll errors can be both an internal artifact of the instrument or a result of changing stability characteristics of the ship. Constant errors which can be associated with the internal design of the heave sensor can be easily investigated and corrected. Errors associated with the stability characteristics of the ship on the other hand will change from time to time with changing conditions. Any change in either the vessel load, weather characteristics or vessel heading will all determine how a vessel rests in the water. Any or all of these situations occur continuously at sea and will affect the angle of the ship that represents the average orientation. In particular this changing offset in the roll will cause a bias in the transformation computation which assumes a zero roll angle when the ship is in stable equilibrium. This bias will map into the heave estimate as a function of the separation between the GPS sensor and the point of interest.

5.6   Comparison Statistics Summary

Table 5.2 summarizes the results of the heave estimation process for each day that contained useful data. The mean and standard deviation of each residual signal were obtained by differencing the GPS heave estimate with the heave sensor heave estimate. Statistics for the actual heave signal are given in the last column as a reference. The mean and standard deviation of the summary statistics for each sensor pair have been provided in

the last row in order to highlight any behaviour which may have been consistent over a period of days.

Table 5.2 – Table of Heave Estimation Residuals (metres)

(100 point 3 degree moving polynomial fit)

	SENSOR PAIRS									
	Hippy - GPS		TSS1 - GPS		TSS2 - GPS		Hippy -TSS1		TSS1	
File Name	Mean	St.Dev	Mean	St.Dev	Mean	St.Dev	Mean	St.Dev	Mean	St.Dev
Day 168 # 4,5,6	0.01	0.05	-0.03	0.06	0.05	0.05	0.02	0.04	0.00	0.26
Day 169 # 12	0.01	0.04	-0.02	0.05	0.03	0.05	0.02	0.05	0.00	0.16
Day 169 # 6,7,8	0.00	0.05	-0.03	0.06	0.05	0.06	0.02	0.04	0.00	0.16
Day 170 # 1,2,3	0.02	0.05	-0.01	0.07	0.07	0.07	0.01	0.07	0.00	0.35
Day 170 # 5,6	0.01	0.05	-0.01	0.08	0.05	0.08	0.00	0.08	0.00	0.35
Day 171 # 5	-0.03	0.12	-0.03	0.14	0.01	0.11	-0.00	0.09	0.00	0.27
Day 171 # 7	0.01	0.07	-0.01	0.07	0.04	0.07	0.01	0.06	0.00	0.27
Day 174 # 6,7,8	0.01	0.06	-0.02	0.07	0.03	0.07	0.02	0.05	0.00	0.27
Day 174 #6,7,8b	0.02	0.06	-0.02	0.07	0.04	0.07	0.02	0.05	0.00	0.27
Day 174 # 11,12	0.03	0.05	-0.01	0.07	0.05	0.06	0.02	0.05	0.00	0.27
Day 177 # 1	-0.00	0.05	-0.04	0.06	0.05	0.06	0.02	0.04	0.00	0.25
Day 179 # 1	-0.02	0.11	-0.05	0.14	0.03	0.13	0.03	0.13	0.00	0.56
Day 179 # 3,4,5	0.02	0.09	-0.01	0.15	0.06	0.13	0.01	0.12	0.00	0.56
Average	0.01	0.06	-0.02	0.08	0.04	0.08	0.02	0.07	0.00	0.31
Standard Dev.	0.02	0.03	0.01	0.03	0.02	0.03	0.01	0.03	0.00	0.13

5.7 Chapter Summary

Chapter Five has introduced the processing of the collected data and the procedure for comparisons between the GPS estimated heave and the measured heave from the accelerometer based heave sensor. The chapter has been structured to deal with the organization of the processing steps and discuss and present the criteria used for judging the comparisons followed by a review of the results obtained from these comparisons. A

discussion of how the relevant errors and biases will affect the heave estimates and the residual signal used for the comparison was concluded with a summary of the statistics of the residual signals for all the data collected and processed.

CHAPTER SIX
CONCLUSION

Chapter Six forms the conclusion of this thesis and begins with a summary and discussion of the issues that were raised during various phases of the research work. The main conclusions drawn from the results of using differential GPS carrier-phase signals for heave estimation and the comparisons with the other heave sensors are presented. The chapter ends with recommendations for future research in this field.

6.1 Summary and Discussion

6.1.1 Vessel Motion

During the investigation of this thesis topic and processing of the data, several aspects of vessel motion have been noted. Heave motion experienced by a vessel is a function of both the driving forces and the characteristics of the vessel itself. In the case of the CSS Hudson, the heave motion exhibited strong characteristic frequencies within a range of 0.2 to 0.1 hertz — the characteristic frequency band being similar at all sensor locations. However, the phase and shape of the heave signal differed substantially between sensor locations, indicating a strong coupling of heave with pitch. The pitch and roll motions were only weakly coupled.

Observation showed that heave experienced by the CSS Hudson was approximately one third of the actual wave height depending on location and was clearly a function of the size and stability of the vessel. Weather for the month of June is usually fair and this is reflected in the heave motion depicted in Table 5.2. During the two week cruise the heave

experienced in the forward laboratory ranged from just ± 0.5 metres to in excess of ± 4 metres.

6.1.2 Current Heave Sensors

Most current heave sensors are accelerometer based and rely on self-stabilizing and filtering to establish and maintain a vertical datum. Both the Hippy 120b and the TSS Model 320 heave sensors are good representatives of current technology in this field with little change expected other than refinements in the filtering. These heave sensors have stated accuracies within ± (0.03 m + 5 %) and performed well during the exercise. Comparisons between heave sensors however, indicated that they may produce a noisier signal than expected (refer to Table 5.1 and Appendix A). The primary shortcomings of these heave sensors appear to be: sensitivity to long period motions such as course changes, a narrow frequency response band, and the limited range of motion they are designed to experience (for example the TSS Model 320 is only rated for ± 4 metres).

6.1.3 Relative vs. Absolute Heave

As GPS heave determination becomes better understood, the trend will move towards precise measurements of absolute vertical motions of ships with respect to global datums such as the geoid or ellipsoid (see section 2.7) rather than relative heave in the context of section 3.5.6.1. As evidence of this trend is the intention of the CHS to use the GPS heave technique to monitor tidal action in future [Rapatz and Wells, 1990]. In this context, this thesis addresses only relative heave and leaves absolute heave for future research.

6.1.4 Transfer of Heave From Sensor to Point of Interest

The transformation from the sensor site to the point of interest has been addressed in this thesis in order that comparisons be made between different sensors. It was found that accurate pitch and roll data as well as accurate relative coordinates of all points were essential for precise heave transfer. The position of the pitch and roll sensor may be arbitrary but should be placed so as to reduce the effect of lateral accelerations. The location of the origin of the ship based coordinate system may also be arbitrary and can be chosen for convenience. One very important consideration is that the transfer algorithm makes the assumption that when the vessel is in stable equilibrium the pitch and roll angles are zero. However, the vessel's equilibrium orientation shifts in response to changing currents, winds and different stability characteristics. As an example, such a shift could occur when the wind shifts to the beam of the vessel. This could offset the orientation of the ship by as much as five degrees of arc and would result in a direct bias of the transferred heave measurements by up to 30 centimetres.

6.1.5 Problems with Data Collection and Processing

The problems with the data set were numerous and required considerable effort to correct. The major difficulties were bad ephemeris, mismatching time-tags, equipment failure, inconsistent data logging and an incorrect master station position. In general, the most troublesome problems were with the time tagging and an inconsistent data rate. A great deal of success was accrued using simple polynomial fitting, interpolation and spline fitting to offset these difficulties.

6.1.6 GPS Technology Then and Now

Quality and accuracy of GPS derived heave results are affected by external factors associated with GPS and receiver technology. The heave results in this thesis are limited by signal noise, a slow data rate, the minimum number of satellites and numerous cycle-slips. The TI 4100 GPS receivers are limited older technology whereas newer receivers are being produced which are more reliable, have increased data rates, reduced signal noise, reduced cycle-slips, and multiple satellite monitoring — all of which will play a major part in the success of GPS derived heave. As the features of modern GPS receivers are improved so will the usefulness of GPS derived heave be increased and extended.

6.2   Conclusions

Several conclusions may be drawn from the results of this investigation regarding GPS derived heave:

- The accuracy of GPS heave determined in this thesis has been shown to be at the five centimetre level. This level represents the limit for the data set studied, using the data processing techniques described in Chapters Four and Five and is comparable with the accuracies found for the other heave sensors used as control.

- Limiting factors for the accuracy of GPS derived heave include: the data sampling rate, biases in the GPS measurement signals, cycle-slips and measurement noise. It is reasonable to expect that without the initial signal interpolation, better signal to noise capabilities of new receivers and better techniques for detecting and correcting cycle-slips the limiting accuracy could conceivably be improved by an order of magnitude to less than a centimetre.

- The datum determination technique is insensitive to long term biases in either the GPS data or the actual sea surface.

- GPS offers advantages over available accelerometer based heave sensors:

    i) larger range of motions that may be accommodated – both in terms of frequencies and amplitudes;

    ii) eliminates sensitivity to resonant frequencies;

    iii) potential for very high accuracy (better than a centimetre).

6.3   Direction of Future Research

This research has accomplished the initial goal of applying GPS to heave measurements. The possibilities for further research are numerous. In particular, application of "on-the-fly" ambiguity resolution or other techniques for solving the carrier-phase ambiguity will help to fully utilize the accuracy of carrier-phase signal. The solution to this particular problem will affect many of the issues in GPS heave determination such as datum determination, signal noise and initial position estimates. Continuing research using receivers capable of multi-satellite data, increased data rates and kinematic positioning will drastically improve GPS heave determination.

Whereas relative heave determination is the detection of the high frequency motion of a ship, it will be possible to measure lower frequency height motions as bias detection and reduction is improved. Further research into reducing the biases in GPS will eventually result in the monitoring of tidal signals and potentially culminating in the monitoring of real time absolute heave.

REFERENCES

Abidin, H. Z. (1989). "Extended Extrawidelaning Technique of Ambiguity Resolution." Graduate seminar paper, Department of Surveying Engineering, University of New Brunswick, Fredericton, N.B., Canada.

Abidin, H. Z. (1990). Personal communication.

ASHTECH, Inc. (1989). "Receiver Specifications." Sunnyvale, California.

Atkinson, L.V. and P.J.Harley (1983). *An Introduction to Numerical Methods with Pascal*. Addison-Wesley Publishers Ltd., London pp. 117-127.

Blagoveshchensky, S.N. (1962). *Theory of Ship Motions*. Iowa Institute of Hydraulic Research, McClelland Stewart Ltd., Canada.

Beach, R. (1988). "TI41LOG." TI 4100 data logging program written in Turbo Pascal.

Bowditch, N. (1984). *American Practical Navigator*. U.S. Department of Defense, Defense Mapping Agency Hydrographic Center, Washington, D.C.

Caldwell, J.M. (1955). "The Step Resistance Wave Gauge." *Proceedings of the First Conference on Coastal Engineering Instruments*. Berkeley, California, Oct. 31 - Nov. 2, 1955, pp 44-60.

Datawell bv. (n.d.). "Manual - HIPPY Sensor 120 sec with analog filter (B filter) from serial no. 19111-B." Datawell bv, Laboratorium voor Instrumentatie, Netherlands.

Evans, A. G. (1986). "Use of GPS Phase Measurements for Dynamic Relative Position and Velocity Estimation: Laboratory Test Results." *Proceedings of the Fourth International Geodetic Symposium on Satellite Positioning,* Austin Texas, vol. II, pp. 1361.

Evans, A., B.R. Herman, D.S. Coco and J.R. Clynch (1985). "Collocation Tests of an Advanced Geodetic Global Positioning System Receiver." *Proceedings of the First International Symposium on Precise Positioning with the Global Positioning System*. Rockville, Md., 15-19 April, 1985, Vol. I, pp. 245-254.

Forrester, W.D. (1984). "Remote Sensing in Hydrography." *Report on Detection of Depth Anomalies*, International Federation of Surveyors, commission 4, August, 1984 second edition, pp. 186 - 236.

Garmulewicz, J.A. (1989). *An Integrated Approach to Monitoring Sea Floor Subsidence: Role of Kinematic Relative GPS Positioning*. MScE Thesis, Department of Surveying Engineering, University of New Brunswick, Fredericton, N.B., Canada.

Gelb, A. (1974). *Applied Optimal Estimation*. The M.I.T. Press, Massachusetts Institute of Technology, Cambridge, Massachusetts.

Green, Colonel G.B., P.D. Massatt and N.W. Rhodus (1988). "The GPS 21 Primary Satellite Constellation." *Proceedings of the Satellite Division's International Technical Meeting.* The Institute of Navigation, Colorado Springs, Colorado, 19-23 September 1988, pp. 15-26.

Grover, S.C. (1954). "Observations on Ship Motions at Sea." *Proceedings of the First Conference on Ships and Waves.* Hoboken, New Jersey, October, 1954, pp 351-363.

Hatch, R. (1989). "Ambiguity Resolution in the Fast Lane." *Proceedings of the Second Annual International Technical Meeting- ION GPS-89,* Institute of Navigation's Satellite Division, The Institute of Navigation, Colorado Springs, Colorado, 19-23 September, 1989.

Hopkins, Lt. Cmd. R. D., L. C. Adamo (1981). "Heave-Roll-Pitch Correction for Hydrographic and Multibeam Survey Systems." *The Hydrographic Journal,* No. 21, pp. 5-12.

Hurley, J.F. (1980). *Intermediate Calculus.* Saunders College/Holt, Rinehart and Winston, Philadelphia, PA 19105.

Hudson (1988). "Hudson 88-020 Montagnais Cruise Report." Atlantic Geoscience Centre, Geological Survey of Canada, Bedford Institute of Oceanography, Dartmouth, Halifax June 15, 1988 - Halifax June 28, 1988.

Jones, Lt. Col. Thomas (1989). "Navstar Global Positioning System - Status and Update." *Proceedings of the Fifth International Symposium on Satellite Positioning,* 13-17 March 1989, New Mexico State University, Las Cruces, NM, pp. 28-52.

Killen, K. (1988). "Operations Segment." *Proceedings of the Satellite Division's International Technical Meeting.* The Institute of Navigation, Colorado Springs, Colorado, 19-23 September 1988, pp. 3-8.

Kleusberg, K. and L. Wanninger (1987). "Analysis of the Juan de Fuca GPS Survey-1986." Final Contract Report to Pacific Geoscience Centre of the Geological Survey of Canada.

Landau H. (1989). "Precise Kinematic GPS Positioning." *Bulletin Geodesique,* Vol. 63, No. 1, pp. 85.

Lattwood, E. and H.S. Pengelly (1967). *Theoretical Naval Architecture.* Longmans, Green and Co. Ltd, London.

Mader G.L. (1986). "Decimeter Level Aircraft Positioning Using GPS Carrier Phase Measurements." *Proceedings of the Fourth International Geodetic Symposium on Satellite Positioning,* Austin Texas, vol. II, pp. 1335.

McCaskill, T.B. and J.A. Buisson (1985). "On-Orbit Frequency Stability Analysis of NAVSTAR GPS Clocks and the Importance of Frequency Stability to Precise Positioning". *Proceedings of the First International Symposium on Precise*

Positioning with the Global Positioning System. Rockville, Md., 15-19 April, 1985, Vol. I, pp. 37-50.

Mertikas, S. (1983). *Differential Global Positioning System Navigation: A Geometrical Analysis*. M.Eng. Thesis, Department of Surveying Engineering, University of New Brunswick, Fredericton, N.B., Canada.

Mikhail, E.M. (1976). *Observations and Least Squares*. Thomas Y. Crowell Company, Inc., University Press of America, Inc., Lanhm, MD 20706.

Nortech Surveys (Canada) Inc. (1987). "Draft Report on Development of Techniques for using the Global Positioning System (GPS) at Sea for Hydrographic Surveying." Prepared for: Canadian Hydrographic Service, Department of Fisheries and Oceans under DSS File No. 5OSS.FP901-5-R531.

Peyton, D.R. (1990). *An Investigation into Acceleration Determination for Airborne Gravimetry using the Global Positioning System*. MScEng thesis, University of New Brunswick, Fredericton, N.B., Canada.

Price, W.G. and R.E. Bishop (1974). *Probabilistic Theory of Ship Dynamics*, John Wiley and Sons Ltd., New York.

Rapatz P.J.V. (1988). "Preliminary Report on Heave Sensor Comparisons." Unpublished report, Department of Surveying Engineering, University of New Brunswick, Fredericton, N.B.

Rapatz, P.J.V. (1989). "Comparison of the TSS Model 320 and HIPPY 120b Heave Sensors." Unpublished seminar report as part of graduate degree requirements at the Department of Surveying Engineering, University of New Brunswick, Fredericton, N.B.

Rapatz, P.J.V. and D.E. Wells (1990). " Algorithm for the Determination of Heave Using GPS Carrier-phase Measurements." Final contract report to Nortech Surveys Inc (Canada).

Rawson, K.J. and E.C. Tupper (1968). *Basic Ship Theory*. Longmans, Green and Co. Ltd., London.

Remondi, B. W. (1985). "Global Positioning System Carrier Phase: Description and Use." National Geodetic Survey Charting and Geodetic Services, National Ocean Services, NOAA Rockville, MD. 20852.

Remondi, B. W. (1986). "Distribution of Global Positioning System Ephemerides by the National Geodetic Survey." Surveying, Instrumentation, and the Global Positioning System Technical Papers, ACSM-ASPRS Annual Convention, Vol. II, pp. 219-225.

Remondi, B.W. (1988). "Kinematic and Pseudo-Kinematic GPS." *Proceedings of the Satellite Division's International Technical Meeting*. The Institute of Navigation, Colorado Springs, Colorado, 19-23 September 1988.

Renouf, K. (1987). "Heave Compensation for Hydrographic Surveys." Graduate paper, Department of Surveying Engineering, University of New Brunswick, Fredericton, N.B., Canada.

Santerre, R. (1989). *GPS Satellite Sky Distribution: Impact on the Propagation of Some Important Errors in Precise Relative Positioning.* Ph.D. dissertation, University of New Brunswick, Fredericton, N.B., Canada.

Seeber, G. and G. Wübbena (1989). "Kinematic Positioning with Carrier Phases and 'On the Fly' Ambiguity Solution". *Proceedings of the Second Annual International Technical Meeting- ION GPS-89,* Institute of Navigation's Satellite Division, The Institute of Navigation, Colorado Springs, Colorado, 19-23 September, 1989.

Staples, H., J.T. Lockhart and G. Eaton (1985). "HIPPY 120c Heave Compensator". *Proceedings of 1st Biennial Canadian Hydrographic Conference,* Halifax, April 1985, pp. 23.

Technical Survey Services Ltd. (n.d.) "Model 320 Heave Compensator Operating Manual." TSS Ltd., U.K.

Tranquilla, J. (1991). Personal Communication. Professor, Department of Electrical Engineering, University of New Brunswick, Fredericton, N.B.

Tucker, M.J. (1955). "A Ship Borne Wave Recorder." *Proceedings of the First Conference on Coastal Engineering Instruments.* Berkeley, California, Oct. 31 - Nov. 2, 1955, pp 112-118.

Vaníček, P. (1973). "Gravimetric Satellite Geodesy." Department of Surveying Engineering Lecture Notes No. 32, University of New Brunswick, Fredericton, N.B., Canada.

Vaníček, P. and E. Krakiwsky (1988). *GEODESY: The Concepts.* 2nd rev. ed., North-Holland Publishing Company, Amsterdam.

Vaníček, P., G. Beutler, A. Kleusberg, R.B. Langley, R. Santerre and D.E. Wells (1985). "DIPOP: Differential Positioning Program Package for the Global Positioning System." Department of Surveying Engineering Technical Report No. 115, University of New Brunswick, Fredericton, N.B., Canada.

Wassef, A.M. and K.M. Kelly (1988). "Enhancing the Usefulness of GPS Two-Frequency Data for Estimating the Ionospheric Correction." *Proceedings of the Satellite Division's International Technical Meeting.* The Institute of Navigation, Colorado Springs, Colorado, 19-23 September 1988, pp 347-354.

Wells, D.E. and A. Kleusberg (1989). "Kinematic Differential Global Positioning System." Contract report for the U.S. Army Engineer Topographic Laboratories, Fort Belvoir, Virginia, March, 36 pp.

Wells, D.E. and E.J. Krakiwsky (1971). "The Method of Least Squares." Department of Surveying Engineering Lecture Notes No. 18, University of New Brunswick, Fredericton, N.B., Canada.

Wells, D.E., N. Beck, D. Delikaraoglou, A. Kleusberg, E.J. Krakiwsky, G. Lachapelle, R.B. Langley, M. Nakiboglu, K.P. Schwarz, J.M. Tranquilla and P. Vaníček (1986). *Guide to GPS Positioning*. Canadian GPS Associates, New Brunswick, Canada.

Zielinski, A. (1986). "A Digital Double Integrating Filter for Heave Measurements." *Oceans 86 Conference Record*, IEEE, vol. 1, page 430.

BIBLIOGRAPHY

Allison, T., R. Eschenbach (1989). "Real-Time Cycle-Slip Fixing during Kinematic Surveys". *Fifth International Symposium on Satellite Positioning*, 13-17 March 1989, New Mexico State University, Las Cruces, NM.

Ashjae, J., R. Lorenz, R. Sutherland, J. Dutilloy, J.B. Minazio, R. Abtaki, J.M. Eichner, J. Kosmalska and R. Helky (1989). "New GPS Developments and Ashtech M-XII". *Proceedings of the Second Annual International Technical Meeting- ION GPS-89,* Institute of Navigation's Satellite Division, The Institute of Navigation, Colorado Springs, Colorado, 19-23 September, 1989.

Bastos, L. and H. Landau (1988). "Fixing Cycleslips in Dual Frequency Kinematic GPS-Applications using Kalman Filtering." *Manuscripta Geodetica* No. 13, pp. 249-256.

Brozena, J.M., G.L. Mader and M.F. Peters (1989). "Interferometric Global Positioning Source for Airborne Gravimetry." *Journal of Geophysical Research.* vol. 94, No. B9 pp. 12.153-12.162, September 10, 1989.

Eran K. (1989). "Effects of Orbital A Priori Information on Baseline Determinations." *ASCE Journal of Surveying Engineering,* vol. 115, No. 1.

Eschenbach, R., T. Allison, K. Mooyman, T. Poplawski and C. Quirion (1988). "Practical Aspects of Kinematic Surveying." *Proceedings of the Satellite Division's International Technical Meeting.* The Institute of Navigation, Colorado Springs, Colorado, 19-23 September 1988.

Frei, E. and G. Beutler (1989). "Some Considerations Concerning an Adaptive, Optimized Technique to Resolve the Initial Phase Ambiguities for Static and Kinematic GPS Surveying - Techniques". *Fifth International Symposium on Satellite Positioning,* 13-17 March 1989, New Mexico State University, Las Cruces, NM.

Georgiadou, Y. and A. Kleusberg (1989). "Multipath effects in Static and Kinematic GPS Surveying". *Proceedings 1989 IAG General Meeting,* Edinburgh, UK, August 3-12.

Hatch, R. (1982). "The Synergism of GPS Code and Carrier Measurements." Magnovox Report, MX-TM-3353-82, January 1982.

Hatch, R. (1986). "Dynamic Differential GPS at the Centimeter Level." *Proceedings of the Fourth International Geodetic Symposium on Satellite Positioning,* Austin Texas, vol. II, pp. 1287.

Hein, G. W., G. Baustert, B. Eissfeller and H. Landau (1988). "High Precision Kinematic GPS Differential Positioning: Experiences, Results, Integration of GPS with a Ring Laser Strapdown Inertial System." *Proceedings of the Satellite Division's International Technical Meeting.* The Institute of Navigation, Colorado Springs, Colorado, 19-23 September 1988.

Hein, G., H. Landau and G. Baustert (1989). "Differentielle Kinematische GPS-Positionierung." *Zietschrift für Vermessungswesen,* Vol 6, pp. 287-302.

Ingham, A.E. (Ed.) (1975). *Sea Surveying - Vol 1.* John Wiley and Sons Ltd., Great Britain.

Kanasewich, E.R. (1981). *Time Sequence Analysis in Geophysics.* The University of Alberta Press, Edmonton.

Keel, G., H. Jones and G. Lachapelle (1988). "A Test of Airborne Kinematic GPS Positioning for Aerial Photography: Methodology." *Proceedings of the Satellite Division's International Technical Meeting.* The Institute of Navigation, Colorado Springs, Colorado, 19-23 September 1988.

Kleusberg A., S.H. Quek, D.E. Wells, G. Lachappelle (1986). "GPS Relative Positioning Techniques for Moving Platforms." *Proceedings of the Fourth International Geodetic Symposium on Satellite Positioning,* Austin Texas, vol. II, pp. 1299.

Krabill, W. B., C. F. Martin and R. N. Swift (1989). "Applying Kinematic GPS to Airborne Laser Remote Sensing." *Proceedings of the Second Annual International Technical Meeting- ION GPS-89,* Institute of Navigation's Satellite Division, The Institute of Navigation, Colorado Springs, Colorado, 19-23 September, 1989.

Krakiwsky, E.J. (Ed.) (1983). "Papers for the CIS Adjustment and Analysis Seminars." The Canadian Institute of Surveying and Mapping, Ottawa.

Kremer, G. T., R. M. Kalafus, P. V. W. Loomis, J. C. Reynolds (1989). "The Effect of Selective Availability on Differential GPS Corrections." *Proceedings of the Second Annual International Technical Meeting- ION GPS-89,* Institute of Navigation's Satellite Division, The Institute of Navigation, Colorado Springs, Colorado, 19-23 September, 1989.

Loomis, P. (1989). "A Kinematic GPS Double-Differencing Algorithm." *Fifth International Symposium on Satellite Positioning,* 13-17 March 1989, New Mexico State University, Las Cruces, NM.

Nord, G. P. and L. Weems (1989). "GPS Geodesy and Kinematic Topography Measurements and Results." *ASCE Journal of Surveying Engineering,* vol 115, No. 2, pp. 166.

Okkes, R.W. (1988). "GPS Relative Navigation for Space Vehicles." *Proceedings of the Satellite Division's International Technical Meeting.* The Institute of Navigation, Colorado Springs, Colorado, 19-23 September 1988.

Prado, G. (1979). "Optimal Estimation of Ships Attitudes and Attitude Rates." *IEEE Journal of Ocean Engineering.* Vol. OE-4, April 1979, pp. 52-59 .

Press, W.H., B.P. Flannery, S.A. Teukolsky and W.T. Vetterling (1987). *Numerical Recipes - The Art of Scientific Computing.* Cambridge University Press, New York.

Remondi, B.W. (1985). "Modelling the GPS Carrier Phase for Geodetic Applications."
Proceedings of the First International Symposium on Precise Positioning with the Global Positioning System. Rockville, Md., 15-19 April, 1985, vol. I, pp. 325.

Remondi, B.W. (1985). "Performing centimeter accuracy relative surveys in seconds using GPS carrier phase." *Proceedings of the First International Symposium on Precise Positioning with the Global Positioning System.* Rockville, Md., 15-19 April, 1985, vol. II, pp. 789.

Remondi, B.W. (1986). "Performing Centimeter Level Surveys in Seconds with GPS Carrier Phase: Initial Results." *Proceedings of the Fourth International Geodetic Symposium on Satellite Positioning,* Austin Texas, vol. II, pp. 1229.

Roth, B. D. (1986). "Applications of Navstar GPS to Precision Attitude Determination." *Proceedings of the Fourth International Geodetic Symposium on Satellite Positioning,* Austin Texas, vol. II, pp. 1345.

Wasef, A. M. and K. M. Kelly (1988). "Enhancing the Usefulness of GPS Two-Frequency Data for Estimating the Ionospheric Correction." *Proceedings of the Satellite Division's International Technical Meeting.* The Institute of Navigation, Colorado Springs, Colorado, 19-23 September 1988.

Weis, I.M. (1977) "Ship Motion Measurement Filter Design." *IEEE Journal of Ocean Engineering,* Vol. OE-2, Oct 1977, pp. 325-330.

Wells, D.E., P. Vaníček and S. Pagiatakis (1985). "Least Squares Spectral Analysis." Department of Surveying Engineering Technical Report No. 84, University of New Brunswick, Fredericton, N.B., Canada.

Wübbena, G. (1989). "The GPS Adjustment Software Package GEONAP, Concepts and Models." *Proceedings of the 5th International Geodetic Symposium on Satellite Positioning.* New Mexico State University, Las Cruces, New Mexico, 13-17 March, vol. 1, pp. 452-461.

Zielinski, A., W.J. Vetter and D. Howse (1984). "Realtime Removal of Source Heave Effects from Marine Seismic Profiles." *Oceans 84 Conference Record,* IEEE, vol. 1, pp. 45.

APPENDIX A

Comparison of the
TSS Model 320 and HIPPY 120b
Heave Sensors

Graduate Seminar Paper II

SE 6910

March 10, 1989

A.1   Introduction

Any vessel that is free to move upon the surface of a body of water will be affected by the motion of that body of water. In response to the motion of the water, the vessel will experience an induced motion which is a function of the properties of the vessel and characteristics of the forcing motion. The motion of the vessel will be the coupled effects of three translations and three rotations of the vessel from some position of equilibrium.

The vertical motion of the vessel is often the most critical parameter when determining the operational limits of offshore activities such as bathymetry, ocean seismic profiling and ocean drilling programs. Traditionally, short period vertical motions caused by wind driven waves are termed heave. These wind driven waves, with periods of between 1 second and 20 seconds [Rawson and Tupper, 1968], can be differentiated from other open ocean related phenomena such as tides, seiche waves and tsunamis, which have longer periods and smaller magnitudes. To facilitate the monitoring of and possible compensation for heave effects, it is necessary to deploy a sensing system designed to operate optimally in the range of conditions likely to be encountered by the vessel.

During the period of June 13 - June 28, 1988, an experiment to determine, by various means, the vertical motion of a ship underway, was conducted aboard the Canadian Survey Ship (C.S.S.) HUDSON. The experiment, a collaborative effort between the Atlantic Geoscience Laboratory of the Geological Survey of Canada, the Geophysics Division of the Geological Survey of Canada, and the Department of Surveying Engineering, University of New Brunswick, took place in an area at approximately 42° 45' N, 64° 15' W. Included in the deployed instrumentation were two commercial heave sensor packages, the Technical Supply and Services Model 320 and the Datawell HIPPY 120b. This report examines these two products by comparing their responses to a similar input motion.

A.1.1   Accelerometer based Heave Sensors

The particular type of heave sensor investigated in this report has a single accelerometer installed on a self-stabilizing platform. These devices are usually but not always located near or at the centre of gravity of the vessel where the sensor will not experience tangential accelerations other than those due to heave. Should the device experience motions outside its dynamic range, the resulting output will be unreliable.

When the sensor is placed away from the point of interest, other orientation sensors monitoring the pitch and roll of the vessel must be used. The roll and pitch may then be used to translate the motion experienced by the sensor to the point of interest.

A.1.1.1 The Reference Platform

The self-stabilized platform is used as the vertical reference plane and attempts to constrain the accelerometer to measure in the vertical direction only. This platform has some resonant period which is a function of the characteristics of the platform as well as the medium in which the working parts are immersed. The reference platform is designed to be insensitive to rotational motions and short period translational motions. However, these motions, which can be the result of wave action, ship maneuvering and pitch and roll, become significant as the frequency of the motion falls below the natural frequency of the platform [Staples et al., 1986]. The resulting horizontal accelerations will cause the orientation of the reference platform to change with respect to the gravitational normal and the accelerometer will no longer register the vertical acceleration alone but a component of both the vertical and horizontal accelerations experienced.

A.1.1.2 The Acceleration Signal

To calculate the vertical position of the sensor with respect to its equilibrium position, the vertical acceleration is doubly integrated and sampled [Renouf, 1987]. However, because the signal from an accelerometer oriented vertically will always contain a DC component as well as spurious low frequency components, the integrator will eventually become overwhelmed. For this reason, low frequency signals must be rigorously filtered from the output signal with the consequent loss of information [Zielinski, 1986].

There are two ways of handling output from the accelerometer. The signal, which is analogue by nature, can be filtered and integrated in an analogue sense or it can be discretely sampled, and then digitally filtered and integrated. Analogue filtering and integration techniques, using only past data, can provide near real time output , whereas digital filtering, utilizing past and future information, can also provide optimally filtered and integrated data in a post event sense [Hopkins and Adamo, 1981].

Filtering techniques are limited in that they are designed to be insensitive to periodic motions within a specific frequency pass band. The appropriate band chosen in the filter and integrator design is determined by the conditions the sensor is expected to operate in.

For vessel operations on the ocean, a low frequency cutoff point of close to 0.05 Hz and a high frequency cutoff point of 1 Hz are commonly used [Renouf, 1987].

A.2 Sensor Descriptions

The TSS Model 320 heave sensor package and the Datawell HIPPY 120b heave sensor package are similar in terms of their theoretical design and accuracy, yet differ with respect to the construction of the sensor as well as the packaging and included peripherals. Whereas the operation of the TSS Model 320 heave sensor is digitally based, the operation the HIPPY 120b heave sensor is based on analogue techniques. Table A.2.1 summarizes the specifications for each heave sensor.

Table A.2.1 – Heave Sensor Specifications

CATEGORIES	TSS MODEL 320	HIPPY 120b
Type	Gimbal Mounted Accelerometer	Pendulum Stabilized Accelerometer
Power Requirements	120 Volts AC, 10 - 30 Volts DC	Bandwidths: 1.0 - 0.05 Hz 1.0 - 0.067 Hz
Dynamic Range	±4 metres	± 10 metres
Accuracy	10% @ high freq bandwidth, 5% @ med. freq bandwidth, 5% @ low freq bandwidth	3.5 % @ full bandwidth
Lag Time	36 msecs	320 msecs
Output	Digital, RS 232, IEEE, Continuous, Interrogation	Analogue,Continuous
Additional Sensors	Pitch, Roll (optional)	Pitch, Roll
Size	height 0.21 m, diam. 0.14 m	height 0.8 m, diam. 0.6 m
Weight	13 kg	120 kg
Included Peripherals	Controller Unit, Cables, Mounting bracket	None

A.3 Experiment Design

The goal of the original experiment was to determine the capability of satellite measurements in monitoring the vertical motion of a ship and the purpose of the heave sensors was to provide reference measurements. However, because of the availability of the two commercial brands of heave sensor, it was additionally decided to compare their capabilities.

A.3.1 Equipment Location

The Datawell HIPPY 120b was mounted near the TSS Model 320 in the forward lab (see Figure A.1). The forward lab, approximately 25 metres forward of the centre of rotation, while not the ideal location, was chosen because of the physical constraints imposed by the size and weight of the HIPPY 120b. Vertical motions measured by the two sensors therefore include a component due to rotation of the vessel about the pitch and roll axis.

A.3.2 Data Collection

Data logging from both heave sensors took place on a single IBM compatible computer connected via standard cabling and connectors. Data collection from the HIPPY 120b required an analog to digital conversion board in the computer, whereas the TSS Model 320 used a standard RS 232 serial communications port.

The logging program, written in the BASIC programming language, used a 1 pulse per second signal to trigger a data collection loop from both the TSS Model 320 heave sensors and the analog to digital conversion board. Time tagging of the data was accomplished using the computer clock. The data was stored in American Standard Code for Information Interchange (ASCII) format on a 20+20 megabyte floppy disk drive.

The experiment was expected to start on June 13, 1988 and end the morning of June 28, 1988. The first three days of that period the ship was delayed in port and so no observations were recorded. During the next 11 days the only problems encountered with recording heave observations occurred with the analog to digital conversion board which would sometimes stop operating for no apparent reason. When this problem occurred, it was a simple matter of restarting the data logging program. Typical duration of an observing session was 4 hours per day and a typical session file size was 2 megabytes. Approximately 22 megabytes of heave data were collected over the 11 days of operation.

A.4 Investigation of Results

The data investigated were the observations from two consecutive days of logging heave. During the first day, day 174, the winds were moderate and the swell was smooth.

The ship responded to the swell with average vertical motions of ± 0.5 m and average pitch rotation of ± 1°. Heave conditions during this day were characterized by the regularity of the seas encountered. Day 175 on the other hand, exhibited a marked increase in the size and irregularity of the seas. The magnitude of both the swell and the pitch rotation doubled and the motions experienced were more complicated than the motions on the previous day.

The data sets chosen for analysis are subsets of the data recorded for the particular day. The data set from day 175 was selected because of the extreme motions encountered during that period, whereas the data set from day 174 was chosen randomly to represent the smooth and moderate vertical motion experienced. The data sets used were 35 minutes in duration and contain 2000 data points from each sensor. Due to the more extreme motions encountered on day 175, the TSS Model 320 experienced some difficulties in measuring the vertical heave. Approximately 20% of the data from the TSS Model 320 over the 35 minute period were internally flagged as being unreliable. These periods of unreliable data spanned between 10 and 20 seconds and were scattered throughout the entire data set. The TSS Model 320 data set from day 175 was "cleaned" by deleting those data points flagged as unreliable.

Various analyses were performed with the data sets including simple differencing, power spectrum analysis, and cross correlation. To determine the character of the unreliable TSS Model 320 observations from day 175, the differencing was performed using both the original data set and the "cleaned" data set from the TSS Model 320. However, for the spectrum density and correlation analysis, only the original TSS Model 320 data set for day 175 was used in order not to further complicate the analysis. The results from these analyses were plotted and are included in the appendix.

A.4.1   Differences

The recorded heave from both the HIPPY 120b and the TSS Model 320 heave sensors for days 174, 175 (see Figures A.2a, A.2b, A.3a and A.3b) were differenced and the residuals inspected (see Figures A.4a, A.4b and A.5). Some statistics determined from the residual data set are summarized in Table A.4.1.

Table A.4.1 — Statistics from Residual Signals

STATISTIC	DAY 174	DAY 175 (original)	DAY 175 (cleaned)
Average Heave (approx)	± 0.5 m	± 1.5 m	± 1.5 m
Dominant Period (approx)	7 sec	9 sec	9 sec
Differenced Mean	2.7 cm	1.9 cm	2.9 cm
Differenced Std Dev.	4.8 cm	20.7 cm	15.5 cm
Largest Differences	0.3 m	1.5 m	-0.7 m

Inspection of the residual series plot for day 175 (uncleaned) shows a number of large spikes representing large discrepancies due to abnormal operation of the TSS Model 320. When such abnormal operation occurs in the TSS Model 320, the heave signal is characterized by an upward "hump" in the data [Technical Survey Services Ltd.]. This observation can be verified by inspecting the output from the TSS Model 320 for day 175 (see Figure A.3b). However, even eliminating the data resulting from the abnormal periods of operation, the largest peak to peak difference is still as much as 1.2 m (see Figure A.5)

Visual inspection also indicates that the differenced signal is 180° phase shifted from the original signals. A 180° phase shift can result if, over the balance of the time series, the amplitude of the second signal is larger than the first signal. This then means that the scale factor of the TSS Model 320 is larger than the scale factor for the HIPPY 120b and therefore the TSS Model 320 consistently registers a greater heave signal than the HIPPY 120b sensor. To illustrate this conclusion consider the difference c between two simple periodic signals a and b:

$$a = A\sin(wt) \ , \ b = B\sin(wt) \ , c = (A-B)\sin(wt) \tag{A.1}$$

where:

w	-	angular frequency
t	-	time
A,B	-	amplitude

$B > A > 0$ and for simplicity $B-A=1$

Therefore the difference **c** is:

$$c = -\sin(wt) = \sin(wt+\pi) \qquad (A.2)$$

where π represents a phase shift of the signal by 180°. The existence of a 180° phase shift between the residual signal and either of the original signals was further tested using correlation analysis (see section A.4.3).

A.4.1.3   Error Analysis

Each heave sensor publishes an error statistic which is a percentage of the measured value. To investigate if the residuals found from differencing are within the specifications given, the given error values of 10% for the TSS Model 320 and 3.5% for the HIPPY 120b were used to predict the differences between the two heave sensors based on the amplitude of the motion experienced. Taking the absolute value of the heave signal and applying error propagation for combining the error for the TSS Model 320 and the HIPPY 120b, the average predicted error is compared against the average of the absolute value of the residuals.

$$Error_{ave} = \frac{1}{n} \sum_{i=1}^{n} \sqrt{\left(\varepsilon_{TSS} H_{iTSS}\right)^2 + \left(\varepsilon_{Hip} H_{iHIP}\right)^2}$$

$$(A.3)$$

where:

n	-	the number of observations
ε_{TSS}	-	percentage error specified for the TSS Model 320
ε_{HIP}	-	percentage error specified for the HIPPY 120b
H_{iTSS}	-	TSS Model 320 heave measurement at epoch i
H_{iHIP}	-	HIPPY 120b heave measurement at epoch i

Using equation A.3, it was found that the average predicted error is consistently less than the average of the absolute value of the residual indicating that either the published error for the sensors is optimistic or the sensors are being affected by external errors not being accounted for. The results of this investigation are summarized in Table A.4.2.

Table A.4.2 – Error Investigation

DAY	Predicted Average Error from Eqn. A.3	Actual Average Residual from (Hippy - TSS 1)
Day 174	2.1 cm	5.1 cm
Day 175 (cleaned)	3.5 cm	15.2 cm

A.4.2 Power Spectrum Analysis

Using visual examination, it was found that each time series, including the residual time series, has an apparent dominant frequency. However, to more precisely determine both the dominant frequencies and any other frequency components not readily visible, power spectrum density analysis was performed. The significant frequencies that make up the signals are of interest in determining if either instrument is inserting a periodicity into the measured heave. One technique for estimating the power spectrum density $P(f_k)$ is by summing the results C_k of a fast Fourier transformation . Specifically the relationship is:

$$P(0) = P(f_0) = \frac{1}{N^2} |C_0|^2$$

(A.4)

$$P(f_k) = \frac{1}{N^2} \left[|C_k|^2 + |C_{N-k}|^2 \right] \quad k = 1, 2, \dots, \left(\frac{N}{2} - 1 \right)$$

(A.5)

$$P(f_c) = P(f_{N/2}) = \frac{1}{N^2} |C_{N/2}|^2$$

(A.6)

where:

C_k - elements of Fourier transform of data set (complex)

N - number of data points

Δ - sampling interval

f_c - nyquist frequency

$$f_k \equiv \frac{k}{N\Delta} = 2f_c \frac{k}{N} \quad k = 0, 1, \dots, \frac{N}{2}$$

[Press et al., 1987]

To reduce the variance of the power estimate, the power spectrum results are summed in groups of K and binned into M+1 frequency bins where: N=2MK. Thus the

variance factor of the power spectrum result can be reduced by a factor of $1/K^{1/2}$ [Press et al., 1987]. For the purposes of this investigation, N=2048, K=8, and M= 128.

Each plot was visually inspected to determine which frequencies contain significant power (see Figures A.6a, A.6b, A.7a, A.7b, A.8a and A.8b). From this, conclusions have been drawn as to the source of the spectral power in the residual time series. It was expected that day 174 and day 175 would show different spectral characteristics. The significant results from the power spectrum density analysis have been summarized in Table A.4.3.

Table A.4.3 – Power Spectrum Density Summary

DATA SET	DAY 174		DAY 175	
	Period (sec)	Magnitude	Period (sec)	Magnitude
HIPPY 120b HEAVE SIGNAL	6.7 6.5 DC Comp	380 340 50	8.5 9.5 26.0	770 550 15
TSS Model 320 HEAVE SIGNAL	6.7 6.5 80.0	425 375 10	8.5 9.5 77.0	950 670 60
RESIDUAL HEAVE SIGNAL	DC Comp 15 20	62 15 41	8.5 9.5 26.0 77.0	14 16 28 61

A.4.3   Cross Correlation Analysis

Cross correlation analysis was applied to the data set to determine if there exists a phase lag between the signals from the two heave sensors and to investigate earlier suspicions of a 180° phase shift between the residual series and either of the original series. The correlation between two time series will be large if the first time series is a close representation of the second time series but lags or leads it in time by τ. The mathematical expression for correlation of a periodic discrete time series with period N as a function of τ is:

$$\text{Corr} (g,h)_\tau \equiv \sum_{k=0}^{N-1} g_{\tau+k} h_k$$

(A.7)

[Press, et al, 1987].

A cross correlation between the data sets from the HIPPY 120b and the TSS Model 320 was performed for both day 174 and day 175. The plot of the results shows a maximum positive peak at zero lag indicating that there is no phase discrepancy between either sensor (see Figures A.9a & A.9b). It is also apparent from the successive high negative and positive correlation peaks at lags consisting of a multiple of the dominant period, that successive waves are highly correlated, with that correlation decreasing in time.

A cross correlation was also performed between the residual data set and the TSS Model 320 signal for day 175. The correlation plot indicates the maximum correlation is negative and occurs at a time lag of 1 second (see Figures A.10a & A.10b). This is further confirmation that the differenced signal is phase shifted by almost 180° from the original TSS Model 320 signal.

A.5 Conclusion

The residuals from the differencing the measurements of both heave sensors over the two day period indicates that, as the magnitude of motion increases, the magnitude of the residuals also increases. The differences can reach magnitudes greater than half the magnitudes of the actual motion. This suggests that the two heave sensors are responding differently to the forcing motion of the vessel. During day 175 the residuals indicated anomalous behavior of one of the heave sensors. This anomalous behavior was traced to the operation of the TSS Model 320 during more extreme motions and while the data during that period is not reliable, the condition was correctly flagged in the output. In general, the vertical motion experienced by the TSS Model 320 during day 175 was not outside of the specified range. However, the problem may be related to the short period bandwidth selected for that day. The short bandwidth is between 1 and 8 seconds, whereas the dominant period for day 175 was between 8.5 and 9.5 seconds.

Power spectrum density plots of the data series from the two heave sensors and the residual series, indicated that there is significant power in the lower frequencies. As both heave sensors should filter any low frequency signals, the plots suggest that the heave sensors are contaminating the measurements. From the power spectrum density plots it appears that, during periods of large motion, the TSS Model 320 introduces the majority of the low frequency power. A possible cause of the low frequency power is the frequent periods of unreliable data. However, the effect is dominant at a period of 77 seconds which does not appear to correspond to the occurrences of the periods of unreliable data.

During the period of lesser motion that was experienced on day 174, the HIPPY 120b introduced a dominant offset into the measurements. This offset appears to be a constant that is associated with the HIPPY 120b and falls within the specifications given for the sensor.

Correlation analysis of the two heave sensors indicated that, at the limit of the sampling interval, there is no phase lag between the recorded measurements from both the TSS Model 320 and HIPPY 120b. Correlation analysis between the residual data set and one of the original data sets does confirm that there exists a 180° phase shift. This phase shift indicates that there is a scale difference between the two sensors and more specifically the TSS Model 320 measurements are larger in magnitude that measurements from the HIPPY 120b of the same heave motion. A contribution to this scale difference is the placement of the TSS Model 320 two metres forward of the HIPPY 120b causing the TSS Model 320 to register a greater vertical motion due to pitch rotation than the HIPPY 120b does. However, the pitch of the vessel does not account for all of the residual signal, suggesting that there does exist a component of the scale difference which is internal to the two sensors.

The results presented indicate that the HIPPY 120b was reliable over a larger dynamic range than the TSS Model 320. However, during low dynamics, and even though the agreement between the two sensors is excellent, the HIPPY 120b introduced an anomalous vertical offset in the order of 3 cms. During high dynamics, the agreement is not as good and seems to include a low frequency effect that can be attributed to the internal operations of the TSS Model 320, rather than external accelerations. In both cases, the differences between the two heave signals are greater than those predicted using the given specifications.

In short, it appears that the TSS Model 320 heave sensor is more appropriate for low dynamic operations due to its greater sensitivity, whereas the HIPPY 120b heave sensor operates better in a high dynamic situation. Finally, these results are based on sensors located well forward of and above the centre of gravity of the vessel and therefore subject to accelerations other than pure heave. These accelerations may introduce errors into the measured heave that the manufacturers never intended the sensor to accommodate.

A. References

Datawell bv. "Manual - HIPPY Sensor 120 sec with analog filter (B filter) from serial no. 19111-B", Datawell bv, Laboratorium voor Instrumentatie, Netherlands.

Hopkins, Lt. Cmd. Robert D., Louis C. Adamo (1981). "Heave-Roll-Pitch Correction for Hydrographic and Multibeam Survey Systems". *The Hydrographic Journal*, No. 21.

Kanasewich, E.R. (1981). *Time Sequence Analysis in Geophysics*. The University of Alberta Press, Edmonton.

Press, W.H., B.P. Flannery, S.A. Teukolsky and W.T. Vetterling (1987). *Numerical Recipes - The Art of Scientific Computing*, Cambridge University Press, New York.

Rapatz P.J.V. (1988). "Preliminary Report on Heave Sensor Comparisons". Unpublished report, Department of Surveying Engineering, University of New Brunswick, Fredericton, N.B.

Rawson, K.J. and E.C. Tupper (1968). *Basic Ship Theory*. Longmans, Green and Co. Ltd., London.

Renouf, K. (1987), "Heave Compensation for Hydrographic Surveys". Graduate paper, Department of Surveying Engineering, University of New Brunswick, Fredericton, N.B.

Staples, H., J.T. Lockhart and G. Eaton, (1985), "HIPPY 120c Heave Compensator". *Proceedings of 1st Biennial Canadian Hydrographic Conference*, Halifax, April, page 23.

Technical Survey Services Ltd. "Model 320 Heave Compensator Operating Manual", TSS Ltd., U.K.

Zielinski, A. and W.J. Vetter, D. Howse (1984), "Realtime Removal of Source Heave Effects from Marine Seismic Profiles". *Oceans 84 Conference Record*, IEEE, vol. 1, page 45.

Zielinski, A., (1986), "A Digital Double Integrating Filter for Heave Measurements". *Oceans 86 Conference Record*, IEEE, vol. 1, page 430.

A.Diagrams

Diagrams and Plots of Analyses results

(Figure A.1 - Figure A.10)

EQUIPMENT LOCATION

Gravimeter

TSS 1

Centre Line

TSS 2

GPS
Antenna
Accelerometre

Hippy

GPS Antenna
Accelerometer package

GPS Antenna &
Accelerometre Package

Fwd Lab) Hippy
TSS 1

Gravity Lab) TSS 2
LG Gravimeter
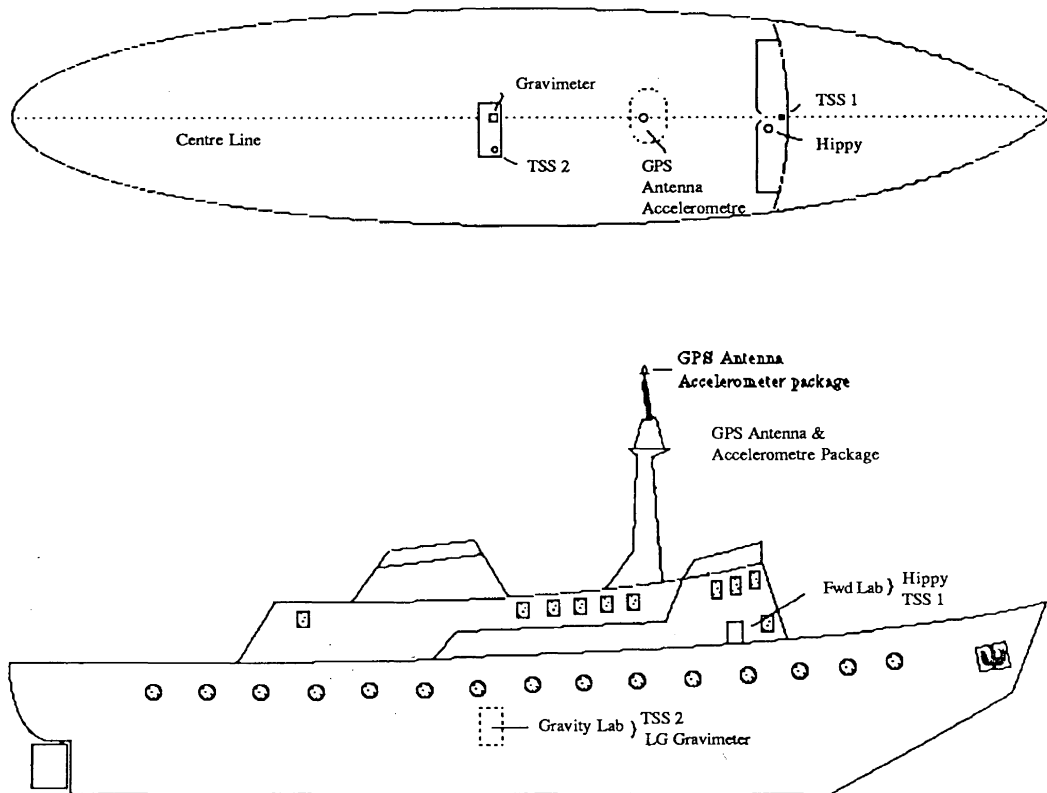
Figure A.1 – Equipment Location
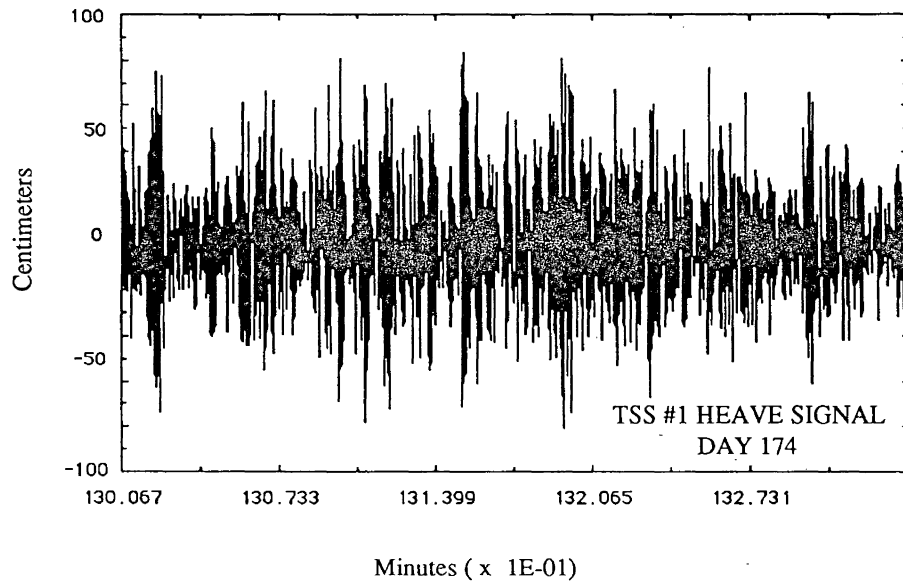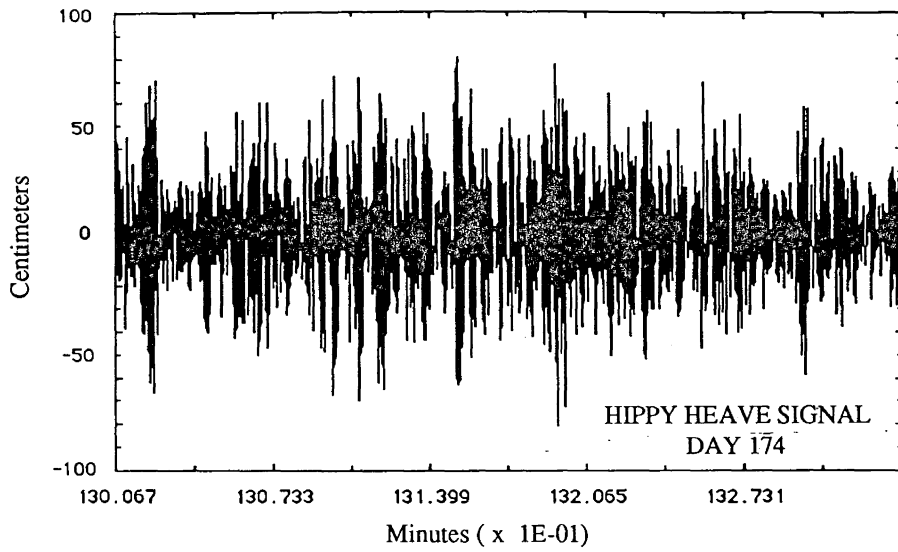
Figure A.2 a & b – Heave Signal Day 174
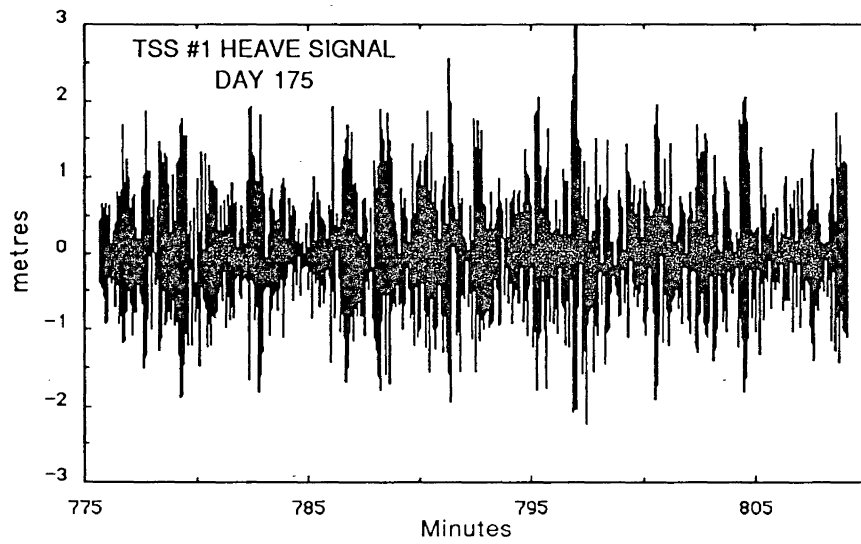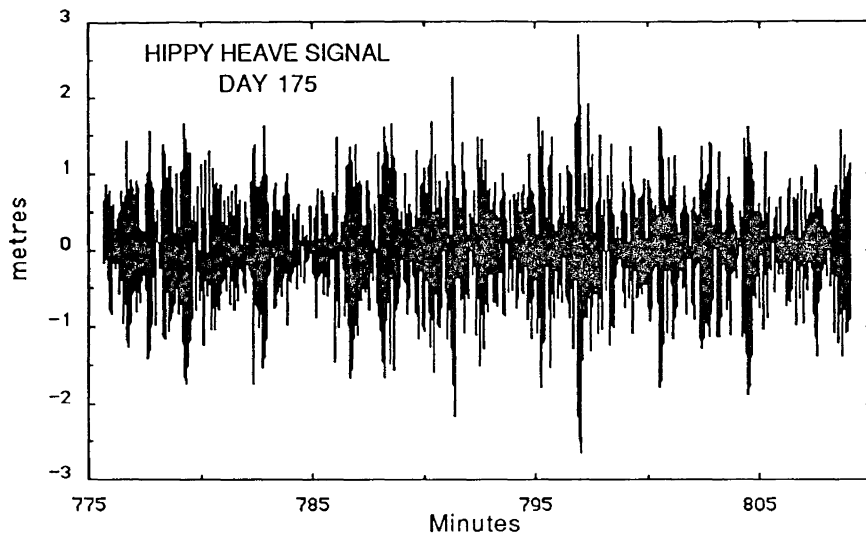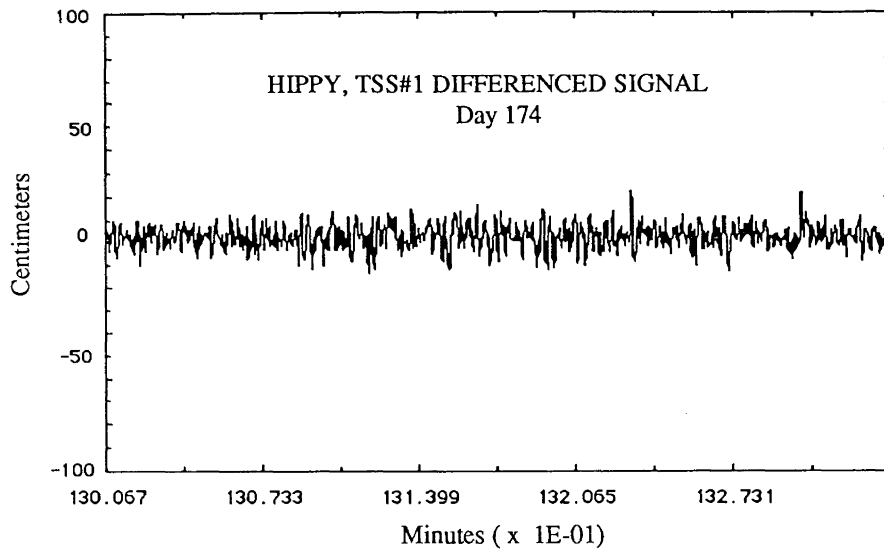
Figure A.3 a & b – Heave Signal Day 175
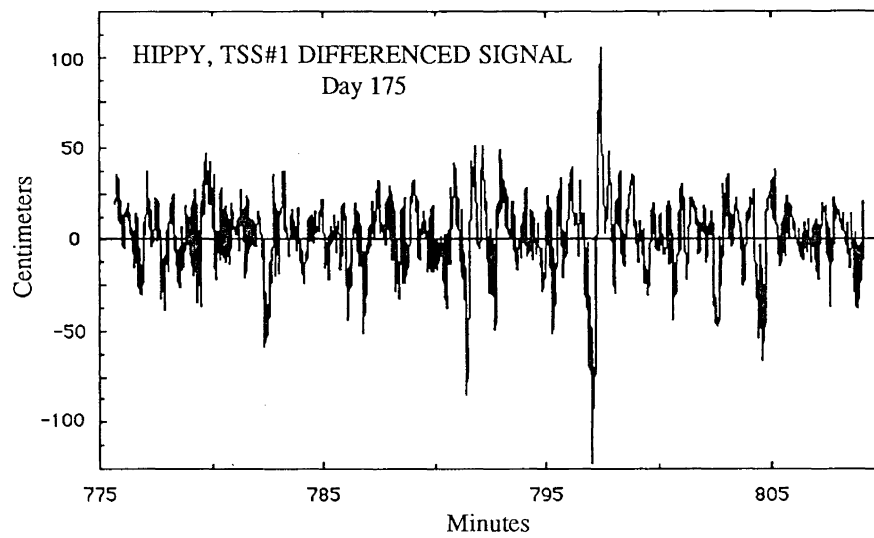
Figure A.4 a & b – Residual Heave Signal Day 174, 175
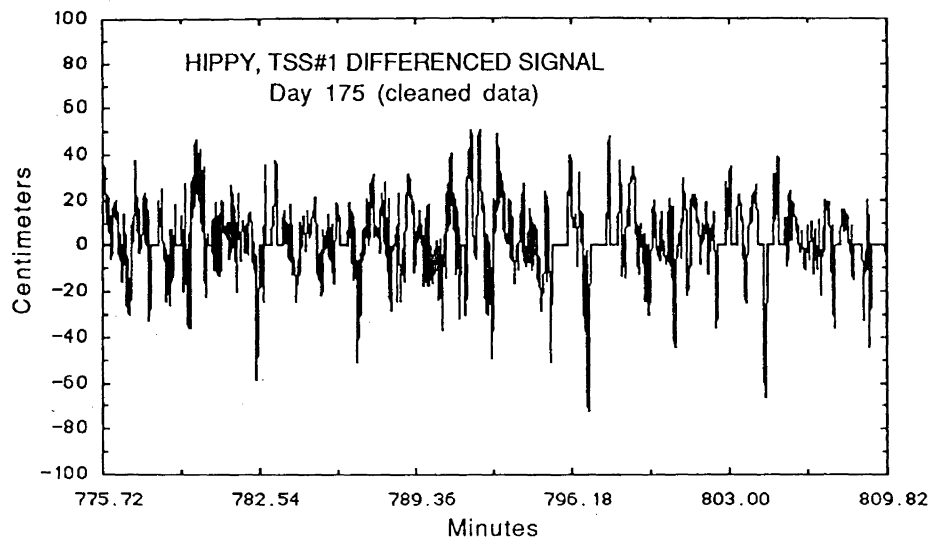
Figure A.5 – Residual Signal Day 175 (Cleaned)
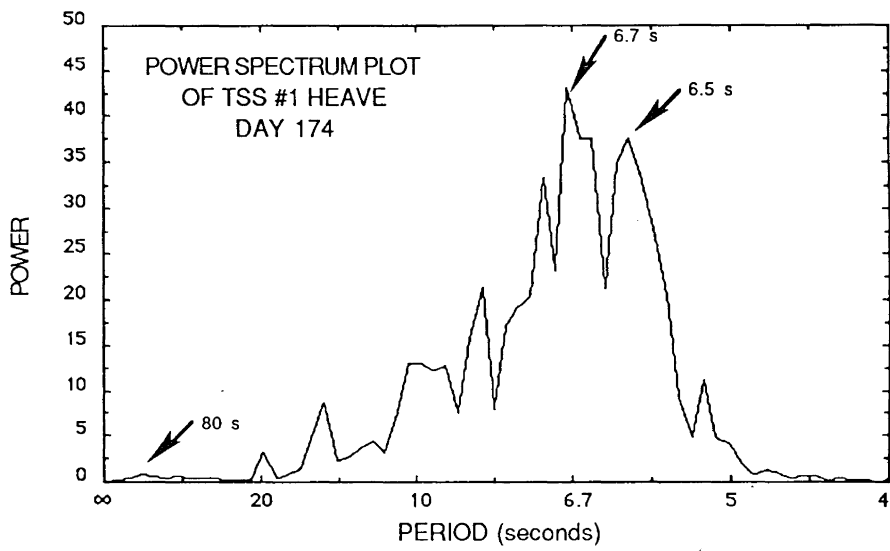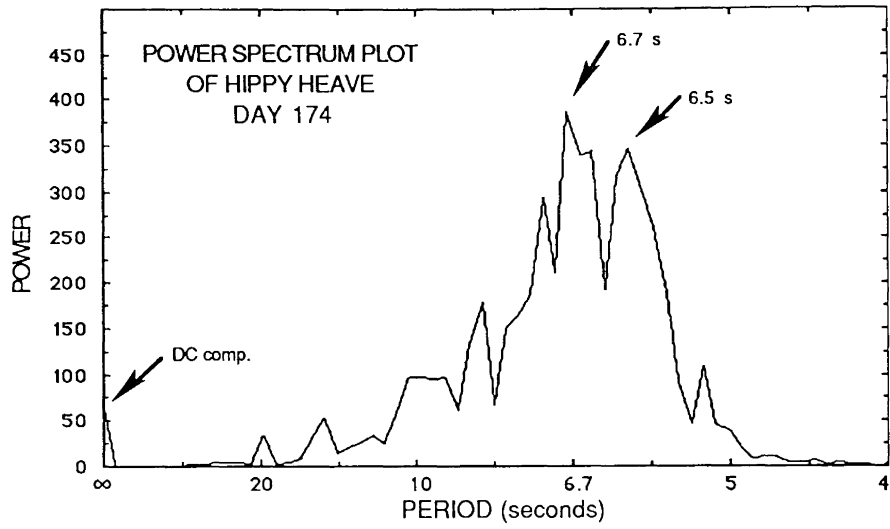
Figure A.6 a & b – Spectral Density Plots Day 174
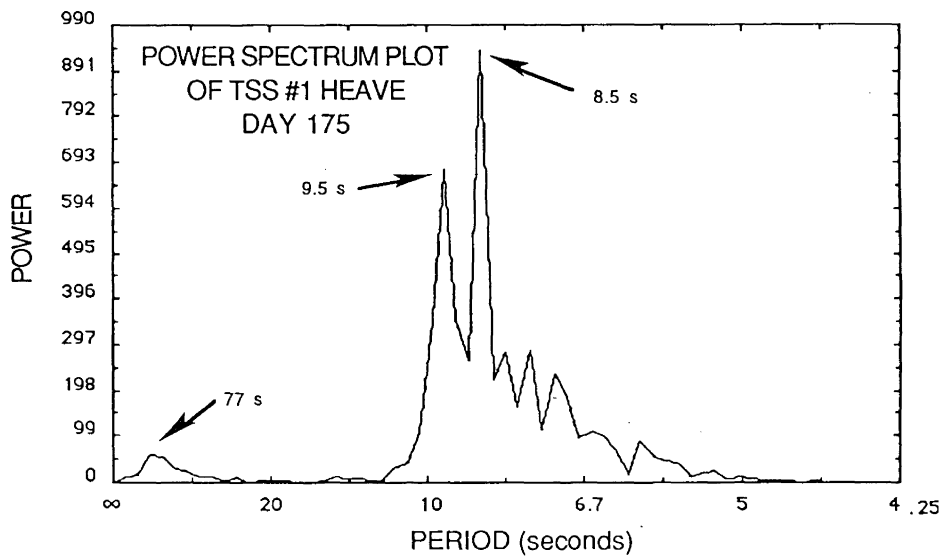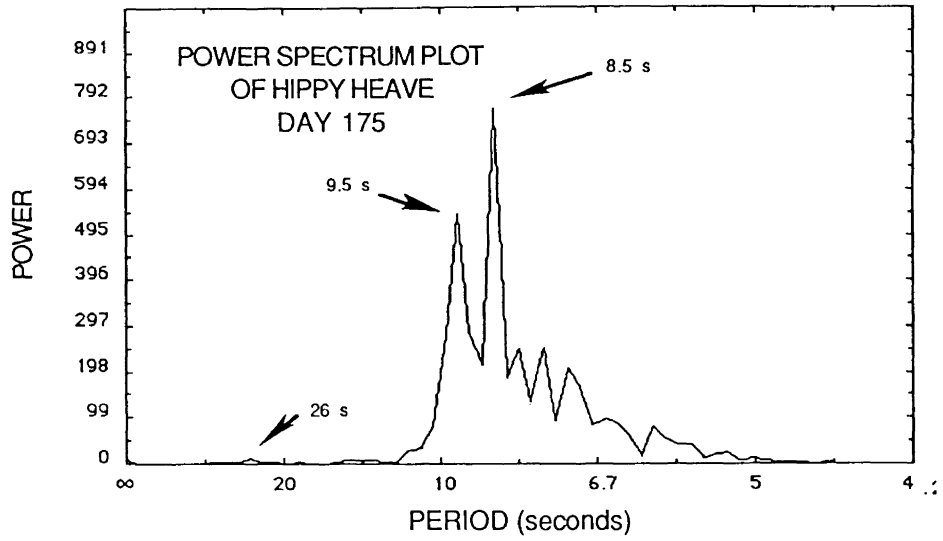
Figure A.7 a & b - Spectral Density Plots Day 175
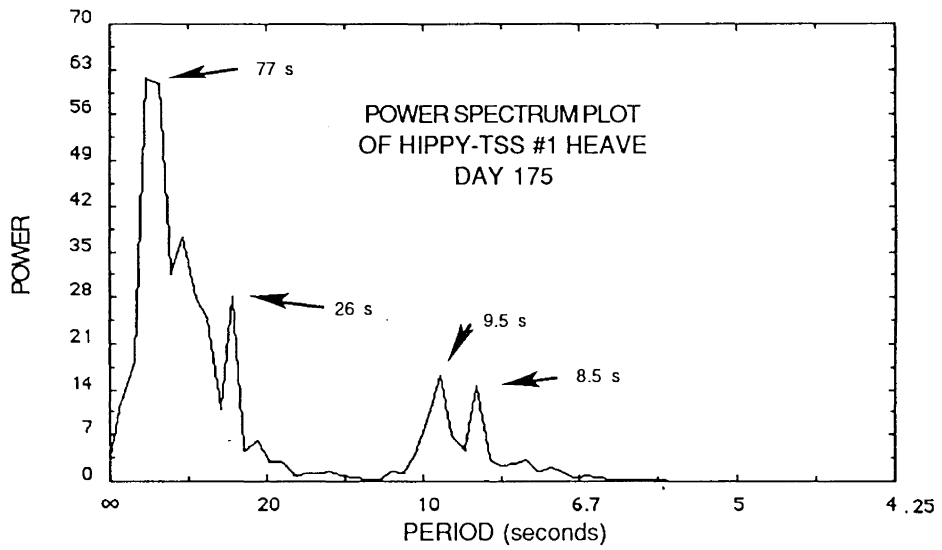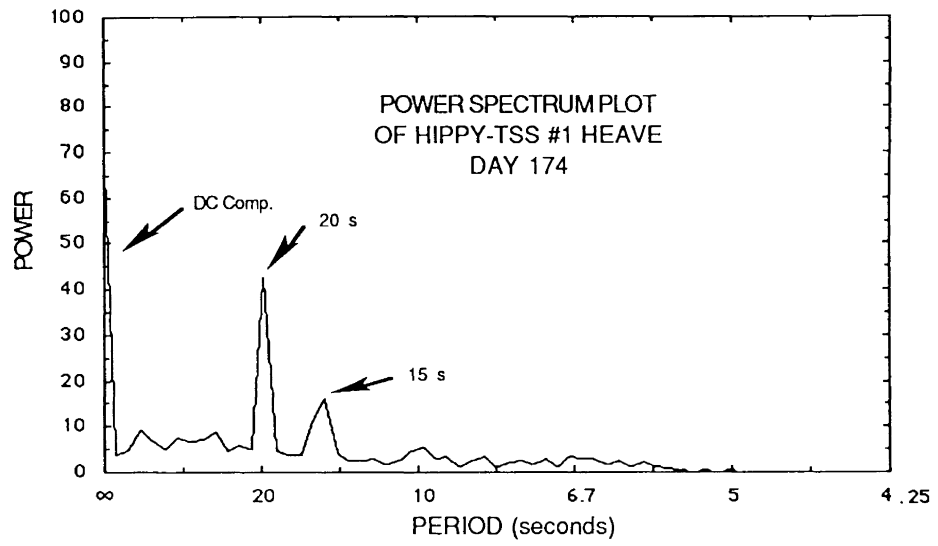
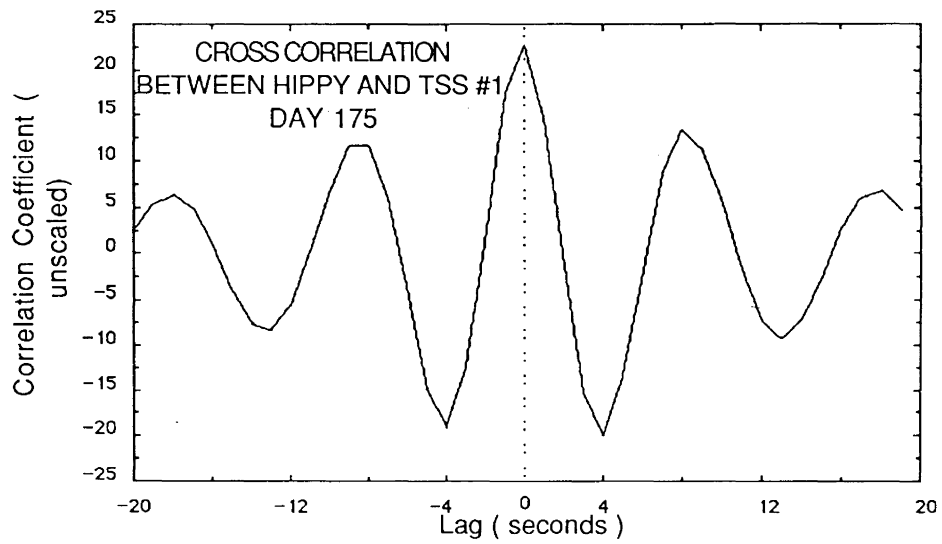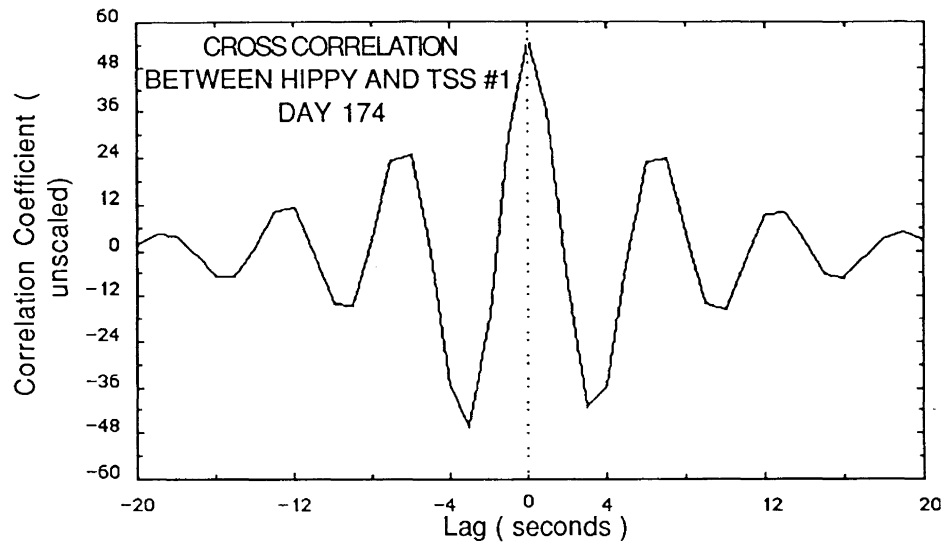Figure A.8 a & b – Spectral Density Plot of Residual Heave Day 174, 175
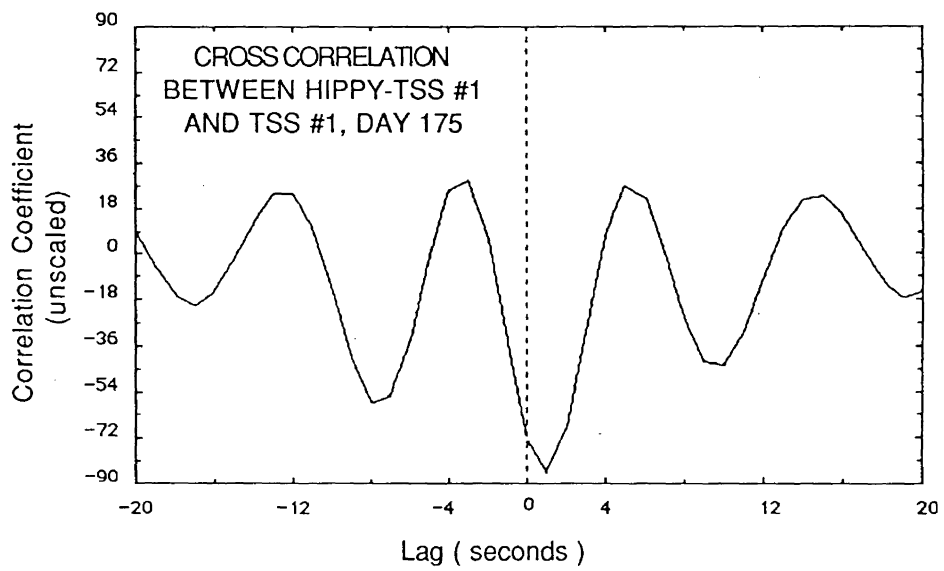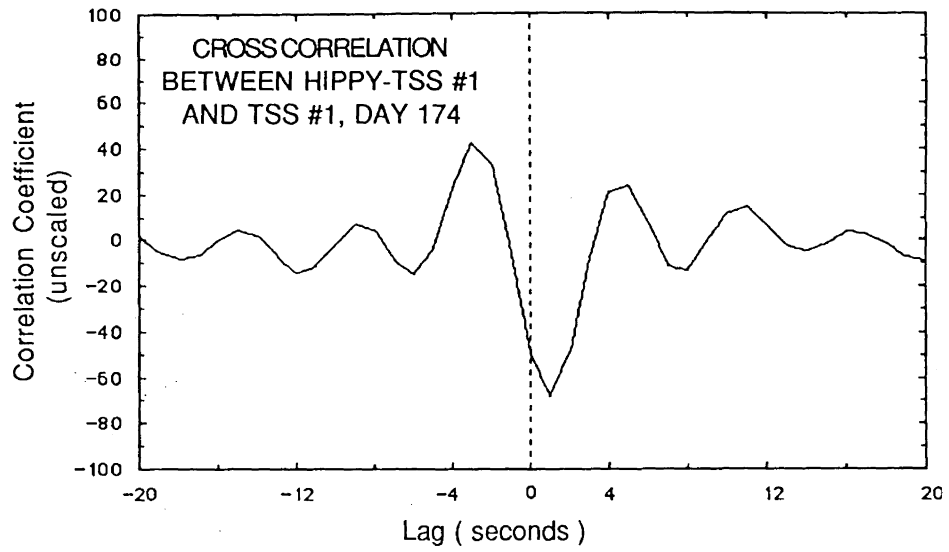
Figure A.9 a & b – Cross Correlation Plots Day 174, 175

Figure A.10 a & b – Cross Correlation Plots Residuals vs. Heave

VITA

Candidate's full name:	Phillip John Victor Rapatz
Place and date of birth:	Victoria, B.C., Canada, February 24, 1961
Permanent address:	339 Aberdeen St. Apt. A, Fredericton, N.B. E3B 1R8 CANADA
Schools attended:	Parkland Senior Secondary School, Sidney, B.C., CANADA 1976 - 1979
Universities attended:	University of Victoria, Victoria, B.C., CANADA 1979 - 1980, 1981-1984 B.Sc. - Physics (1984)

Publications:

Rapatz, P.J.V., M. Craymer, A. Kleusberg, R.B. Langley, S.H. Quek, J. Tranquilla, D.E. Wells (1987). "Specifications and procedures for urban GPS surveys." Department of Surveying Engineering Technical Report No. 131, University of New Brunswick, Fredericton, N.B., Canada.

Rapatz, P.J.V., M. Craymer, A. Kleusberg, R.B. Langley, S.H. Quek, J. Tranquilla, D.E. Wells (1987). "Specifications and procedures for urban GPS surveys." Paper presented at the ASCE Symposium on Satellite Positioning–Technical Papers, Nashville, Tennessee.

Rapatz, P.J.V. and D.E. Wells (1990). " Algorithm for the determination of heave using GPS carrier-phase measurements". Final contract report to Nortech Surveys Inc (Canada).